NTNU

Norwegian University of
Science and Technology

Modal Analysis of Weak Networks with the Integration of Wind Power

Asbjørn Benjamin Hovd

Master of Science in Energy and Environment
Submission date: June 2008
Supervisor: Olav B Fosso, ELKRAFT

Norwegian University of Science and Technology
Department of Electrical Power Engineering

Problem Description

When increasing the integration of wind power, both the steady-state and the dynamic behaviour of the system are affected. Since wind power facilities often are located in areas with weak networks (low short circuit capacity), disconnection of generators leading to power outage might occur at small disturbances. New requirements are therefore introduced, demanding that the facilities are not disconnected at a defined type of disturbance with specified time duration (fault-ride-through).

The main objective is the focus on how different types of wind power facilities affect a network's dynamic stability when exposed to small disturbances. This implies dynamic simulations for typical wind series and systematically use of linear analysis (eigenvalues, sensitivities, etc) in order to identify critical variables.

Analyses shall be carried out for wind power facilities based on both constant speed wind turbines and variable speed wind turbines. Dynamic models of SVC and traditional condenser batteries can be used if found necessary.

The following activities shall be included:

- Describe the current models for wind power turbines and demonstrate an understanding of the different models and how these interact.
- Identify crucial parameter values and evaluate the optimal placement of critical eigenvalues.
- Demonstrate how the linear analysing technique can be used to find the interaction between components in a dynamic system and by that contribute to optimal system behaviour.
- Analysis of a small-scale network with a combination of different production sources. Obtain results which are illustrative.

The analyses shall in general be based on the simulation software SIMPOW. MATLAB can also be used to evaluate the results.

The Master Thesis is a continuance of a project during the fall of 2007.

Assignment given: 17. January 2008
Supervisor: Olav B Fosso, ELKRAFT

Abstract

In this master thesis the theory and practical use of modal analysis is explained, giving an introduction to the possibilities of modal analysis. The master thesis starts with a look at wind power and the design of a modern wind turbine. Two models, one for constant wind speed wind turbines and one for variable speed wind turbines, are presented. An example shows how modal analysis can be utilized to evaluate a network's dynamic stability. Simulations are performed on a two-area network where different wind power models are tested and compared.

A two-mass model is used to model a constant wind turbine. The model consists of an asynchronous generator, a turbine, and a low speed shaft with a tensional stiffness. The model representing the variable speed wind turbine is based on a DFIG model included in the simulation software.

The two-area network consists of two areas connected together through a long line between Bus 5 and Bus 6. Area 1 has two production sources, one placed in Bus 1 and one placed in Bus 2. The second area represents a large network modelled as a very large synchronous generator with a high inertia.

The calculations have showed how modal analysis can be used to evaluate a system by using linearized differential equations and how the systems robustness against small disturbances can be altered by changing the systems parameters.

Simulations have verified that a two-mass model must be used when modelling a constant speed wind turbine. The inertia of the turbine will greatly influence the model's behaviour and must therefore be included in the model. Eigenvalues analysis performed during different wind speeds have documented that wind power will not become less stable towards small disturbances when operated at low wind speed conditions.

Preface

This master thesis has been written at the Department of Electric Power Engineering at the Norwegian University of Science and Technology during the spring of 2008. The thesis represents the end of my two years international master study.

Wind power facilities are often located in areas with weak networks, disconnection of generators leading to power outage for small disturbances. This thesis deals with the possibilities of applying modal analysis to a weak network with the integration of wind power.

The master thesis is written in the text formatting system LaTeX, calculations are done in MATLAB and simulations have been executed in SIMPOW.

I would like to thank my subject teacher and supervisor Prof. Olav Bjarte Fosso for his valuable guidance and help. I would also like to thank Ph.D. student Jarle Eek and Trond Toftevaag at SINTEF Energiforsking AS for important help with the simulations.

Trondheim, June 2008

Asbjørn Benjamin Hovd

Contents

List of Figures

List of Tables

Nomenclature

Scalars

β	Turbine blade angle
$\Delta\omega_r$	per unit speed deviation
ΔW	Speed deviation
δ	rotor angle
Λ	Tip speed ratio
λ	Eigenvalue
Ω	Rotational speed of wind turbine
ω	Imaginary part of the eigenvalue
∂	Partial derivative
ρ_{air}	Density of wind
σ	Real part of the eigenvalue
ζ	Damping ratio
A_{rotor}	Areal of rotor
C_p	Turbine efficiency
E	Steady state internal emf
f	Frequency
H	Mechanical inertia
I	Current
J	Inertia
K	Speed calculation coefficient
K_D	Generator damping power
K_s	Synchronizing torque coefficient
k_s	Torsional Spring Constant
P_{ord}	Power order

P_{wind} Power extracted from wind

Peg Optimal generated power

Q_{ord} Reactive power order

R Resistance

R_{blade} Length rotor blades

S Apparent power

T_e Electrical Torque

T_m Mechanical Torque

V Voltage

$V_{ac,ref}$ node reference voltage

v_{wind} Wind speed

W_{ref} Rotational speed reference

X Reactance

Z Impedance

P_e Power produced

$T_d^{'}$,$T_d^{''}$ short-circuit d-axis transient and sub-transient time constants

T_e Electrical Torque

$T_q^{'}$,$T_q^{''}$ short-circuit q-axis transient and sub-transient time constants

$T_{d0}^{'}$,$T_{d0}^{''}$ open-circuit d-axis transient and sub-transient time constants

$T_{q0}^{'}$,$T_{q0}^{''}$ open-circuit d-axis transient and sub-transient time constants

X_d,$X_d^{'}$,$X_d^{''}$ d-axis synchronous, transient and sub-transient reactance

X_q,$X_q^{'}$,$X_q^{''}$ q-axis synchronous, transient and sub-transient reactance

Vectors and Matrices

u Input vector

x State vector

y Output Vector

$\dot{x}$ State vector derivatives

A System matrix

B Control matrix

B Feed-forward matrix

C Output matrix

I Identity matrix

P Participation matrix

X_L Left eigenvector

X_R Right eigenvector

Units

m meters

m/s Meter per second

$p.u.$ Per unit

rpm Revolutions per minute

AC Alternate Current

MVA Megavoltampere

MW Megawatt

Hz Hertz

Abbreviations

DDSG Direct Drive Synchronous Generator

DFIG Doubly Fed Induction Generator

HVDC High Voltage Direct Current

SCRC Static Constant Reactive Compensation

SVC Static Var Control

VC Voltage Control

emf Electro-motive force

SCIG Squirrel Cage Induction Generator

Chapter 1

Introduction

1.1 Motivation

Norway has with its long coastline and good wind conditions the possibility to extend its current wind utilization greatly. Several wind farms are therefore planned which will considerably increase the amount of wind power in the Norwegian power system.

Since wind power must be placed along the coast or at other locations where the wind conditions are good, most wind farms will be located far away from the load centres and in relatively weak networks with low short circuit power.

Wind power is an fluctuating power source where the amount of produced power varies with the wind speed power. Combined with the fact that wind power technology differs from the technology used in the synchronous water power plants dominating the Norwegian power systems today, leads to new and demanding challenges.

1.2 Background

The recent years' considerable growth of installed wind power has led to considerable research concerning the performance of wind turbines towards power system dynamics, transient stability and their response to short circuits. Small small signal stability on the other hand has so far received much less attention. Small signal stability is as described in chapter 4 the systems ability to reach a steady state condition after a small disturbance. This is mainly a problem due to insufficient damping of electromechanical modes, which are related to power oscillations occurring in the rotor of electrical machines [13].

1.3 Research Objective

The scope of this master thesis is to see how different types of wind power facilities affect a network's dynamic stability when exposed to small disturbances. This includes dynamic simulations for typical wind series and a systematically use of linear analysis (eigenvalues, sensitivities, etc) in order to identify critical variables.

Description of the currents models for wind power models shall be presented and a demonstration on how linear analysing techniques can be used to find the interaction between components in a dynamic system and by that contribute to optimal system behaviour are to be carried out.

A small SMIB network and a network with an sufficient degree of freedom are to be used to simulate and evaluate the different wind farm representations.

1.4 Content of the Thesis

The master thesis can in general be divided into three main parts:

Chapter 2-5. These chapters contains the theory part of the thesis. Chapter 2 present wind power in a historical perspective and explains the design of a modern wind turbine, while chapter 3 looks closer into a general wind turbine model and presents the models used in the simulations. The theory behind small signal stability and the mathematical expressions are presented in chapter 4-5.

Chapter 6. This chapter uses a small network with an synchronous generator to demonstrate how linear analysis can be applied on a power system.

Chapter 7. Two SMIB systems, one with a constant speed wind turbine and one with a variable speed wind turbine is simulated and several models are tested on a two area network.

Chapter 2

Wind Power

This chapter gives a brief introduction to the history and development of wind power. The design of a modern wind turbine is explained and a market overview for Europe is presented.

2.1 Historical Perspective

Wind power have been used to pump water, grind corn and cross oceans for thousands of years, and early examples of wind powered machines were used in Persia as early as 200 BC. The first known practical windmills were probably built in Sistan, Afghanistan around the seventh century. These windmills were vertical axles with rectangle shaped blades and were used to grind corn and pump water. Windmills for grinding corns were also used in a large scale in Europe and by the late nineteenth century more than 100.000 "Dutch" windmills were in use [1].

Figure 2.1: Traditional "Dutch" windmill [1]

In 1887 the first known electrical wind turbine was built in Scotland and there were in 1908 around 70 wind-driven electric generators ranging from 5 kW to 25 kW. Some larger mills were built later on, but due to large scale grid electrification projects all interest for windmills halted in the late 1930's [14].

2.2 Modern Wind Turbines

A wind turbine is by definition a machine that converts wind power into electrical power. Most turbines in use today are of a fairly large size, ranging from 500 Kw and up 4 MW. Most new turbines are also, in order to better utilize the space, constructed in clusters, more commonly known as wind farms.

Modern wind turbines uses the aerodynamic force of lift and converts it into a mechanical torque on a rotating shaft which is transformed into electricity by a generator. The amount of power from a wind turbine highly depends on the wind speed and since the wind is always changing, wind turbines must be treated as fluctuating and non-dispatchable energy sources. Power systems with installed wind power generation must therefore be designed with this factor taken into consideration.

Formula 2.1 shows the produced power as a function of wind speed, wind density and the area covered by the blades. The formula indicate that the produced power increases with the cubic of the wind speed.

$$P_{wind} = \frac{1}{2} C_p \rho_{air} A_{rotor} v_{wind}^3 \tag{2.1}$$

When the wind speed is low there is very little energy in the wind. A wind turbine will therefore not start to produce power until the wind reaches a predefined cut-in speed, normally around 3-5 m/s. As the speed increases and reaches nominal speed, around 12-15 m/s, the power taken out from the wind must be reduced or the wind turbine can be exposed to large forces that eventually will damage the wind turbine.

All commercially available wind turbines today are based on the horizontal axis design and aligned with the wind. The principal subsystem of a modern wind turbine is shown in figure 2.2:

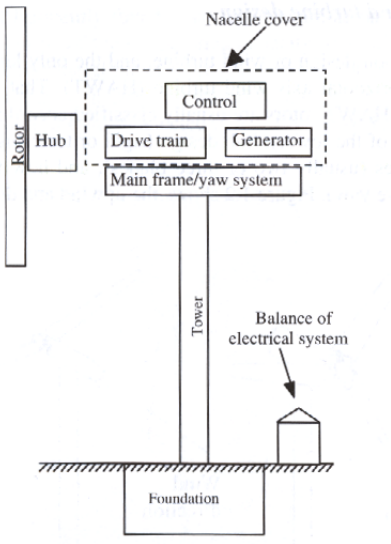

Figure 2.2: Components of a wind turbine

An in-depth explanation of the various components in a wind turbine can be found in the book "Wind energy Explained, Theory, Design and application" [15]

2.3 Wind Resources

Small changes in wind will drastically change the amount of power produced from a wind turbine. It is therefore vital to investigate the wind resources in a area before planning of building a wind farm.

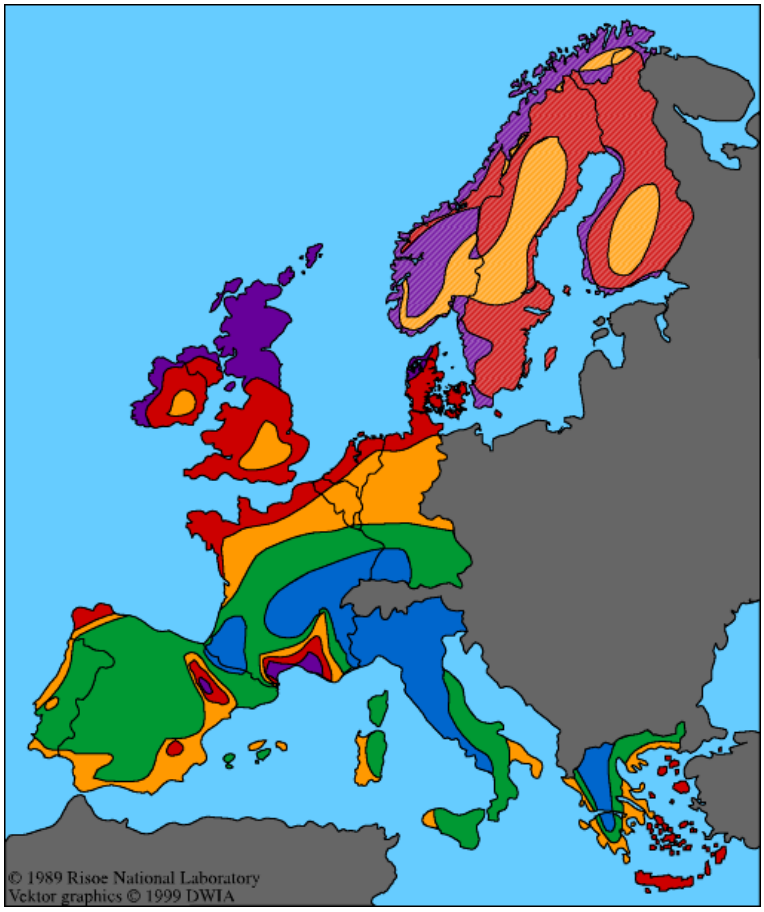

Figure 2.3: European wind map [2]

Figure 2.3 shows the onshore European wind resources at a height of 50 metres. Darker colour indicates stronger wind and it is clear that the United Kingdom and especially the coast of Norway have an exceptional potential for wind power.

2.4 Market overview

Figure 2.4 shows the amount of installed wind power in Europe. Around two-thirds of all the installed capacity is located in Germany and Spain, countries that according to the wind atlas experiences small amounts of wind, while Norway with its huge potential only have 0.005 percentage of the installed capacity in Europe. This implicates that

even though a large amount of wind parks are planned to be erected in Norway, giving an considerable increased installed capacity, there is still potential for much more wind power in the years to come [16].

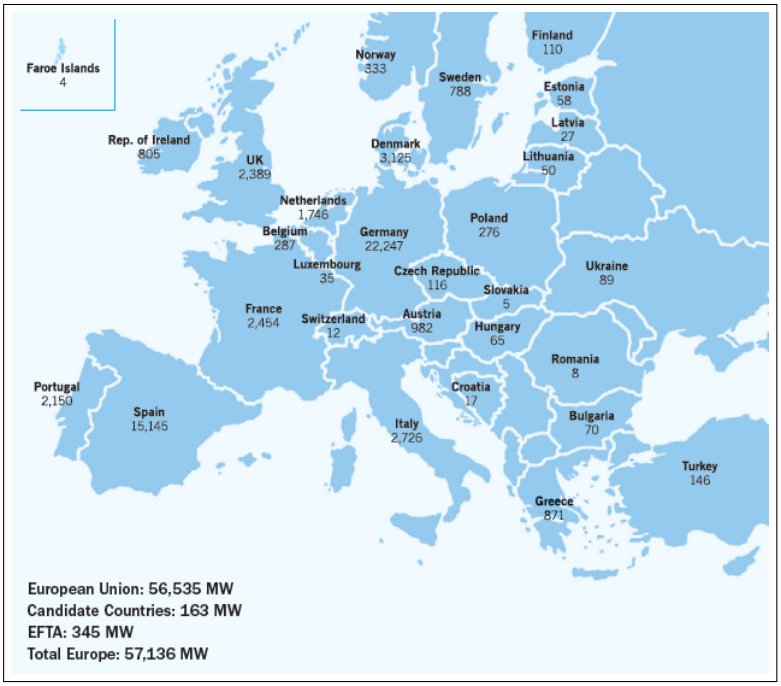

Figure 2.4: Installed wind power in Europe [3]

Chapter 3

Wind Turbine Modelling

This chapter explains the importance of using a model intended for the required application. A general model is explained and models for constant speed wind turbines and variable speed wind turbines are presented

3.1 Introduction

A typical power system consists of many components such as overhead lines, underground cables, transformers, generators and loads. Since most components can be described by differential equations, a large system would need several thousands of differential equations to describe the system. It is therefore necessary to take into account a model's intended application and ensure that the model gives reliable results while not being too complex.

Since the scope of this project is to look into linear stability, it is only necessary to study phenomena occurring in the frequency range of 0.1 Hz and up to 10 Hz. Phenomena with a frequency above or below this range can therefore be neglected because they most likely do not affect the investigated phenomena [5].

3.2 General Model

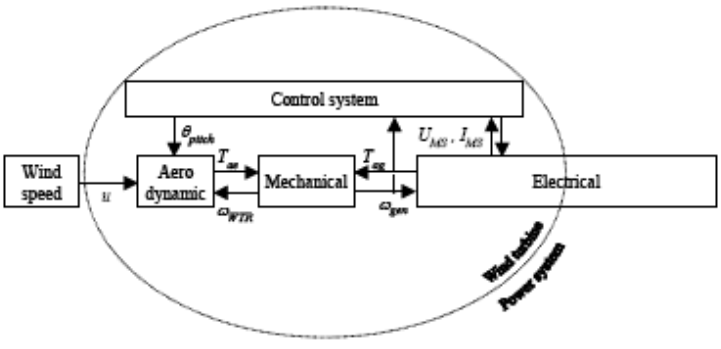

Figure 3.1: General model of a wind turbine [4]

The basic working principle of all wind turbines is, as described in chapter 2, basically the same. It is therefore possible to use a general model of a wind turbine in order to visualize the working principle. The model in figure 3.1 is one example on how such

a model could look like. The wind speed model simulates the wind passing the wind turbine, while the aerodynamic model translates this wind into mechanical power which goes trough the shaft and other mechanical components and into the generator. A more detailed description of the different parts are given in the specialisation project [17]

It is how ever not always sufficient to use a general model to describe all wind turbines and it is often common to divide different wind turbine technologies into two different types:

- Constant speed wind turbines
- Variable speed wind turbines

The constant speed turbine uses a generator directly coupled to the network. This means that the speed of the generator will follow the system frequency and the speed variations will due to the slip in the generator only be around 1 or 2 percents. A variable speed turbine's frequency is on the other hand decoupled from the electrical grid. This allows for variable speed operations since the electrical stator and rotor frequency can be matched independently of the mechanical rotor speed [5]. This differences in working principles necessitate the use of two different model when simulating wind power.

3.3 Constant Speed Wind Turbines

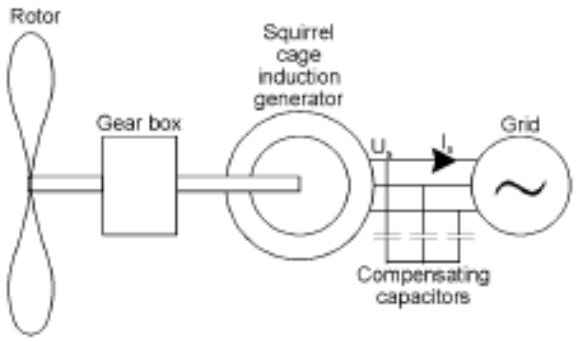

Figure 3.2: Constant speed wind turbine with squirrel cage induction generator [5]

Most constant-speed wind turbines in use today are based on the squirrel-cage induction generator, hereby referred to as SCIG. The Generator is directly coupled to the grid and since the slip and the rotor speed variations are so small the SCIG is described as fixed speed.

SCIG wind turbines normally uses stall control to limit the power from the wind. This means that the blades are constructed in such a way that they start stalling when the wind reaches a predefined value, thereby reducing the lift.

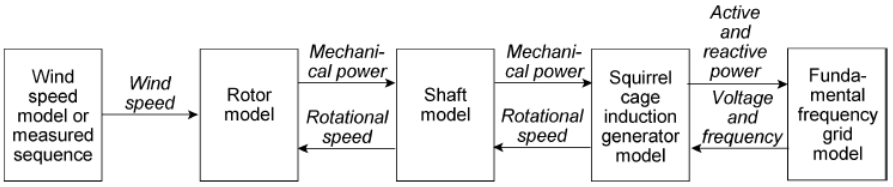

Figure 3.3: General SCIG model [5]

3.3.1 Constant Speed Wind Turbine Modelling

Figure 3.3 shows the general structure of a SCIG wind turbine as presented by [5]. This model includes all the parts necessary to perform a complete analysis of the turbine, including the power system model.

Since the main objective of this thesis is to perform small signal stability studies, which must be performed when the system is at steady state, it is not critical to include the "Wind speed" block. This block is therefore not included in the simulated model. The "Rotor model" is modelled using a turbine where an arbitrary time function $f(t)$ is multiplied with the initial value of the mechanical torque Tm_0 [7]. Since the time function is given as a table it is also possible in a simplified way to simulate wind speeds by changing the amount of torque during the simulation.

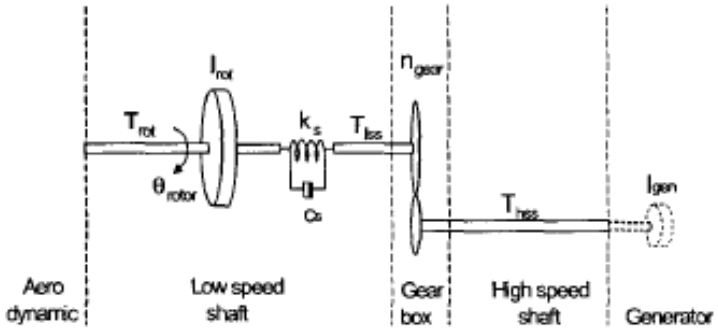

Figure 3.4: Two mass model [6]

Figure 3.4 shows the drive train of a wind turbine. Since the resonance frequency of the high speed shaft and the gearbox are much higher than the bandwidth of interest, only the spring constant of the low speed shaft needs to be modelled [5]. The drive train can therefore be modelled using a two-mass model where the rotor is modelled with an inertia J_{wtr} and generator inertia J_{gen} is implemented in the generator. The torsional spring constant of of the low speed shaft is modelled by the stiffness constant k_s.

The squirrel cage induction generator is modeled according to the parameters used in [4]. They represent the values of a single wind turbine in the wind farm Hagesholm in Eastern Denmark. These values are changed into PU values and aggregated in order to simulate a large wind farm.

A full list of all the wind turbine parameters, calculations for implementation into SIMPOW and the SIMPOW simulation files can be found in appendix B.2

3.4 Variable Speed Wind Turbines

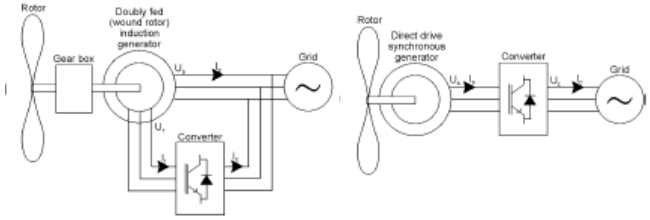

(a) DFIG **(b)** DDSG

Figure 3.5: Variable speed wind turbines. From left: doubly fed induction generator and direct drive synchronous generator [5]

Figure 3.5 illustrates the two main types of variable speed wind turbines on the market. They both use power electronics to decouple the mechanical rotor speed from the electrical frequency, enabling them to change the rotor speed independently of the grid frequency. The DFIG uses a back-to-back converter feeding the three phase rotor winding, while the DDSG uses a full scale converter completely decoupling the generator from the grid [5].

Both solutions have a several advantages and drawbacks. In the DFIG only 30 % of the power passes through the converter while the converter in the DDSG must be of full scale. The DDSG does on the other hand not need a gear box but must use a large, heavy and complex ring generator. A more in-depth explanation on the differences between DFIG and DDSG can be found in [15].

3.4.1 Variable Speed Wind Turbine Modelling

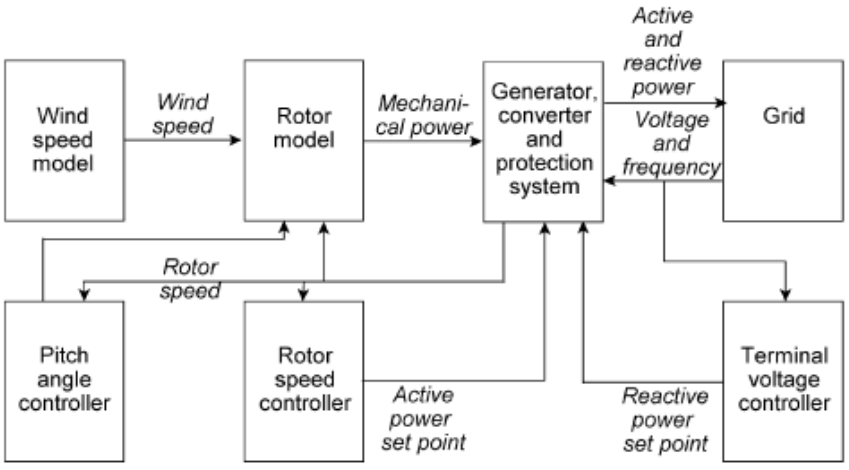

Figure 3.6: General variable speed wind turbine model [5]

A general model for a variable speed wind turbine as presented in [5] is shown in figure 3.6. Simulations performed on both DFIG and DDSG in [5] revealed that there is a high degree of similarity in the simulation results for these technologies. This occurs since only the rotor speed controller and the pitch angle controller governs the frequency

bandwidth of interest. Since these controllers often are similar in both the DFIG and the DDSG, it can be concluded that both types can be represented by the same model in power system dynamics simulations [5].

SIMPOW includes a model of a DFIG wind turbine designed for system analysis of power flow and electromechanical transients. This models have all the components necessary to perform a full analysis of a variable wind turbine and has therefore been used in this thesis to simulate a variable speed wind turbine.

The model in SIMPOW consists of six modules as shown in figure 3.7. The explanations on this model is mainly from [7] and [18].

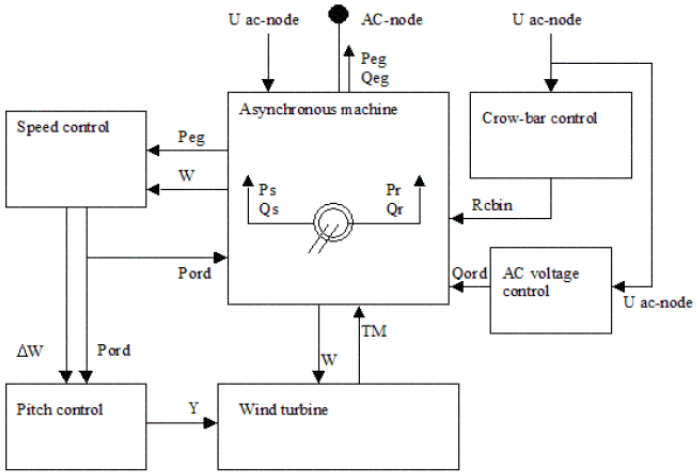

Figure 3.7: Block diagram of DFIG model [7]

The asynchronous machine model consists of a wound rotor induction generator. The rotor uses slip rings for the external rotor circuit where an simplified loss-less frequency converter modelled as a voltage source is placed. The frequency converter transfers during negative slip, real power from the rotor to the grid and real power from the grid to rotor during positive slip.

The inertia of the DFIG wind turbine is modelled as one rotating mass placed in the generator. This can be done since the controllers of the turbine will minimize the effects of the turbine shaft and it is therefore not necessary to use a two mass model [5].

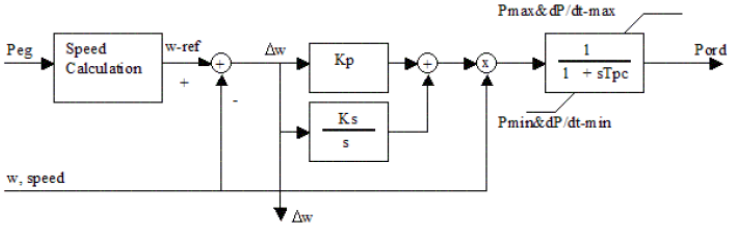

Figure 3.8: The speed control [7]

The speed control is used to control the rotational speed and generated real power. A speed reference (W_{ref}) is found by using the real power generation in the formula:

$$W_{ref} = A_2 P_{eg}^2 + A_1 P_{eg} + A_0 \tag{3.1}$$

Where A_0, A_1 and A_2 are coefficients defined in such a way that optimal wind power is captured (see appendix B.1).

When the optimal speed reference is obtained, the difference between the reference and real speed is calculated and sent through a PI-controller and multiplied with the real speed. This gives the Power order P_{ord}, which is sent trough a filter and back to the generator. The power order now ensures that the generator's rotational speed is optimal compared to the wind speed. The control range of the speed is about $+/-0.25-0.30pu$.

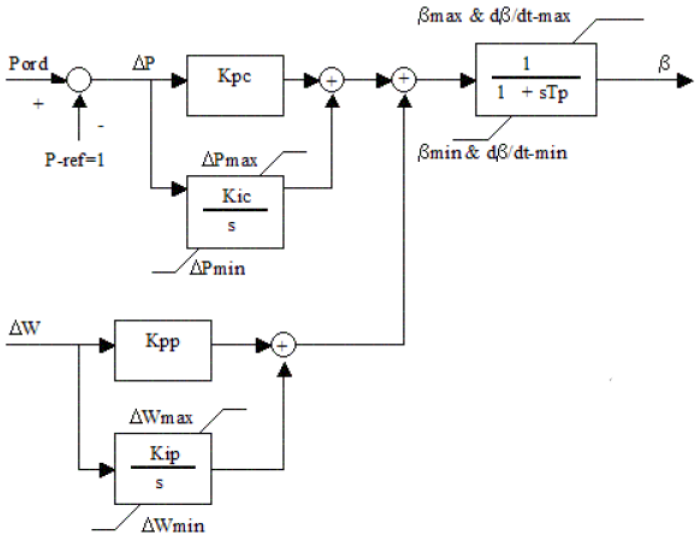

Figure 3.9: The pitch control [7]

All variable wind turbines uses a form of pitch control in order to reduce the force of power obtained from the wind. This ensures that the wind turbine can be safely operated even though the wind speed exceeds the wind needed to obtain rated generator power. Figure 7.5 in section 7.1.2 shows how the wind turbine starts to pitch the blades as the wind speed increases in order to keep the power output constant.

The pitch control uses the power order (P_{ord}) obtained from the speed control and compares it with the speed deviation (ΔW) which is also from the speed control. The sum of these outputs gives the optimum blade angle for the turbine. The blade angle (β) is then filtered to ensure that it does not exceed the maximum or minimum blade angle of the wind turbine.

If a fault appears on the line resulting in a large voltage change on the wind turbine terminals, it is vital that the frequency converter is quickly disconnected to prevent it from failure. If such a fault should appear the Crow-bar resistor control will measure the node voltage and if the voltage is found to be outside the boundaries, the frequency converter will be disconnected and the external rotor circuit will be connected to a crow-bar resistor.

When the DFIG is set to control the voltage at the node, this is ensured by changing

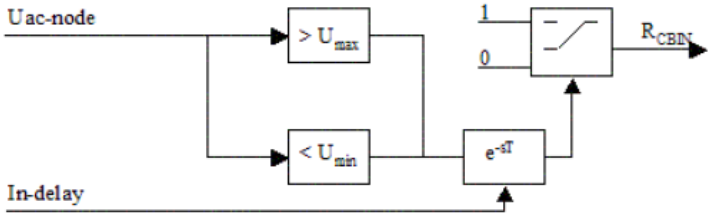

Figure 3.10: The crow-bar resistor control [7]

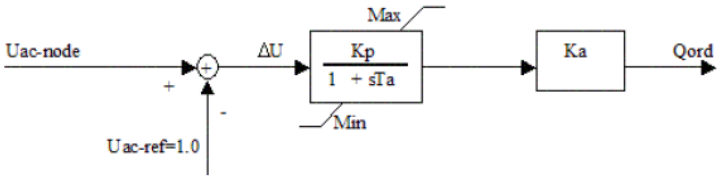

Figure 3.11: The AC bus control [7]

the amount of reactive power produced or consumed by the generator. The AC voltage control regulator does this by measuring the node voltage and comparing it with a reference voltage ($V_{ac,ref} = 1.0pu$). If the measured voltage is below or above the reference, a reactive power order (Q_{ord}) is sent to the generator, making it produce or consume reactive power

SIMPOW uses as default a DFIG with a rated size of $S_n = 2.05MVA$. The model used in the simulation is much larger and it is important to ensure that the ratio between nominal power, blade length and turbine speed remains the same. The aggregation of the DFIG wind turbine and the complete SIMPOW files can be found in appendix B.1.

Chapter 4

Power Oscillations

This chapter explains the nature of power oscillations, why they occur, and how they can be mitigated. A quick look at wind power versus power system oscillations is presented.

4.1 Introduction

Power systems contain many modes of oscillation due to a variety of interactions among components. Most of these oscillations originate from generators swinging relative to one another. The modes involving these masses most often occur in the frequency range of 0.1 to 2 Hz [19] and can cause the oscillation of other power system variables (bus, voltages, bus frequency, transmission lines, active and reactive power, etc).

Oscillations in the 1 to 2 Hz range are most often a result of a single generator or a group of generators oscillating against the rest of the system. These oscillations are most often referred to as "local-area oscillations" . Oscillations occuring in the 0.1 to 0.5 Hz range are referred to as "inter-area oscillations", and involve groups of generators in one area oscillating against generators in another area. These oscillations are particularly troublesome and can in some cases constrain system operation.

Power system oscillations can be stimulated trough a number of mechanisms. Oscillations may be triggered trough a disturbance on the power system, or by crossing some steady-state stability boundaries. Undamped oscillations can, once started, grow in magnitude over a few seconds and lead to the loss of synchronism, loss of part or losses of all electrical network. Network outage can also occur if the oscillations are strong and persistent enough to cause uncoordinated automatic disconnection of key generators or loads.

The two most common reasons for instability is:

- Steady increase in generator rotor angle due to lack of synchronizing torque.
- Rotor oscillations of increasing amplitude due to lack of sufficient damping torque.

Small signal stability or steady state stability is the systems ability to maintain synchronism during small disturbances, or as given by IEEE [20]:

> *A power system is steady-state stable for a particular steady-state operating condition if, following any small disturbance, it reaches a steady-state operating condition which is identical or close to the pre-disturbance operating condition. This is also known as Small Disturbance Stability of a Power System*

The disturbances must be so small that the equations describing the dynamics of the power system can be linearized for the purpose of analysis. This is further explained in chapter 5.

4.2 Historical perspective

Oscillations between generators have appeared since the first ac-generators where operated in parallel. These oscillations where expected due to synchronous generators power vs. phase-angle curve gradient, forming an equivalent mass and spring system. Varying load of the generators would therefore continually trigger the oscillations.

Power system oscillations were for a long time not regarded as a problem and most analytical tools seemed to ignore damping entirely. This changed rather suddenly in the 1960's when an increasing number of networks, were interconnected, and more negative damping was introduced by the increasing use of high responsive generator voltage regulators. The increasing complexity of the power systems and tie-lines of limited capacity led to the reappearance of power system oscillations.

4.3 Types of Power System Oscillations

Power system oscillations can in general be divided into four types:

- Local plant mode oscillations
- Inter-area mode oscillations
- Torsional mode oscillations
- Control mode oscillations

Local plant mode oscillations are the most common oscillations and are associated with the swinging of units at a generating station against the rest of the power system. These oscillations normally occur in the range of 1 to 2 Hz.

Inter-area mode oscillations are associated with the swinging of a group of machines in one part of the system against groups of machines in other parts of the system. They are caused by two or more groups of machines being interconnected by weak tie-lines. These oscillations normally occur in the range of 0.1 to 1 Hz and are normally the oscillations which present the greatest challenge.

Torsional mode oscillations comes from the turbine-generator rotational components and can lead to instability due to interactions with the generating units and prime mover control.

Control mode oscillations are associated with the control of generating units and other equipment and are normally caused by poorly tuned controls of excitation systems, prime movers, static var compensators and HVDC converters.

Figure 4.1 shows an inter-area oscillations between two areas. The generators in each area are in phase with each other and in anti-phase with the generators in the another area.

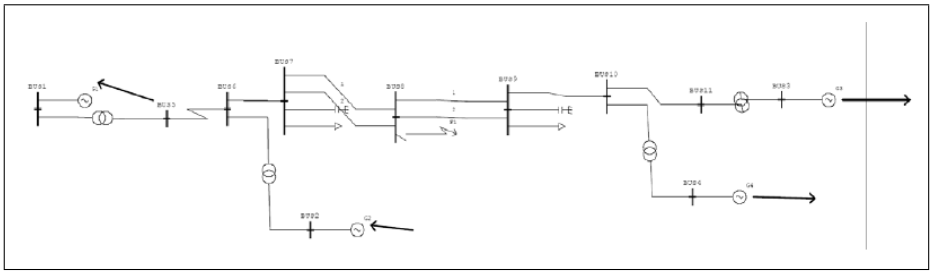

Figure 4.1: Inter-area oscillation [8]

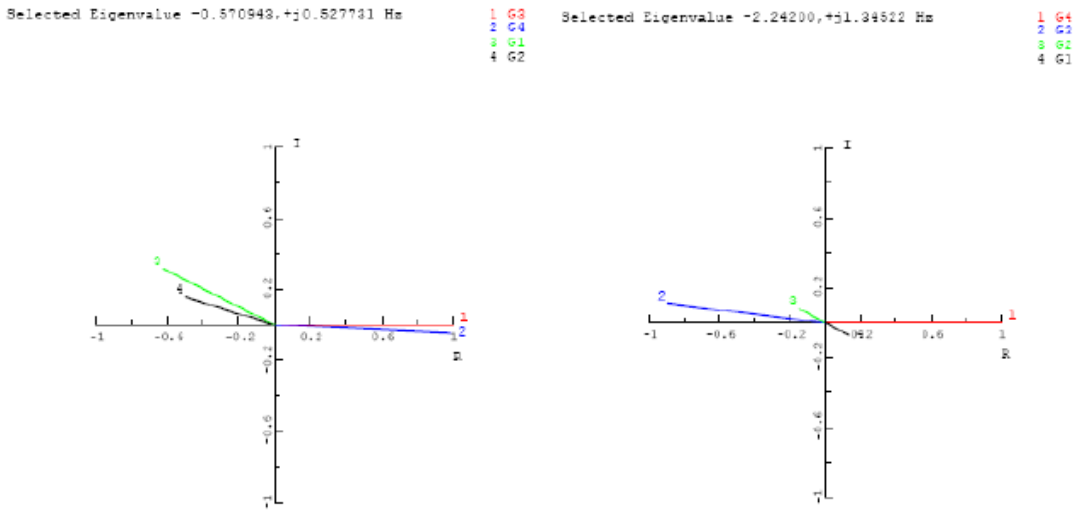

(a) Inter-area **(b)** Local-area

Figure 4.2: Inter-area and local-area oscillations [8]

The left picture figure in 4.2 shows the same inter-area oscillation as in figure 4.1. The picture in the right side show a local-area oscillation where the two generators in area 1 are oscillating against each other

4.4 Reasons for Power System Oscillations

Power system oscillations are as previous mentioned, normally a result of the power vs. phase-angle characteristic in synchronous generators, but the damping can be improved or worsen by many different factors. When only a few generators are paralleled in a closely connected system, oscillations are damped by the generators damper windings and only small variations in system voltage can occur. The generators voltage regulators will therefore not participate in the activity, and increasing the regulators' response will not decrease the system damping, but only improve the transient stability.

If this system is now connected to a similar system by a tie-line with only a fraction of the system capacity, this would due to the tie-line's high impedance, greatly reduce the damper positive damping. The generators' terminal voltage will become more responsive to angular swings and cause the regulators to react, thereby producing negative damping.

Tie-line oscillations are likely to occur, which can lead to transfer restriction on the tie-line.

4.5 Wind Power and Power System Oscillations

Since the mechanical parts of a synchronous machine have low damping of low oscillations the damping must come from other sources, such as the damper windings, the machine's controllers and other parts of the power system. But the very low frequency of the power system oscillations are hardly damped by the damper windings, thus leaving the controllers and the rest of the system as the main contributors to the damping of the rotor speed oscillations. Most wind turbines however, including the models used in this thesis, uses an asynchronous generator which in contrast to the synchronous generator does not show oscillatory behaviour since the generator have a correlation between rotor slip and electrical torque. The mechanical part is therefore of first order and does not oscillate. The generator used in variable speed wind turbines such as the DFIG, is decoupled from the power system by power electronic converters. The generator does therefore not react to any oscillations in the power system as they are not transferred trough the converter [5].

Chapter 5

Modal Analysis

Modal analysis is a powerful and helpful tool in order to locate and mitigate power system oscillations. Modal analysis assumes a linearized model of the system in a state space form. This chapter explains the linearization of a system and presents the modal analysis methods used by most simulations software.

5.1 Introduction

Analyzing power system oscillations require a combination of analytical tools. Oscillations are often observed in transient non-linear simulations and a complete understanding of the system will therefore require programs both for linear analysis and for non-linear analysis.

Programs capable of analyzing power system oscillations have historically been, due to the mathematical nature of the techniques required, restricted to fairly small networks. The recent years development of mathematical tools for analyzing the oscillatory behaviour of power systems have led to a large number of commercially available tools, capable of both linear and non-linear simulations.

5.2 Modal Analysis

Modal analysis is used to find the nature of the oscillations and it is a very useful tool to determine the characteristic modes of a system linearized around a specific operating point. By applying modal analysing to a power system it is possible to locate the devices participating in the oscillations and use this information to do the required action in order to solve the problem.

Models of power systems uses non-linear algebraic differential equations to represent the components. When using modal analysis, these equations are linearized about an operating point by the use of Taylor series expansion. This sections describes the mathematical methods used in power system modal analysis.

5.2.1 State-Space Model

A state-space model is in many ways just a defined way to write a system's differential equations. The variables used in the state-space model amount to the system's state variables. The state variables of the dynamic system can be physical quantities such as

angle, speed or differential equations describing the dynamics of the system. Together with the inputs to the system, the state variables give a complete description of the system behaviour.

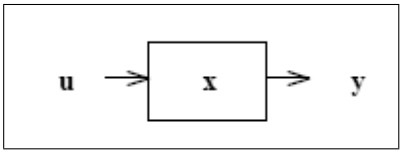

Figure 5.1: Dynamic system [9]

Figure 5.1 shows a dynamic system with its input vector u, output vector y and the state vector x, containing the state variables of the dynamic system.

When given a non-linear continuous time dynamic system, one equation is used to determine the state of the system and another equation to determine the output of the system.

The equation describing the state of the system will then have the form [21]:

$$\dot{x} = f(x, u) \tag{5.1}$$

$$x = \begin{pmatrix} x_1 \\ x_2 \\ \vdots \\ x_n \end{pmatrix} u = \begin{pmatrix} u_1 \\ u_2 \\ \vdots \\ u_n \end{pmatrix} f = \begin{pmatrix} f_1 \\ f_2 \\ \vdots \\ f_n \end{pmatrix} \tag{5.2}$$

The equation describing the system's output will have the form:

$$y = g(x, u) \tag{5.3}$$

$$y = \begin{pmatrix} y_1 \\ y_2 \\ \vdots \\ y_m \end{pmatrix} g = \begin{pmatrix} g_1 \\ g_2 \\ \vdots \\ g_m \end{pmatrix} \tag{5.4}$$

5.2.2 Linearization

Linearization is a useful tool when studying a systems behaviour around an operating point. Linear equations can be used to describe the new system, assuming that all deviations are small. The non-linear system can then be made into a linear system, since linear equations are sufficient to describe the system.

Linearization methods can generally be classified into three groups [22]:

- System identification

- Numerical linearization
- Analytical linearization

System identification measures or simulates the response of non-linear systems to change of inputs. A suitable model is selected and parameter identification techniques are used to obtain parameters for the linear system. System identification methods are rarely used for linearization of power system components models.

Numerical linearization measures the response of the system by calculating deviation of state derivatives after a small change has been applied to the inputs and the states. This enables the calculation of the states space matrices by the use of difference equations:

$$A_{ij} = \frac{\Delta f_i}{\Delta x_j} = \frac{f_i(x_\delta u_0) - f_i(x_0, u_0)}{x_{\delta,j} - x_{0,j}} \tag{5.5}$$

where subscript δ is used for vector with changed j^{th} and subscript δ, j is used for the value of that specific component.

This method is widely used in power systems, such as PSS/E. It is quick and simple, but can only provide an approximation of the precise analytical solution. It is also necessary to repeat the linearization procedure each time the operating point changes.

Analytical linearization is based on analytical computation of system Jacobians. Analytical linearization is very precise and when the operation point changes, new matrices are easily obtained by substituting the new operating points in the Jacobians.

The simulation software used in this thesis, SIMPOW, uses analytical linearization where all differential equations are linearized by their analytical expressions [23]. The eigenvalues of matrix A is then solved using the QR-method, which is further explained in section 5.3.1.

5.2.3 Principles of Linearization

By applying a small disturbance in both the state vector and the input vector the new state of the system presented in section 5.2.1 can be written as:

$$\dot{x} = \dot{x_0} + \Delta\dot{x} = f[(x_0 + \Delta x), (u_0 + \Delta u)] \tag{5.6}$$

Formula 5.1 can now, by using Taylor series expansion, and neglecting second and higher order terms, be written in linearized form, also known as the state space equation:

$$\Delta\dot{x} = A\Delta x + B\Delta u \tag{5.7}$$

$$A = \begin{pmatrix} \frac{\partial f_1}{\partial x_1} & \cdots & \frac{\partial f_1}{\partial x_n} \\ \cdots & \cdots & \cdots \\ \frac{\partial f_n}{\partial x_1} & \cdots & \frac{\partial f_n}{\partial x_n} \end{pmatrix} B = \begin{pmatrix} \frac{\partial f_1}{\partial u_1} & \cdots & \frac{\partial f_1}{\partial u_r} \\ \cdots & \cdots & \cdots \\ \frac{\partial f_n}{\partial u_1} & \cdots & \frac{\partial f_n}{\partial u_r} \end{pmatrix} \tag{5.8}$$

Matrix A is the system matrix, and relates to how the current state affects the state change. Matrix B is the control matrix, and determines how the system input affects the state change [10].

The linearized form of the output equation 5.3 is written as:

$$\Delta y = C\Delta x + D\Delta u \tag{5.9}$$

$$C = \begin{pmatrix} \frac{\partial g_1}{\partial x_1} & \cdots & \frac{\partial g_1}{\partial x_n} \\ \cdots & \cdots & \cdots \\ \frac{\partial g_m}{\partial x_1} & \cdots & \frac{\partial g_m}{\partial x_n} \end{pmatrix} D = \begin{pmatrix} \frac{\partial g_1}{\partial u_1} & \cdots & \frac{\partial g_1}{\partial u_r} \\ \cdots & \cdots & \cdots \\ \frac{\partial g_m}{\partial u_1} & \cdots & \frac{\partial g_m}{\partial u_r} \end{pmatrix} \tag{5.10}$$

Matrix C is the output matrix, and determines the relationship between the system state and the system output. Matrix D is the feed-forward matrix, and allows for the system input to affect the system output directly [10].

A more comprehensive deduction of the linearization process can be found in [24] and [17].

5.2.4 Eigenvalues

A power systems eigenvalues are important for determining the systems response. Each eigenvalue describe one special dynamic behavior of the system called a mode. This mode is calculated based on the A matrix.

The eigenvalues of the system determines the relationship between the individual system state variables, the response of the system to inputs, and the stability of the system. Eigenvalues consist of a real and an imaginary part. The real part tells about the swing of the mode and the imaginary part tells about the oscillating frequency of the mode [25].

Eigenvalues with no imaginary part i.e. real eigenvalues, indicate modes which are aperiodic. Eigenvalues with an imaginary part i.e. complex eigenvalues, indicate modes which are oscillatory.

A power system is stable if the real parts of all the eigenvalues are negative. If any one of the eigenvalues has a positive real part, a small disturbance would lead to exponentially increase of a modes oscillations. The power system is then said to be unstable.

The eigenvalues of the A matrix are given by the values of the scalar parameter λ as written in the non-trivial solution:

$$det(A - \lambda I) = 0 \tag{5.11}$$

A complex pair of eigenvalues can then be written as:

$$\lambda = \sigma \pm j\omega \tag{5.12}$$

Where σ represents the real component of the eigenvalue, giving the damping of the oscillation. A negative σ indicates a damped oscillation while a positive σ indicates an oscillation with increasing amplitude. The real component tells how much time it takes before the amplitude of the oscillation reaches 37%. The imaginary part, ω, is the oscillation's frequency where the real frequency is given by the formula [24]:

$$f = \frac{\omega}{2\pi} \tag{5.13}$$

A complete deduction of the eigenvalue calculation can be found in the specialisation project [17].

To better visualize an eigenvalue, it is often useful to place it in the complex plane . A damped eigenvalue with $\sigma < 0$ will then be located in the open left half of the complex plane. Eigenvalues in the left-half plane are called stable eigenvalues.

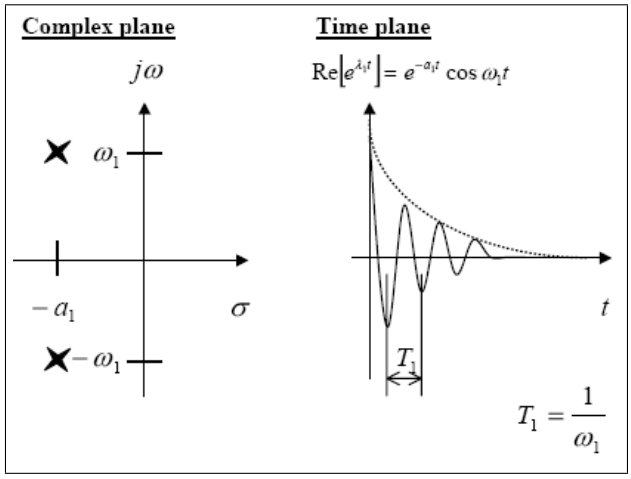

Figure 5.2: An Eigenvalue in the complex plane and the time plane [9]

The left side in Figure 5.2 shows an stable eigenvalue in the complex plane. The eigenvalue is non-real-valued meaning that it has both damping and oscillation. The right side shows the eigenvalue in the time plane. The frequency of the oscillation is ω_1 and the period of the oscillation is T_1.

5.2.5 Damping Ratio

Since oscillatory modes can have a wide range of frequencies it is often more appropriate to use the damping ratio in order to express the degree of damping.

For an oscillatory mode with a complex eigenvalue $\lambda = \sigma \pm j\omega$, the damping ratio is given by :

$$\zeta = \frac{-\sigma}{\sqrt{(\sigma)^2 + (\omega)^2}} \tag{5.14}$$

The minimum acceptable damping ratio is system dependent and must be based on operation experience and sensitivity analysis. Experiences at the Ontario's Hydro power plant however, has shown that a damping ratio of less than 3% must be accepted with caution [19]

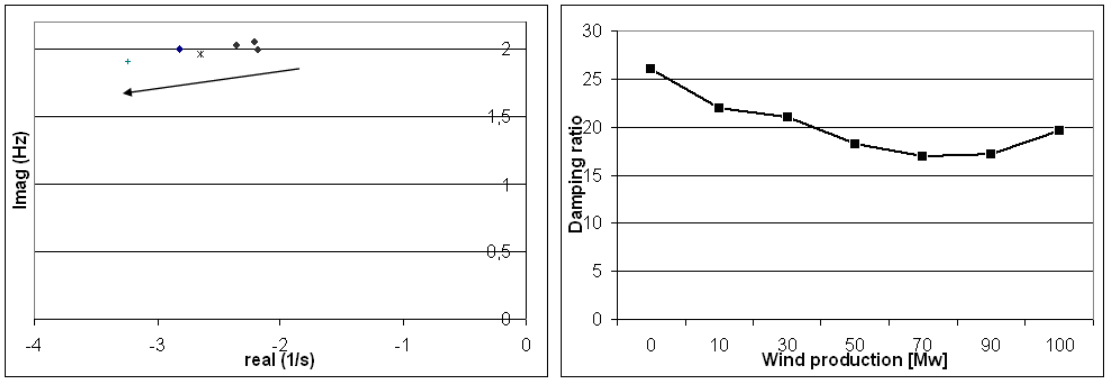

(a) Complex plane **(b)** Damping ratio

Figure 5.3: Eigenvalues in complex plane and with damping ratio

Figure 5.3 shows an example of how eigenvalues can be presented. Both pictures are taken from the same simulation where a wind turbine's productions is increased from 0 MW up to 100 MW. This leads to a change in the oscillatory modes of the power system. The left figure illustrates this by plotting the eigenvalues in the complex plane and the right picture plots the same eigenvalues by using the damping ratio.

5.2.6 Eigenvectors

Eigenvectors are a special set of vectors associated with a linear system of equations. Determining the eigenvectors is important in physics and engineering in order to analyze small oscillations in vibrating systems or stability analysis. Each eigenvector is paired with its corresponding eigenvalue and there are two types of eigenvectors, right eigenvector and left eigenvector [26]. The right eigenvector define the relative distribution of the mode throughout the system's dynamic states. It measures the activity of the state variables to an eigenvalue. The left eigenvector weights the contribution of the activity of the state variable to an eigenvalue. It gives the distribution of the states within a mode. It is for most problems sufficient to only consider the right eigenvector. The term "eigenvector" used without qualification in such applications can therefore be understood to refer to the right eigenvector [24].

The right eigenvector X_R has the form:

$$X_R = \begin{pmatrix} X_{R1} \\ X_{R2} \\ \vdots \\ X_{Rn} \end{pmatrix} \tag{5.15}$$

The left eigenvector X_L has the form:

$$X_L = \begin{pmatrix} X_{L1} & X_{L2} & \dots & X_{Ln} \end{pmatrix} \tag{5.16}$$

The eigenvectors can be normalized so that the product of the them are:

$$X_R X_L = 1 \tag{5.17}$$

While the product of eigenvectors belonging to different eigenvalues will always be 0.

$$X_{Ri} X_{Li} = 0 \tag{5.18}$$

5.2.7 Participation Factors

Using right and left eigenvectors to identify the relationship between a state and a mode can be a problem since the elements of the eigenvectors are dependent on units and scaling associated with the state variables. To solve this problem a matrix called the participation matrix which combines the right and the left eigenvectors, can be used to measure the association between the state variables and the nodes [24]. The participation matrix indicates better than the eigenvectors the effect of a physical component in a system to a mode. Participation factors can by looking at generators speed participations, indicate which generators in the power system that is most suitable for power system stabilizer placement.

$$P_i = \begin{pmatrix} P_{1i} \\ P_{2i} \\ \vdots \\ P_{ni} \end{pmatrix} = \begin{pmatrix} X_{R1i} X_{Ri1} \\ X_{R2i} X_{Ri2} \\ \vdots \\ X_{Rni} X_{Rin} \end{pmatrix} \tag{5.19}$$

or written in general form:

$$P_{ki} = X_{Rki} X_{Lik} \tag{5.20}$$

This formula shows how one state variable contributes to one eigenvalue. This can further be used in small signal stability analysis in order to locate the source of a poorly damped eigenvalue.

5.2.8 Block Diagram Representation

By laplace transforming equation 5.7 and 5.9 the following equations are obtained in the frequency domain [24]:

$$s\Delta x(s) - \Delta x(0) = A\Delta x(s) + B\Delta u(s) \tag{5.21}$$

$$s\Delta y(s) = C\Delta x(s) + D\Delta u(s) \tag{5.22}$$

It is now based on the equations in the frequency domain possible to draw a power systems linearized block diagram, this is shown in figure 5.4

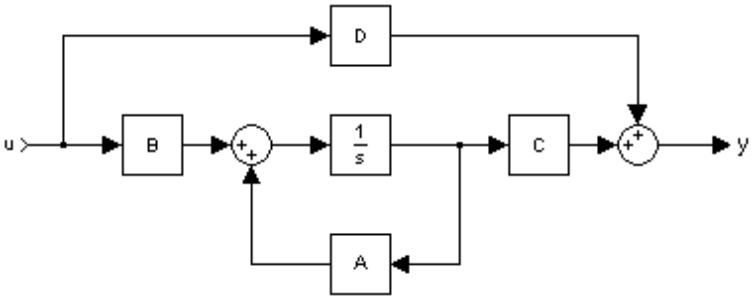

Figure 5.4: Block diagram representation [10]

5.2.9 Transfer Function

Transfer function representation are in contrast to the state-space representation only concerned with the input/output behaviour of the system. It is therefore possible to randomly choose state variables when a system is only specified with a transfer function and the spate-space representation is therefore in many ways a more complete description of the system.

Eigenvalue analysis of the state matrix (matrix A) is normally the best way to perform eigenvalue analysis. But since modal analysis is often done in order to construct better control designs, it is often useful to see how the open-loop transfer function is related to the state matrix and the eigenvalues.

The transfer function has the general form:

$$G(s) = K\frac{N(s)}{D(s)} \tag{5.23}$$

By applying the method used in [24] it can be shown that $G(s)$ may be written as.

$$G(s) = \sum_{i=1}^{n} \frac{R_i}{s - \lambda_i} \tag{5.24}$$

where

$$R_i = cX_{Ri}X_{Li}b \tag{5.25}$$

Equation 5.24 now shows that the poles of $G(s)$ is given by the eigenvalues of matrix A.

5.3 Methods for Modal Analysis

Since an adequate model for small signal stability must include detailed information about the power system, it is not uncommon to have power system of an order of several thousands states. The eigenvalue analysis presented in the previous section would therefore require an enormous amount of computer power and such calculations are therefore limited to small-sized power system. In order to enable modal analysis of larger systems several methods have been developed [27]. This methods are further explained in this section.

5.3.1 Analysis of Small Size Power Systems

The QR-method is a widely used method to determine the eigenvalues of a matrix. This is done by applying a set of transformations to the A matrix in order to construct another matrix, say Q. Real eigenvalues will appear as diagonal elements in Q and complex eigenvalues will appear as a block diagonal 2x2 elements. When the eigenvectors of the Q matrix are found, the eigenvectors of the original matrix can be found by reversing the transformations or by inverse iteration .

Most power system analysis program's are due to computer limitations restricted to about 800 modes when using the QR method. This means that only around 80 generators can be modelled. But using the QR-method will reveal all the systems eigenvalues and eigenvectors, and it is therefore the preferred method to use if the system falls within the limitations [19].

5.3.2 Analysis of Large Size Power Systems

When a power system is to large to be analyzed using a full modal analysis, it is necessary to use partial modal analysis. Partial modal analysis virtually removes the size limitations for modal analysis of power systems. The only remaining limits are the programs capabilities and the availability of data.

The first algorithm using this technique was the AESOPS [19]. This algorithm used the quasi-Newton method iteration to find system eigenvalues close to the defined starting value and was capable of handling up to about 2000 states. The algorithm has now been replaced by other more efficient methods such as:

- Inverse iteration and generalized Rayleigh Quotient iteration
- Modified Arnoldi
- Simultaneous inverse iteration

All this methods are quite similar and they all uses repetitive multiplication of a vector by the state matrix A.

Selective modal analysis on the other hand is a complete different method that only focuses on the relevant eigenvalues in a specific area. The method avoids having to deal with the large system matrix and can therefore greatly reduce storage and computer requirements [27].

Chapter 6

Practical use of Modal Analysis

This chapter evaluates the modal analysis technique by linearization a small power system with a synchronous generator. A MATLAB program capable of testing the systems eigenvalues, damping factors and participation factors when the network parameters are altered is presented.

6.1 Linearization of a Synchronous Generator

A synchronous generator connected to an infinite bus through a line is used to illustrate the possibilities of small-signal stability studies.

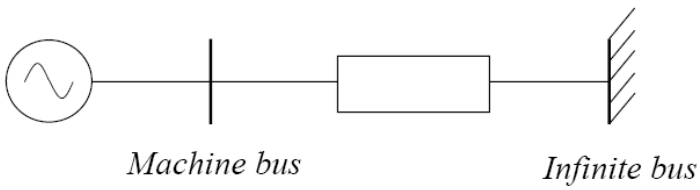

Figure 6.1: SMIB system [11]

Figure 6.1 shows the single machine infinite bus system. Since the system is simple, it allows linearization of formulas to be performed in an understandable way.

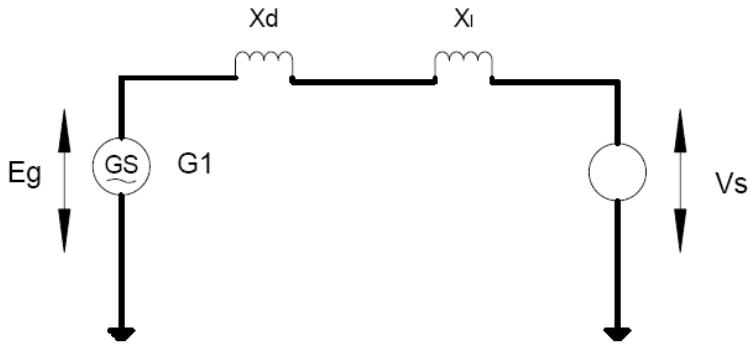

Figure 6.2: Equivalent circuit in the sub-transient state

The equivalent circuit of figure 6.1 is shown in figure 6.2. The generator is modelled as a constant voltage source behind a reactance (X_d) and the line is modelled as a pure reactance.

The real power produced by a generator with a salient-pole rotor ($x_d \neq x_q$) calculated with pu units is as given by [12]:

$$T_e = P_e = \frac{E_q\, V_s}{x_d} \sin\delta + \frac{V_s^2}{2} \frac{x_d - x_q}{x_q x_d} \sin 2\delta \tag{6.1}$$

When the generator uses a round rotor ($x_d = x_q$) or a classic presentation is used, formula 6.1 can be simplified to:

$$T_e = P_e = \frac{E_q\, V_s}{x_d} \sin\delta \tag{6.2}$$

where $x_d = X_d + X_l$ and $x_q = X_q + X_l$

Most of a generators damping effect comes from the damper windings . If the rotor speed is different from the system frequency an emf and a current will be induced. This will produce a damping torque which will try to restore the synchronous speed of the rotor. The effect of the damper winding must therefore be included in stability analysis [12].

Figure 6.3 shows an equivalent circuit of a synchronous machine where the damping windings are given as X_D

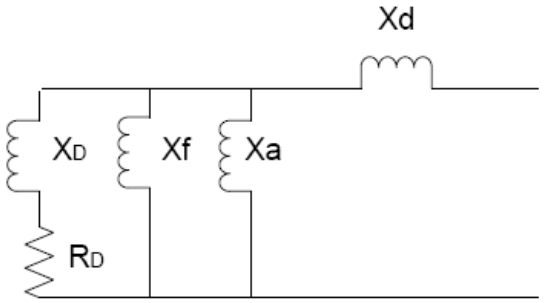

Figure 6.3: Equivalent circuit of synchronous generator [12]

The damping power can be calculated as described in [12], by using the power angle during steady state operation and the generators values for transient and sub-transient reactance and time constants. The following formula will then describe the damping power of the generator when saliency is disregarded:

$$K_D = V_s^2 \frac{X_d^{'} - X_d^{''}}{(X + X_d^{'})^2} \frac{X_d^{'}}{X_d^{''}} \frac{T_d^{''}\Delta\omega}{1 + (T_d^{''}\Delta\omega)^2} \tag{6.3}$$

By taking saliency into account and replacing the voltage V_s in d and q by applying, $V_d = -V_s * sin\delta$ and $V_q = -V_s * cos\delta$, a similar formula can be derived [12]:

$$K_D = V_s^2 \left(\frac{X_d^{'} - X_d^{''}}{(X + X_d^{'})^2} \frac{X_d^{'}}{X_d^{''}} \frac{T_d^{''} \Delta\omega}{1 + (T_d^{''} \Delta\omega)^2} * \sin^2(\delta) + \frac{X_q^{'} - X_q^{''}}{(X + X_q^{'})^2} \frac{X_q^{'}}{X_q^{''}} \frac{T_q^{''} \Delta\omega}{1 + (T_q^{''} \Delta\omega)^2} * \cos^2(\delta) \right) * \omega_s \tag{6.4}$$

During large speed deviations the damping power is a non-linear function of the speed deviation while it is proportional to the speed deviation when the deviation is small. A small deviation such as $s = \Delta\omega/\omega_s \ll 1$, would therefore allow the term $(T_d^{''}\Delta\omega)^2$ in the denominator of formula 6.4 to be neglected. The formula can then be simplified to:

$$K_D = V_s^2 \left(\frac{X_d^{'} - X_d^{''}}{(X + X_d^{'})^2} \frac{X_d^{'}}{X_d^{''}} T_d^{''} * \sin^2(\delta) + \frac{X_q^{'} - X_q^{''}}{(X + X_q^{'})^2} \frac{X_q^{'}}{X_q^{''}} T_q^{''} * \cos^2(\delta) \right) * \omega_s \tag{6.5}$$

By calculating the close loop and open loop time constants, the relationship will be:

$$T_d^{''} = T_{do}^{''} \frac{X_d, ,}{X_d^{'}} \quad T_q^{''} = T_{qo}^{''} \frac{X_q, ,}{X_q^{'}} \tag{6.6}$$

By applying this to formula 6.5 and since $x_d^{'} = X + X_d^{'}$ and $x_q^{'} = X + X_q^{'}$, the formula can be simplified to:

$$K_D = V_s^2 \left(\frac{X_d^{'} - X_d^{''}}{(x_d^{'})^2} T_{do}^{''} * \sin^2(\delta) + \frac{X_q^{'} - X_q^{''}}{(x_q^{'})^2} T_q^{''} * \cos^2(\delta) \right) * \omega_s \tag{6.7}$$

The damping K_D can now be calculated and used in order to find the systems stability

6.1.1 Swing Equation

The angle between the rotor axis and the magnetic field in a synchronous machine is known as the power angle or torque angle. When a perturbation occurs the rotor will accelerate or decelerate and a relative motion begins. The equation describing this relative motion is known as the swing equation [28].

A change from steady state due to a perturbation will result in a positive or negative torque causing acceleration or deceleration:

$$T_a = T_m - T_e \tag{6.8}$$

when including the moment of inertia , J, and neglecting frictional damping the equation becomes:

$$J \frac{d\omega_m}{dt} = T_a = T_m - T_e \tag{6.9}$$

This equation can be expanded to include the per unit inertia constant H, which is further explained in appendix B.2:

$$J = \frac{2H}{w_{0m}^2} V A_{base} \tag{6.10}$$

and the damping factor K_D in pu torque/pu speed deviation, such that [24]:

$$\frac{2H}{\omega_o}\frac{d^2\delta}{dt^2} = T_m - T_e - K_D\Delta\omega_r \tag{6.11}$$

Formula 6.11 is now the swing equation of a synchronous machine and it represents the swings in rotor angle (δ) during disturbances.

Since the state-space representation requires a set of first order differential equations , formula 6.11 must be expressed as two first order differential equations, which can be written in per unit as:

$$\frac{d\Delta\omega_r}{dt} = \frac{1}{2H}(T_m - T_e - K_D\Delta\omega_r) \tag{6.12}$$

$$\frac{d\delta}{dt} = \omega_o\Delta\omega_r \tag{6.13}$$

6.1.2 Linearization

The swing equations 6.12 and 6.13 are nonlinear functions of the power angle. It is however possible to assume that they may be linearized, with little loss of accuracy, for small disturbances:

By linearizing formula 6.1 around an initial operating point where $\delta = \delta_0$, the formula can be written in linearized form as:

$$\Delta T_e = \frac{\partial T_e}{\partial\delta}\Delta = \left(\frac{E'V_s}{x_d}\cos\delta * \Delta\delta + E_B^2\frac{x_d - x_q}{x_q x_d}\cos(2\delta)\right) * \ \Delta\delta = K_s * \Delta\delta \tag{6.14}$$

and for formula 6.2:

$$\Delta T_e = \frac{\partial T_e}{\partial\delta}\Delta = \frac{E'V_s}{x_d}\cos\delta * \Delta\delta = K_s * \Delta\delta \tag{6.15}$$

K_s in formula 6.14 and 6.15 is referred to as the steady state synchronising power coefficient and describes the generator's pull-out power.

Equation 6.12 and 6.12 can now be linearized to:

$$f_1(\delta,\omega) = \frac{d\Delta\omega_r}{dt} = \frac{d^2\delta}{dt^2} = \frac{1}{2H}(T_m - K_s\Delta\delta - K_D\Delta\omega_r) \tag{6.16}$$

$$f_2(\delta,\omega) = \frac{d\Delta\delta}{dt} = \omega_o\Delta\omega_r \tag{6.17}$$

Using formula 5.8 it is ossible to find the elements in the A and B matrix . Applying the formula to Element A_{11} in the A matrix yields:

$$\begin{aligned}\frac{\partial_1}{\partial x_1} = \frac{\delta}{\Delta\omega_r} = \\ &= \frac{1}{2H}(T_m - K_s\Delta\delta - K_D\Delta\omega_r) \\ &= \frac{1}{2H}(0 - 0 - K_D) \\ &= -\frac{K_D}{2H}\end{aligned} \tag{6.18}$$

And using the same method for the rest of the elements the complete A and B matrix will be:

$$A = \begin{pmatrix} \frac{\partial f_1}{\partial x_1} & \frac{\partial f_1}{\partial x_2} \\ \frac{\partial f_2}{\partial x_1} & \frac{\partial f_2}{\partial x_1} \end{pmatrix} = \begin{pmatrix} -\frac{K_D}{2H} & -\frac{K_S}{2H} \\ \omega_0 & 0 \end{pmatrix} \tag{6.19}$$

$$B = \begin{pmatrix} \frac{\partial f_1}{\partial u_1} \\ \frac{\partial f_2}{\partial u_1} \end{pmatrix} = \begin{pmatrix} \frac{1}{2H} \\ 0 \end{pmatrix} \tag{6.20}$$

Which gives the following state space equation 5.7:

$$\begin{pmatrix} \dot{\Delta\omega_r} \\ \dot{\Delta\delta} \end{pmatrix} = \begin{pmatrix} -\frac{K_D}{2H} & -\frac{K_S}{2H} \\ \omega_0 & 0 \end{pmatrix} \begin{pmatrix} \Delta\omega_r \\ \Delta\delta \end{pmatrix} + \begin{pmatrix} \frac{1}{2H} \\ 0 \end{pmatrix} \Delta T_m \tag{6.21}$$

The eigenvalues for the system can now according to formula 5.12 be:

$$det(\begin{pmatrix} -\frac{K_D}{2H} & -\frac{K_S}{2H} \\ \omega_0 & 0 \end{pmatrix} - \lambda \begin{pmatrix} 1 & 0 \\ 0 & 1 \end{pmatrix}) = 0 \tag{6.22}$$

$$det \begin{pmatrix} -\frac{K_D}{2H} - \lambda & -\frac{K_S}{2H} \\ \omega_0 & 0 - \lambda \end{pmatrix} \tag{6.23}$$

$$-\frac{K_D}{2H} - \lambda(0 - \lambda) + (\frac{-K_S}{2H}\omega_0) = 0 \tag{6.24}$$

$$\frac{K_D}{2H}\lambda + \lambda^2 - \frac{-K_S}{2H}\omega_0 = 0 \tag{6.25}$$

$$\lambda^2 + \frac{K_D}{2H}\lambda - \frac{-K_S}{2H}\omega_0 = 0 \tag{6.26}$$

Since this is a second order equation the eigenvalues (λ) can be found by :

$$\begin{aligned}\lambda_{1,2} &= \frac{-\frac{K_D}{2H} \pm \sqrt{(\frac{K_D}{2H})^2 - 4 * 1 \frac{K_S}{2H}\omega_0}}{2 * 1} = \\ &= -\frac{K_D}{4H} \pm \sqrt{(\frac{K_D}{4H})^2 - \frac{K_S}{2H}\omega_0}\end{aligned} \tag{6.27}$$

The general form of an eigenvalue is:

$$\lambda = \sigma \pm j\omega \tag{6.28}$$

The real component of the eigenvalue also known as the damping σ, and the oscillation of the eigenvalue ω will be:

$$\sigma = -\frac{K_D}{4H} \quad \omega = \sqrt{(\frac{K_D}{4H})^2 - \frac{K_S}{2H}\omega_0} \tag{6.29}$$

And the damping ratio will according to formula 5.14 be:

$$\zeta = \frac{-\sigma}{\sqrt{(\sigma)^2 + (\omega)^2}} \tag{6.30}$$

The right eigenvectors are given by:

$$(A - \lambda I)X_R = 0 \tag{6.31}$$

$$\left(\begin{pmatrix} -\frac{K_D}{2H} & -\frac{K_S}{2H} \\ \omega_0 & 0 \end{pmatrix} - \lambda \begin{pmatrix} 1 & 0 \\ 0 & 1 \end{pmatrix}\right) \begin{pmatrix} X_{R1i} \\ X_{R2i} \end{pmatrix} = 0 \tag{6.32}$$

The left eigenvectors are given by:

$$X_R = X_L^{-1} = \frac{adj(X_L)}{|X_L|} \tag{6.33}$$

The participation matrix can now be found by multiplying the right and left eigenvector for each eigenvalue:

$$P = \begin{pmatrix} P_{1i} \\ P_{2i} \end{pmatrix} = \begin{pmatrix} X_{L11}X_{R11} & X_{L12}X_{R21} \\ X_{L21}X_{R11} & X_{L22}X_{R22} \end{pmatrix} = \begin{pmatrix} P_{11} & P_{12} \\ P_{21} & P_{22} \end{pmatrix} \tag{6.34}$$

The first column of the participation matrix shows how mode 1 involves each state variable. The second column shows how mode 2 involves each state variable [11]

This matrix shows how a participation matrix can be understood:

$$\begin{pmatrix} & \lambda_1 & \lambda_2 \\ \Delta\omega_r: & P_{11} & P_{12} \\ \Delta\delta: & P_{21} & P_{22} \end{pmatrix} \tag{6.35}$$

For each mode λ_1 and λ_2, the participation matrix shows how each state variables, in this case ω_r and δ, is involved

6.2 Small System With Synchronous Generator

Network 1 in section 7.3 is simplified by removing Bus 2 and Bus 4. The line from Bus 5 to Bus 6 is removed and the generator is modelled as a constant voltage behind the transient reactance. The derived formulas in the previous section are used to construct a MATLAB file able to calculate all relevant values for small-signal analysis. The MATLAB code can be found in appendix A.2 and the values for the system including the generator can be found in appendix A.1.

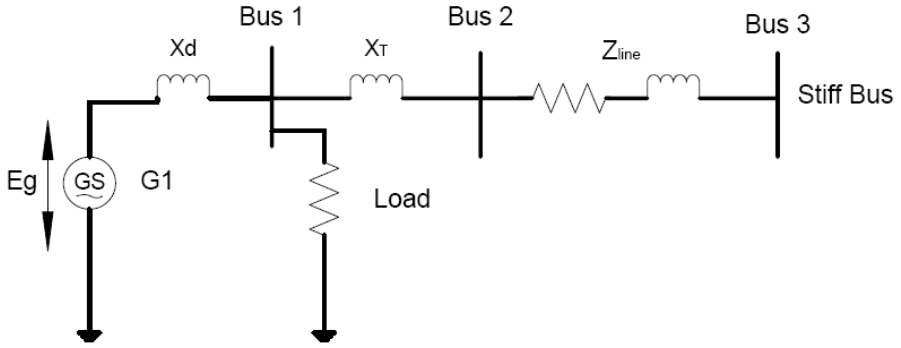

Figure 6.4: Three bus example

6.2.1 Calculations with Initial Values

The values given for the network and the generator are used to calculate the properties of the network. By using the derived formulas all relevant values for small-signal analysis can now be calculated.

The first thing required to find is the Voltage at Bus 1.

The voltage at Bus 1 can be found by adding the voltage at Bus 3 and the line losses:

$$\begin{aligned} V_1 &= V_3 + \Delta V_{line} \\ &= V_3 + I * (X_T + Z_{line}) \end{aligned} \tag{6.36}$$

and the line can current be find with:

$$I_l = \frac{(P_1 + JQ_1)^*}{V_1} \tag{6.37}$$

Combining formula 6.36 and 6.37 and ignoring the line resistance ($X = X_T + X_{line}$) yields:

$$\begin{aligned} V_1 &= V_3 + \frac{(P_1 + JQ_1)^*}{V_1} * X \\ &= V_1^2 - V_3 * V_1 - (P_1 + JQ_1)^* * X \\ &= \frac{V_3 \pm \sqrt{V_3^2 - (4 * 1 * -(P_1 - JQ_1) * X}}{2} \end{aligned} \tag{6.38}$$

And by using the predefined values found in appendix A.1:

$$\begin{aligned} V_1 &= \frac{1.0 \pm \sqrt{1.0^2 + (4 * 1 * (0.5 - J0.1) * J0.35}}{2} \\ &= 1.0565 + J0.157 \\ &= 1.068\angle 8.46 \end{aligned} \tag{6.39}$$

The current trough the line can now be found using formula 6.37:

$$\begin{aligned} I_l &= \frac{(P_1 + JQ_1)^*}{V_1} \\ &= \frac{(0.5 + j0.1)^*}{1.0565 + J0.157} \\ &= 0.45 - J0.161 = 0.477\angle - 19.76 \end{aligned} \tag{6.40}$$

and for the local load

$$I_l = \frac{P_1}{V_1} = \frac{0.5}{1.068} = 0.467 \tag{6.41}$$

The total current from the generator will then be

$$\begin{aligned} I_{tot} &= I_{load} + I_{line} \\ &= 0.467 + 0.45 - J0.161 \\ &= 0.918 - J0.161 = 0.933\angle - 9.947 \end{aligned} \tag{6.42}$$

The transient voltage behind the transient reactance:

$$\begin{aligned} E_g^{'} &= V_1 + JX_d^{'} * I_{tot} \\ &= 1.0565 + J0.157 + J0.3 * (0.918 - J0.161) \\ &= 1.1050 + 0.4324i = 1.187\angle 21.36 \end{aligned} \tag{6.43}$$

Since the generator is using a salient rotor ($x_d \neq x_q$) formula 6.14 must be used to find the synchronizing torque coefficient ,K_s:

$$\begin{aligned} K_s &= \left(\frac{E^{'} V_s}{x_d} \cos\delta * \Delta\delta + V_s^2 \frac{x_d - x_q}{x_q x_d} \cos(2\delta) \right) \\ &= \frac{1.1050 + 0.4324i * 1.0 + 0i}{0.65} * \cos 21.37 + 1.0^2 \ \frac{0.65 - 0.90}{0.65 * 0.90} * cos(2 * 21.37) \\ &= 1.3861 \end{aligned} \tag{6.44}$$

The same applies for the damping power, K_D, where formula 6.7 must be used:

$$\begin{aligned} K_D &= V_s^2 \left(\frac{X_d^{,} - X_d^{,,}}{(x_d^{,})^2} T_{do}^{,,} * \sin^2(\delta) + \frac{X_q^{,} - X_q^{,,}}{(x_q^{,})^2} T_q^{,,} * \cos^2(\delta) \right) * \omega_s = \\ &= 1.0^2 \left(\frac{0.3 - 0.25}{(0.65^2} 0.03 * \sin^2(21.37) + \frac{0.55 - 0.25}{(0.9)^2} 0.05 * \cos^2(21.37) \right) * \omega_s = \\ &= 5.2 \end{aligned} \tag{6.45}$$

All values necessary to find the eigenvalues are now either given or calculated and it is therefore possible to find the systems eigenvalues using the formulas from 6.18 and up to 6.28. The eigenvalues in the general form will then be:

$$\begin{aligned} \lambda_{1,2} &= -0.1997 \pm J5.7842 \ rad/s \\ \lambda 1,2 &= -0.1997 \pm J0.92 \ hz \end{aligned} \tag{6.46}$$

And the right and left eigenvectors according to formula 6.31 and 6.33:

$$\begin{aligned} X_R &= \begin{pmatrix} -0.0006 + J0.0184 & -0.0006 + J0.0184 \\ 1 & 1 \end{pmatrix} \\ X_L &= \begin{pmatrix} 0.0000 - J27.1612 & 0.5001 - J0.0173 \\ -0.0000 + J27.1612 & 0.5001 + J0.0173 \end{pmatrix} \end{aligned} \tag{6.47}$$

Combining the right and left eigenvector by using formula 6.34 gives the participation matrix:

$$\begin{aligned} P &= \begin{pmatrix} 0.5000 + J0.0173 & 0.5000 - J0.0173 \\ 0.5000 - J0.0173 & 0.5000 + J0.0173 \end{pmatrix} \\ &= \begin{pmatrix} 0.5003\angle 1.9777 & 0.5003\angle -1.9777 \\ 0.5003\angle -1.9777 & 0.5003\angle 1.9777 \end{pmatrix} \\ &= \begin{pmatrix} & \lambda_1 & \lambda_2 \\ \Delta\omega_r & 0.5009\angle 1.9777 & 0.5009\angle -1.9777 \\ \Delta\delta & 0.5009\angle -1.9777 & 0.5009\angle 1.9777 \end{pmatrix} \end{aligned} \tag{6.48}$$

This shows that each state variable has the same amount of contribution to the eigenvalues.

6.2.2 Data Scanning

The main advantage of using modal analysis is that it makes it possible to predict the systems behaviour. While planning a new power system or testing a system already in use, it is possible to use modal analysis to see how a change in a parameter can change the robustness against oscillations, see where the source of the problem is, and where it most effectively can be improved.

Formula 6.29, here repeated for convenience, shows how the eigenvalue in the SMIB system can be altered:

$$\sigma = -\frac{K_D}{4H} \quad \omega = \sqrt{(\frac{K_D}{4H})^2 - \frac{K_S}{2H}\omega_0} \tag{6.49}$$

The formula clearly shows that the inertia constant H have an influence on both the damping of the oscillation and the frequency. This constant, which is more thoroughly explained in appendix B.2, is mainly decided my the mass of the generators moving part, hence the rotor.

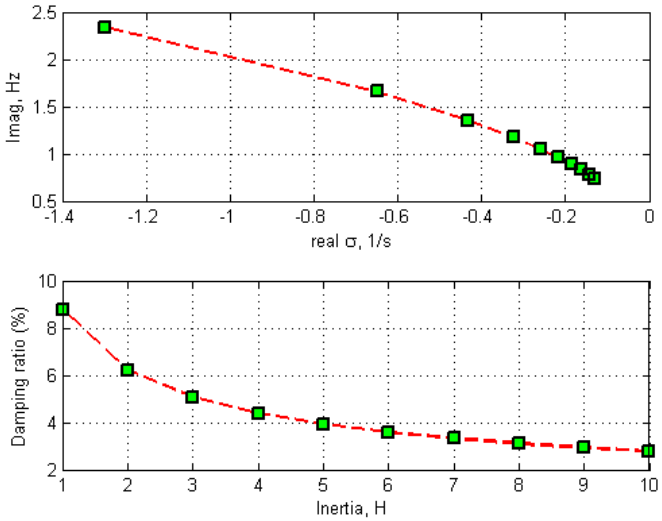

Figure 6.5: Different inertia values

Figure 6.5 display the results obtained from the MATLAB program, when the inertia of the generator is changed from $H = 1$ to $H = 10$. The damping is as predicted, by looking at formula 6.29, decreased when the inertia is increased. A generator with a high inertia would therefore have a more negative impact on the system's ability to withstand small-signal stability than a generator with a low inertia.

The connection between a production source or a group of connections sources and the rest of the power system will often greatly impact the systems small-signal stability. Increasing the line impedance will, by looking at the formulas, affect the voltage at Bus 1, reduce the synchronizing torque coefficient, the damping power , and due to this reduce the damping of the system.

This is tested by changing the line reactance from $X_{line} = 0.2$ and up to $X_{line} = 2.0$.

Table 6.1: Different line reactance values

	Load Flow				Eigenvalues		
X_{line}	V_1	E_g	K_s	K_d	1/s	Hz	DR [%]
0.2	1.068 ∠8.46	1.187 ∠21.37	1.70	5.19	-0.20	0.92	3.45
0.4	1.122 ∠11.82	1.251 ∠23.00	1.36	3.40	-0.13	0.85	2.46
0.6	1.178 ∠14.39	1.312 ∠24.16	1.14	2.39	-0.09	0.79	1.86
0.8	1.233 ∠16.39	1.369 ∠25.04	0.99	1.77	-0.07	0.75	1.46
1.0	1.286 ∠18.00	1.423 ∠25.74	0.88	1.36	-0.05	0.71	1.18
1.2	1.338 ∠19.33	1.473 ∠26.32	0.80	1.08	-0.04	0.68	0.98
1.4	1.387 ∠20.44	1.521 ∠26.81	0.73	0.88	-0.03	0.65	0.82
1.6	1.435 ∠21.39	1.568 ∠27.24	0.68	0.73	-0.03	0.63	0.71
1.8	1.481 ∠22.21	1.610 ∠27.62	0.63	0.61	-0.02	0.61	0.61
2.0	1.525 ∠22.93	1.654 ∠27.96	0.60	0.52	-0.02	0.59	0.53

Since the voltage is set to be 1.0 pu at Bus 3, the voltage at Bus1 must be increased when the line losses increases. The internal generator voltage will also increase and the angle between the generator and the stiff network increases. This factors combined with the reduced K_s and K_d leads to a damping ratio dropping from a low but acceptable 3.45 % down to a very low 0.53 %.

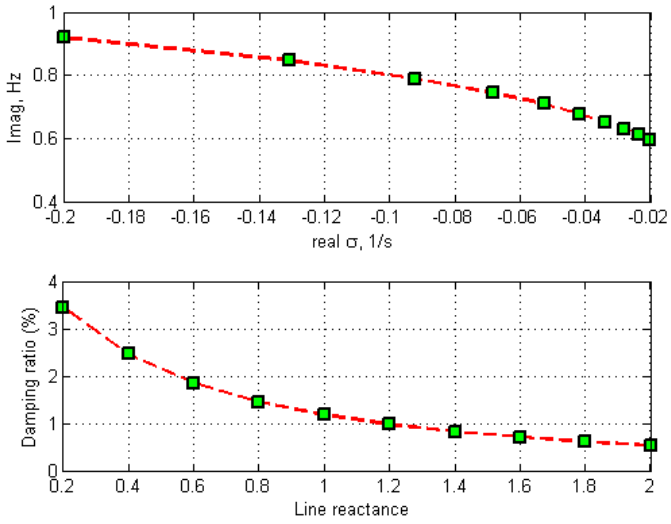

Figure 6.6: Different line reactance values

The graphical representation of the changes in eigenvalues is as shown in figure 6.6 also showing that the increased line reactance greatly reduces the system's damping.

Chapter 7

Simulations

The models presented in chapter 3 are evaluated and tested using a single machine infinite bus network (SMIB).A two area network is used to compare how different wind models affect the system's small signal stability

7.1 Variable Speed Wind Turbine

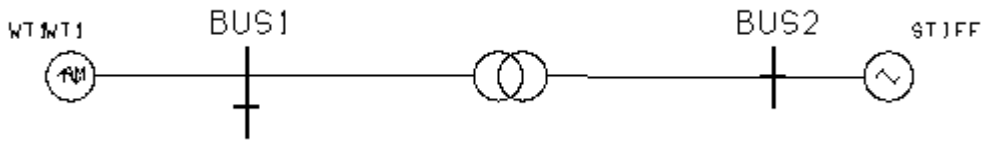

Figure 7.1: 2 Bus system, DFIG and infinite bus

The DFIG is connected to a stiff network through a transformer. This is done in order to simplify the system as much as possible, thereby allowing a more in-depth analysis of the DFIG. Small systems like this are often referred to as SMIB , Single-Machine-Infinite-Bus.

Modelling of the DFIG is done as described in chapter 3.4. The aggregated values and the calculated power coefficients are also used in order to make the system as realistic as possible. Simulations at a defined constant power and simulations where the wind speed is varied are performed. The model is tested with the voltage controller module connected, this allows the DFIG to adjust the production of reactive power, keeping the Bus voltage at $V_{pu} = 1.0$, see more in section 3.4.1.

The full Simpow files and calculations can be found in appendix B.1.

7.1.1 DFIG at Constant Power

The generator is operated at constant power, $P = 100$. This ensures that the produced power from the DFIG remain the same in the dynamic part as the static part. The same values are also used in section 7.3, where the DFIG is compared to other wind turbines models.

Table 7.1 shows the oscillatory eigenvalues of the system without iterative improvement and with iterative improvement. The improvement failed with eigenvalue no. 1, 3, 6, 9 and 10, indicating that the results must be handled with caution. Especially eigenvalue

Table 7.1: Eigenvalues for DFIG

	Not Improved			Improved		
Number	1/s	Hz	Dr [%]	1/s	Hz	Dr [%]
2	-0.34	7.59	0.70	-9.98	0	100
3	-0.34	-7.59	0.70	-0.34	7.59	0.70
4	-30.01	3.06	84.18	-30.01	3.06	84.18
5	-30.01	-3.06	84.18	-30.01	-3.06	84.18

2 and 3 are strange since Simpow is only able to improve one of them with the result being a large change. The full list of eigenvalues can be found in appendix C.1

Table 7.2: Sensitivity overview eigenvalue 4

Sensitivity overview	
Component	Sensitivity
Voltage Control	20.112
Asynchronous Machine	20.025
Transformer	0,03873
Pitch Controller	2,54E-15

By running a sensitivity analysis it is possible to see which components in the system that contributes most to the selected eigenvalue. The parameters in table 7.2 indicate how much each component influence the selected eigenvalue and it reveals that the voltage controller is the component which to a largest degree influence the selected eigenvalue.

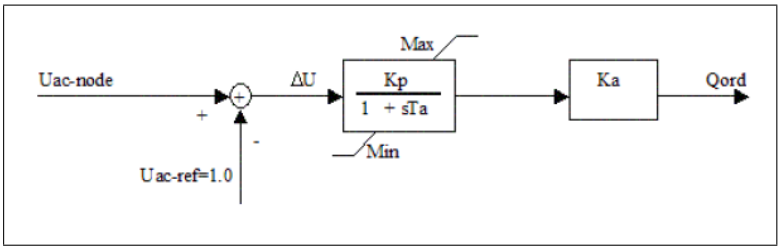

Figure 7.2: The AC bus control [7]

The voltage controller is as described in section 3.4.1, controlling the voltage at the node. When the voltage is below a pre-set reference value, a reactive power order is sent to the generator which increases the reactive power production. The most relevant changeable parameters in the voltage controller are the gain factor, KA, in the controller and the gain factor in the proportional part, KP.

Figure 7.3 shows how eigenvalue 4,5 changes when altering the gain factors in the voltage controller. Increasing either the KP or the KA gives a steady decrease in damping factor. Reducing the gain factors should therefore according to the simulations lead to a better damped system. A full list of the eigenvalues can be found in appendix C.1

Figure 7.3 shows the eigenvalues after changing the KP from $KP = 10$ to $KP = 5$ and KA from $KA = 4$ to $KA = 2$. The new gain factors have led to a non-oscillatory system, although eigenvalue 2,3 still have the same values as before. This is as mentioned most likely due to a problem in the DFIG model.

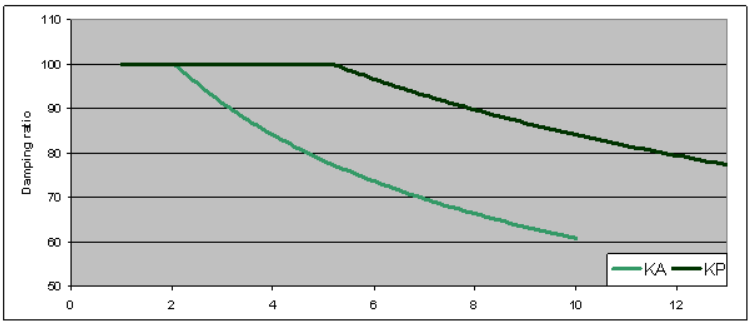

Figure 7.3: Change of eigenvalue 4,5

Table 7.3: Eigenvalues

	Improved Eigenvalues		
Number	1/s	Hz	DR [%]
2	-9.98	0	100
3	-0.34	7.59	0.70
4	-44.42	0	100

If eigenvalue 2 and 3 are disregarded, the system appears to be very well damped with little or non oscillatory behaviour. This is tested by adding a three phase short circuit to Bus 1. The fault was connected to earth through a small reactance for two seconds.

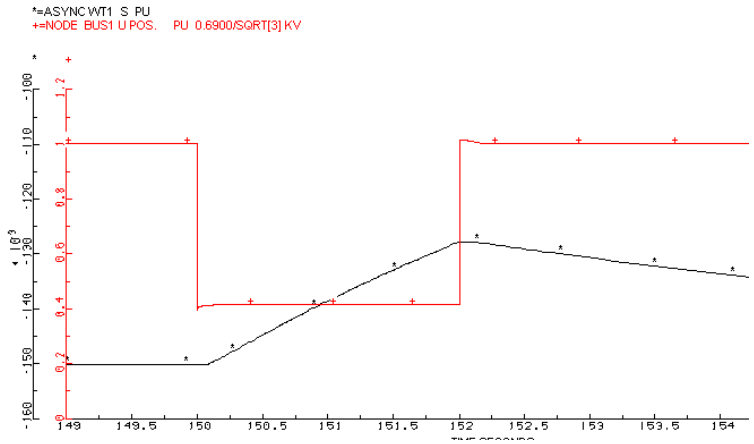

Figure 7.4: Three phase fault at Bus 1

The voltage as Bus 1 drops from 1 pu to 0.4 pu at the moment the fault is connected. This lead to an increase of generator speed. As soon as the fault is removed the speed of the generator goes back to pre-fault state. No oscillatory behaviour is seen but Simpow is reporting that the frequency converter is at maximum current. The flow of current is therefore restricted by the converter and the severity of the fault is smaller than what it realistically should be.

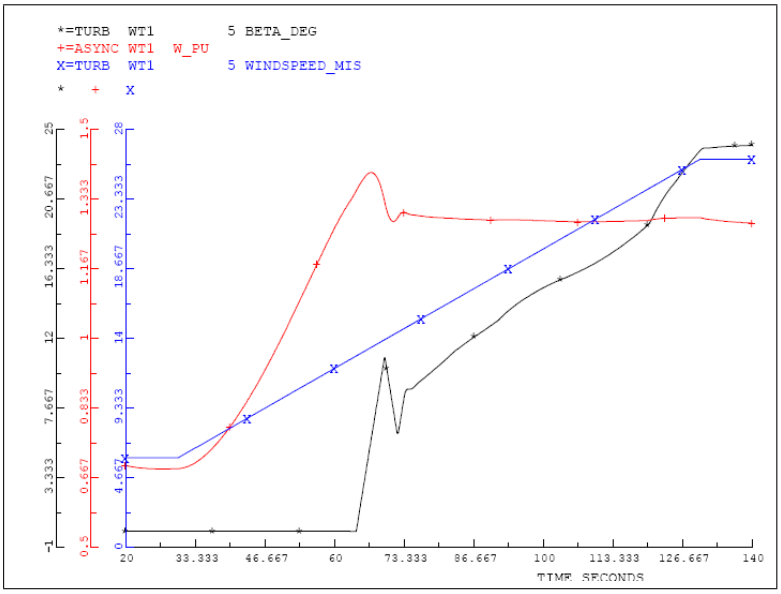

Figure 7.5: Correlation between wind speed, blade angle and produced power

7.1.2 DFIG at Different Wind Speeds

Figure 7.5 shows how the power production increases when wind speed increases. The blades starts pitching when the wind turbine reaches rated power and keeps power production constant.

Since the generator operates at a different slip at different wind speeds, a comparison between the eigenvalues is done by testing three different wind speeds.

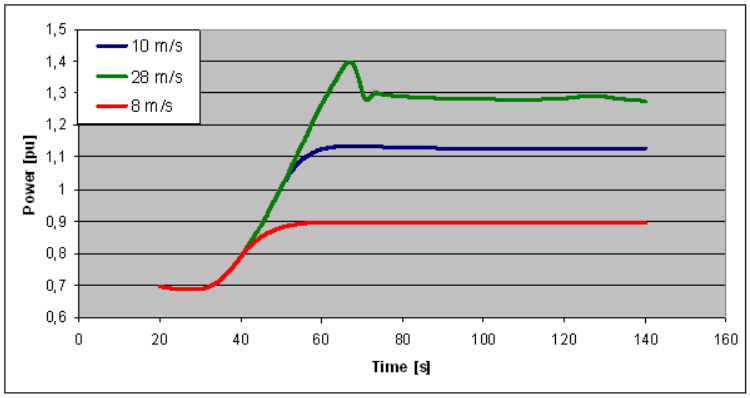

Figure 7.6: Power curves for different wind speeds

As shown in figure 7.5 the blades will start pitching at around $12-14m/s$. The produced power will therefore remain constant during winds above these values. The wind speeds $8m/s$, $10m/s$ and $28m/s$ was therefore chosen as relevant values. KA and KP was set back to default value.

The same eigenvalue problem as in 7.1.1 occurs and eigenvalue 2 and 3 are most likely not correct. The rest of the eigenvalues are quite similar, indicating that the working point of the asynchronous generator have little or non influence on the DFIGs small signal

stability. The eigenvalues found when operating at three different wind speeds are listed in appendix C.1.2.

A three phase fault was connected in the same way as the previous section but revealed no oscillatory behaviour as generator speed went back to previous values without oscillating.

7.2 Constant Speed Wind Turbine

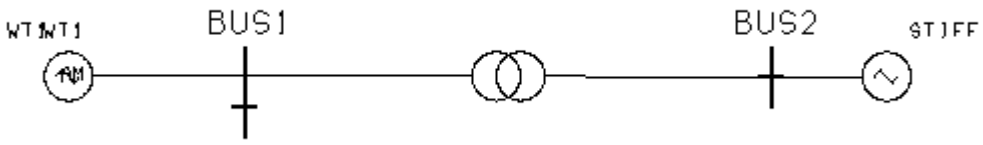

Figure 7.7: 2 Bus system, SCIG and infinite bus

The SCIG modelled in section 3.3 is connected to a stiff network through a transformer. All parameters are modelled as in appendix B.2.

7.2.1 SCIG at Constant Power

The SCIGs power production is set by using a power controller in Optpow. Power production is set to $P = 100$ and no reactive compensation is provided.

Table 7.4: Eigenvalues with constant power

	Eigenvalues		
Number	1/s	Hz	DR [%]
3,4	-5.64	± 3.86	22.65
6,7	-2.70	± 0.61	57.62

Linear analysis found a total of 7 eigenvalues. Two pairs have oscillatory modes but the damping factor is high for both pairs. The full list of eigenvalues can be found in appendix C.2.1.

The sensitivity analysis in figure 7.8 revealed that although the generator contributes most to the eigenvalue, the turbine with inertia, representing the shaft and the wind

Sensitivity overview	
Component	Sensitivity
Generator	13.167
Inertia	1.57
Transformer	0.62

(a) 3,4

Sensitivity overview	
Component	Sensitivity
Generator	7.69
Inertia	3.14
Transformer	0.25

(b) 6,7

Figure 7.8: Sensitivity overview for eigenvalue 3,4 and 6,7

turbine rotor, is also a large contributor. This is due to the inertia of the prime mover combined with the torsional stiffness of the shaft connecting it to the generator.

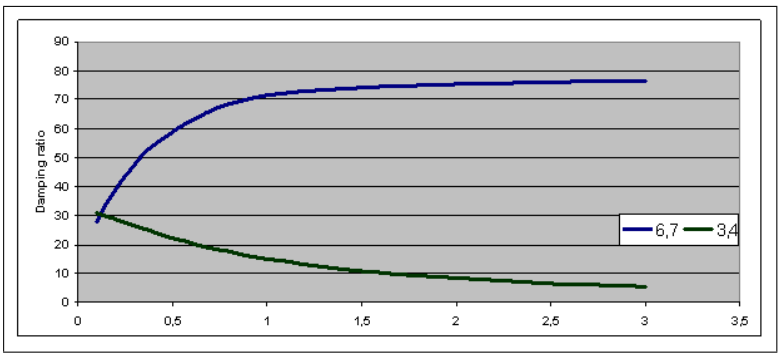

Figure 7.9: Change of Torsional stiffness, eigenvalue 3,4 and 6,7

Changing the inertia of the prime mover did not affect any of the eigenvalues, but changing the torsional stiffness of the shaft between the prime mover and the generators will as figure 7.9 shows, have a large influence on the damping. The torsional stiffness is as explained in section 3.3.1, and calculated in formula B.16, a representation of the shaft connecting the rotor of the wind turbine and the rotor of the generator. Increasing the torsional stiffness of the shaft can be interpreted as equivalent to using a thicker shaft or a shaft made of a more stiff material. Since the damping of eigenvalue 3,4 decreases when the inertia constant is increased, while the damping of eigenvalue 6,7 increases, it is difficult to say what an optimal torsional stiffness would be. But given the low frequency eigenvalue 6,7 it is most critical for the system to have a high damping of this mode. Increasing the torsional stiffness should therefore have the most positive impact on the overall system stability.

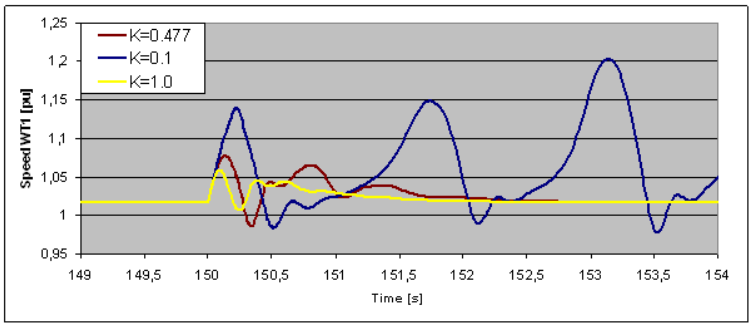

Figure 7.10: Oscillations after fault

A three phase fault is connected at Bus 1 and disconnected after 0.2 seconds. The generator's speed variations are measured with three different torsional constants for the shaft between the turbine rotor and the generator.

Figure 7.10 shows the large influence the shaft stiffness have for the stability of the system. When the stiffness is at its lowest, $K = 0.1$, the oscillations never die out. When the torsional stiffness is at its highest, $K = 1.0$ they extinguish after only 1.5 seconds.

7.2.2 SCIG at Different Wind Speeds

Unlike the DFIG there is no possibility to include wind speed in the SCIG model. But it is possible to simulate wind by adding a torque table to the turbine. Increasing the torque with time can therefore in many ways replace the missing wind speed. The limitation is however that a real SCIG wind turbine uses stalling to reduce the power output when the wind speed get to high. This is not included in the SCIG model and wind speeds (i.e. torque) above nominal power is therefore not possible.

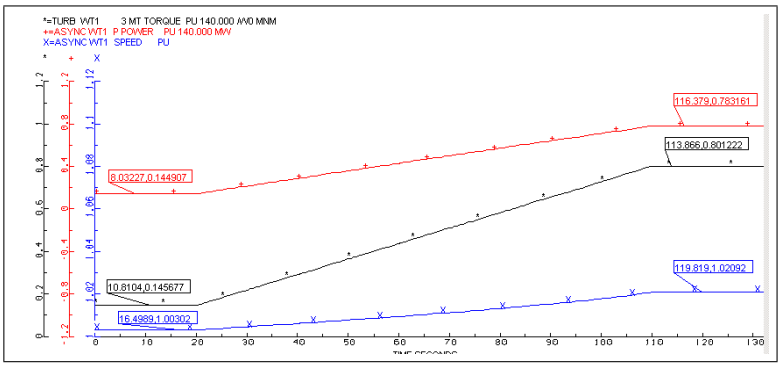

Figure 7.11: Speed increase when torque is increased

Figure 7.11 shows how the generator speed increases when the torque delivered from the turbine increases. Since this is an asynchronous generator directly connected to the stiff network, the speed will follow the frequency of the network. There will only be a small speed deviation as the slip increases when production increases. The slip of the generator changes as shown in the figure, from 0.3% and up to 2.1%.

Table 7.5: Eigenvalues with changed torque

Torque	Eigenvalue 3,4			Eigenvalue 6,7		
MT	1/s	Hz	DR [%]	1/s	Hz	DR [%]
0.2	-3.60	± 4.64	12.36	-2.34	± 0.78	43.12
0.5	-3.70	± 4.60	12.68	-2.56	± 0.77	46.82
0.8	-2.92	± 4.50	13.73	-3.29	± 0.73	57.79
1.1	-4.46	± 4.29	16.27	-5.86	± 1.00	68.30

The eigenvalues of the system changes to a certain degree when the torque from the turbine is changed from $MT = 0.2$ and up to $MT = 1.1$. Since the SCIG unlike the DFIG is directly coupled to the network, changes will in the generator will to a larger degree influence the rest of the system. The full list of eigenvalues can be found in appendix C.5

7.3 Two Area Network

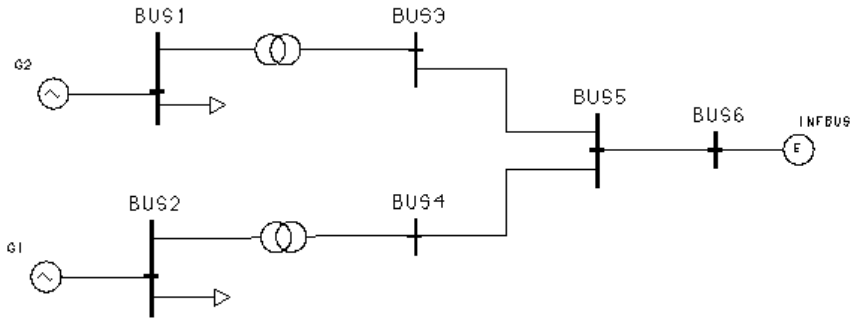

Figure 7.12: Two area network

The network consists of two areas connected together through a tie-line between Bus 5 and Bus 6. Area 1 has two production sources, one placed in Bus 1 and one placed in Bus 2. A local load of 50 MW is located at Bus 1 and Bus 2. The second area represents a large network modelled as a very large synchronous generator with a high inertia. This makes it very stiff but still able to oscillate against area 1.

A synchronous generator (G1) is placed in Bus 2 and produces 100 MW while maintaining a voltage level of pu=1.0 by producing reactive power. The production source in Bus 1 is changed in order to too see if it is sufficient to represent a wind turbine using simpler models.

Five different production sources are tested:

A: Synchronous Generator. The generator is identical to the generator placed in Bus 2. Data for this generator can be found in appendix B.3.

B: Asynchronous Generator. An asynchronous generator connected to a stiff turbine is used. Data can be found in appendix B.4.

C: Static Production. Modelled by using a negative load and will therefore be static without any oscillatory behaviour.

D: DFIG Wind Turbine. The doubly fed induction generator wind turbine included in Simpow is used. The DFIG is further explained in section 3.4 and in appendix B.1.

E: SCIG Wind Turbine. An asynchronous generator connected to a turbine with inertia. The model is explained in section 3.3 and appendix B.2.

In addition to testing different production sources, different types of voltage regulation on Bus 1 are also tested. This types are:

1: VC, Voltage Control. When possible the production sources' ability to control the node voltage is used to ensure node voltage of 1.0 pu.

2: SVC, Static Var Compensation. Static production of reactive power with a regulator connected to ensure correct node voltage.

3: SCRC, Static Constant Reactive Compensation. A negative load producing a fixed amount of reactive power.

Table 7.6: Configurations on Bus 1 (NA=not available)

Production source		Voltage regulation		
Nr		1	2	3
A	Synchronous generator	√	√	√
B	Asynchronous generator	NA	√	√
C	Static Production	NA	√	√
D	DFIG	√	√	√
E	SCIG	NA	√	√

Since some of the production sources are not equipped with regulators they are not able to control the bus voltage. This apply to the asynchronous generator, the static production and the SCIG. The total number of configurations is therefore as shown in table 7.6, twelve different combinations. All productions sources are set to produce $P = 100$ while the reactive power is regulated or pre-defined to ensure a bus voltage as close to pu=1.0 as possible. Apart from the differences in the types of systems and the voltage regulation, all configurations are kept as equal as possible.

There is one inter-area mode in all the configurations, this mode is for each production source compared to the different voltage control systems (VC, SVC, SCRC). The contribution factors for the inter-area modes are tested for the most relevant configurations, A1, B2, C2, D1 and E2. Non-linear time simulations are performed when possible and the generators' speed deviations are compared.

Section C.3 in the appendix includes all the network data, OPTPOW and DYNPOW file, and all the recorded eigenvalues.

7.3.1 A : Synchronous Generator

The synchronous generator is modelled in Simpow as a Type 4 generator. This means that it includes one field winding, one damper winding in d-axis, and two damper windings in q-axis [7]. The parameters for the synchronous generator are taken from [24], but altered slightly to fit the network. It is identical to the synchronous generator at Bus 2. This configuration will therefore consist of two identical generators in two different buses, producing the same amount of power. The modelling of the synchronous generator can be found in appendix B.3.

A1 : Synchronous Generator with VC

The Synchronous generator's voltage regulator measures the voltage at the node and regulates the production of synchronous power in order to maintain a bus voltage of 1.0 pu.

A total number of 26 eigenvalues where found, the oscillatory eigenvalues are listed in table 7.7. Eigenvalue 15,16 is an inter-area oscillation, while 11,12 is a local oscillation.

Table 7.7: Eigenvalues, A1 : Synchronous generator with VC

Number	Real part [1/s]	Imaginary part [Hz]	Damping ratio [%]
7,8	-19.60	±2.39	79.41
9,10	-19,47	±0.77	97.05
11,12	-2.15	±1.00	32.39
15,16	-0.49	±0.57	13.53

The two other pairs of eigenvalues have a very high damping factor and are not of high importance.

A2 : Synchronous Generator and SVC

The voltage regulator is disconnected and the generator will only produce active power. An SVC is connected at the same bus and produces reactive power to control the bus voltage.

Table 7.8: Eigenvalues, A2 : Synchronous generator and SVC

Number	Real part [1/s]	Imaginary part [Hz]	Damping ratio [%]
7,8	-19.64	±1.65	88.39
9,10	-1.19	±0.92	20.10
11,12	-10.39	±0.05	99.65
15,16	-0.32	±0.56	9.08

The eigenvalues are slightly different from the ones in configuration A1, but there is still one inter-area oscillation (15,16) and one local-area oscillation (9,10) of interest.

A3 : Synchronous Generator and SCRC

The voltage controller at the synchronous generators is still disconnected and an acceptable bus voltage is now ensured by a static negative load. Since there is no regulation the negative load is predefined to produce the amount of reactive power needed to get as close to 1.0 pu as possible.

Table 7.9: Eigenvalues, A3 : Synchronous generator and SCRC

Number	Real part [1/s]	Imaginary part [Hz]	Damping ratio [%]
3,4	-19.38	±1.81	86.00
8,9	-1.11	±0.91	18.99
13,14	-0.56	±0.56	8.79

The negative reactive load is not oscillating. But since the synchronous generators are still oscillation against each other, there is still a local-area eigenvalue.

Summary of A1,A2 and A3

All the different configurations appeared to have both an inter-area eigenvalue of interest and a local-area eigenvalue. The eigenvalues are compared in table 7.10.

Table 7.10: Inter-area and local-area eigenvalues

	Local-area			Inter-area		
Case	1/s	Hz	DR [%]	1/s	Hz	DR [%]
A1	-2.15	± 1.00	32.39	-0.49	± 0.57	13.53
A2	-1.19	± 0.92	20.10	-0.32	± 0.56	9.08
A3	-1.11	± 0.91	18.99	-0.56	± 0.56	8.79

The inter-area eigenvalue remains quite unchanged for the different oscillations but the local-area eigenvalue changes quite significant when the voltage regulator is removed and the damping is reduced.

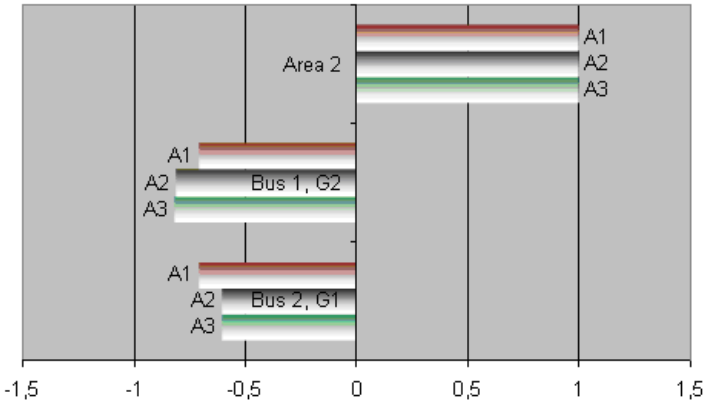

Figure 7.13: Mode shape for inter-area mode

Looking more closely at the mode shape for the inter-area mode it is clear as seen in figure 7.13, that G1 and G2 oscillates against the stiff network in Area 2. When the regulator in G2 is disconnected and replaced with an SVC or SCRC, the contribution from G2 is reduced and the contribution from G1 is increased.

Figure 7.14, showing the participation factors for the inter-area mode indicates that the mode can be best controlled at both G1 and G2. But since the generators have little or non possibility to be altered it is most likely best to use the generators' controllers to improve the inter-area mode.

Figure 7.11 displays the results from the speed deviations that occurred when a three phase fault was connected at Bus 5 and removed after 0.1 seconds. G1 and G2 are in phase and the eigenvalue of the oscillation is found to be $\lambda = -0.33 \pm J0.57\ hz$, close to the inter-area oscillation. An example on how to calculate the eigenvalue from a non-linear time simulation can be found in appendix C.3.4.

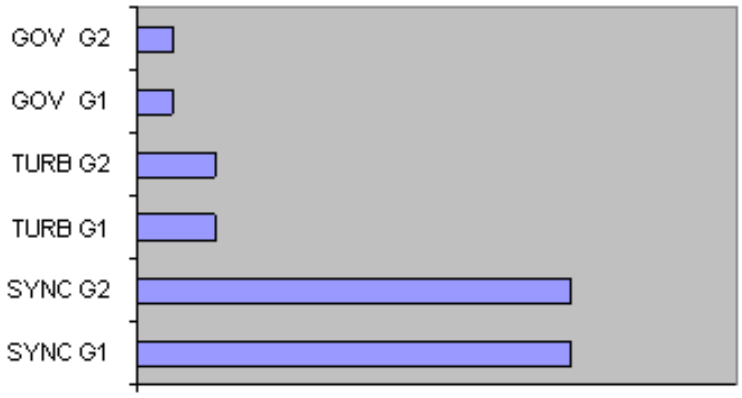

Figure 7.14: Dominant participation factors for inter-area mode

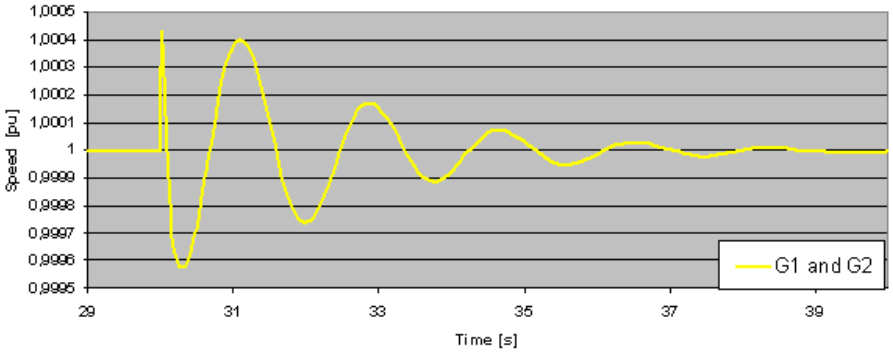

Figure 7.15: Speed response for configuration A1

7.3.2 B : Asynchronous Generator

The asynchronous generator is apart from the lack of a low speed shaft and a turbine with inertia, identical to the SCIG modelled in section 3.3.1. The generator is not equipped with any form of regulation and will consume reactive power.

B2 : Asynchronous Generator and SVC

Around 70 Mvar is required to ensure an acceptable bus voltage. Most of this reactive power is consumed by the asynchronous generator. Using this generator as a production source without any compensation of reactive power would therefore in most cases lead to a voltage collapse.

Table 7.11: Eigenvalues, B2 : Asynchronous generator and SVC

Number	Real part [1/s]	Imaginary part [Hz]	Damping ratio [%]
7,8	-19.59	±1.64	88.48
9,10	-2.19	±1.06	31.2
14,15	-0.58	±0.61	14.98

Looking at the frequency of the eigenvalues it can be observed that eigenvalue 9,10 is a

local-area mode while 14,15 is an inter-area mode. The damping is relatively high.

B3 : Asynchronous Generator and SCRC

The SVC used in the previous configuration is replaced with a negative reactive load, denoted as SCRC. The amount of reactive power produced is set to the same amount as found by the SVC.

Table 7.12: Eigenvalues, B3 : Asynchronous generator and SCRC

Number	Real part [1/s]	Imaginary part [Hz]	Damping ratio [%]
6,7	-19.46	±1.77	86.85
9,10	-2.71	±1.03	38.57
12,13	-0.63	±0.60	16.44
14,15	-2.67	±0.06	98.99

One more highly damped, but very low frequency eigenvalue has appeared since the previous configuration. The other eigenvalues are quite similar to before with only small deviations.

Summary of B2 and B3

Table 7.13: Inter-area and local-area eigenvalues

	Local-area			Inter-area		
Case	1/s	Hz	DR [%]	1/s	Hz	DR [%]
B2	-2.19	±1.06	31.20	-0.58	± 0.61	14.98
B3	-2.71	± 1.03	38.57	-0.63	± 0.60	16.44

Only small deviations occurred when the SVC was replaced with an SCRC. This is not unexpected since both the SCRC is set to produce the same amount of power as the SVC and since an SVC is an stable, almost non-oscillatory construction.

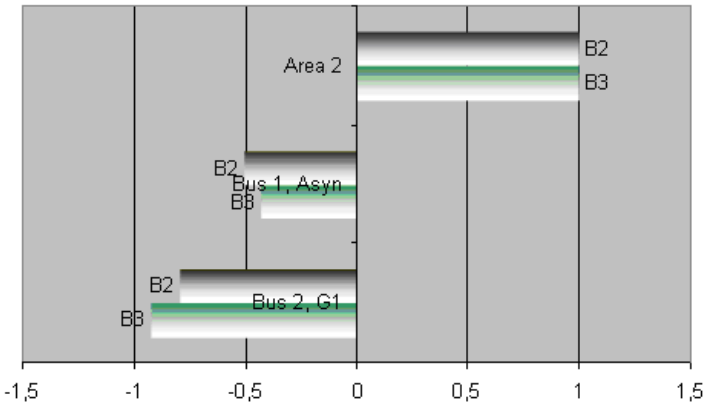

Figure 7.16: Mode shape for inter-area mode

The asynchronous generator and G1 in area 1 oscillates against the stiff network in area 2. When the SVC is replaced with an SCRC the contribution from the asynchronous generator is reduced, thereby increasing the contribution from G1.

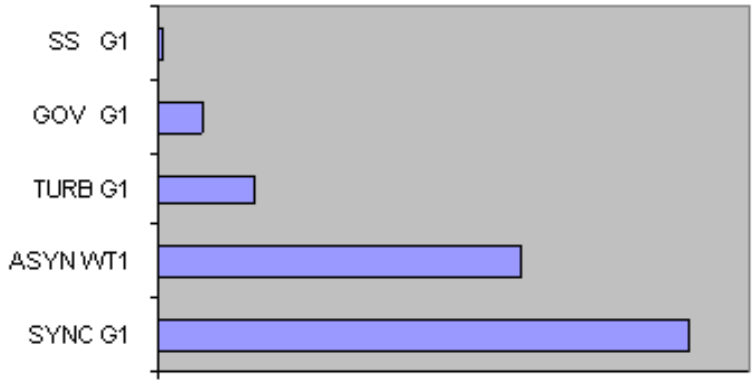

Figure 7.17: Dominant participation factors for inter-area mode

The best place to control the inter-area mode is according to figure 7.17 at Bus 2 where the synchronous generator is located. This is as expected due to the power-angle characteristic for a synchronous generator. But altering the asynchronous generator's properties would also lead to a considerable change of the inter-area mode, which is not expected since the asynchronous generator have as described in section 4.5, a correlation between rotor slip and electrical torque .

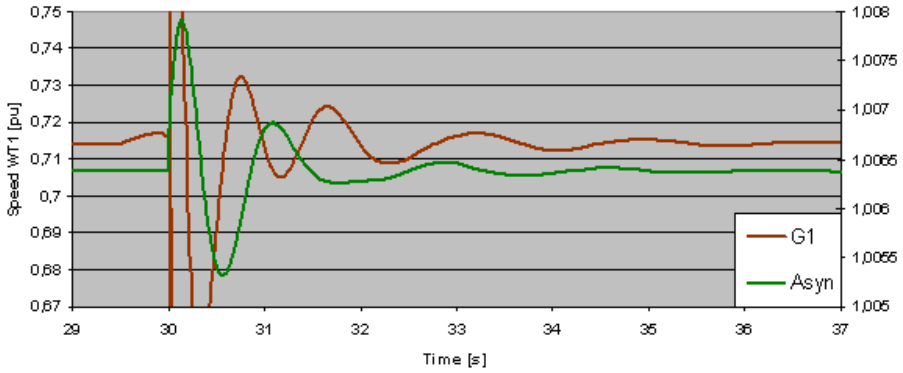

Figure 7.18: Speed response for configuration B2

The synchronous generator's (G1) Y-axis is on the left side in figure 7.18 and the asynchronous generator is on the right side. The speed deviations are much smaller for the asynchronous generator and its contribution to the inter-area oscillation is also smaller.

7.3.3 C : Static Production

All the other production sources are rotating machines that will, due to their construction, have some form of oscillatory behaviour. A static production source is therefore tested to see how much different a non-oscillatory production source representation would give. The power is produced by a load, set to produce instead of consuming active power

C2 : Static Production and SVC

Since there is no reactive power consumer, the SVC will only have to produce enough reactive power to compensate for the losses in the line. Two different types of regulators have been tested, but since no significant differences where found, all simulations are done with the same type.

Table 7.14: Eigenvalues, C2 : Static production and SVC

Number	Real part [1/s]	Imaginary part [Hz]	Damping ratio [%]
5,6	-20.14	±1.68	88.58
8,9	-0,80	±0.69	18.09

When looking at the oscillatory eigenvalues in figure 7.14 it is interesting, and not surprising to see that since G2 does not have any local oscillatory production source to oscillate against there is not a local-area swing mode.

C3 : Static Production and SCRC

The negative load producing the active power is now also used to produce a predefined amount of reactive power.

Table 7.15: Eigenvalues, C3 : Static production and SCRC

Number	Real part [1/s]	Imaginary part [Hz]	Damping ratio [%]
4,5	-19.67	±2.03	83.86
7,8	-0.65	±0.69	14.88

The eigenvalues have only shown small changes compared to the configuration with an SVC. This as previous explained not unexpected.

Summary of C2 and C3

Table 7.16: Inter-area and local-area eigenvalues

	Local-area			Inter-area		
Case	1/s	Hz	DR [%]	1/s	Hz	DR [%]
C2	–	–	–	-0.80	± 0.69	18.09
C3	–	–	–	-0.65	± 0.69	14.88

The non-oscillatory productions source in Bus 1 will as mentioned mean that there are not any local-area eigenvalues in any of the configurations. The differences in the inter-area mode between configuration B2 and B3 might be due to a slightly altered load flow.

As the mode shape for the inter-area mode in figure 7.19 shows, there is no contribution from the static load to the eigenvalue. The differences in the inter-area eigenvalue in case B2 and B3 is therefore most likely due to some load flow differences occurring when the SVC is replaced with the SCRC.

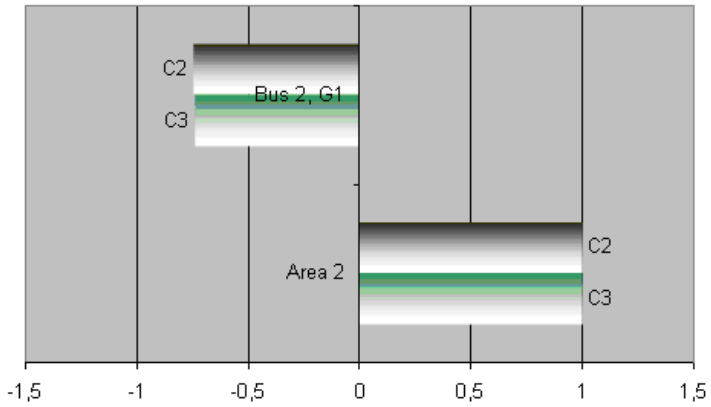

Figure 7.19: Mode shape for inter-area mode

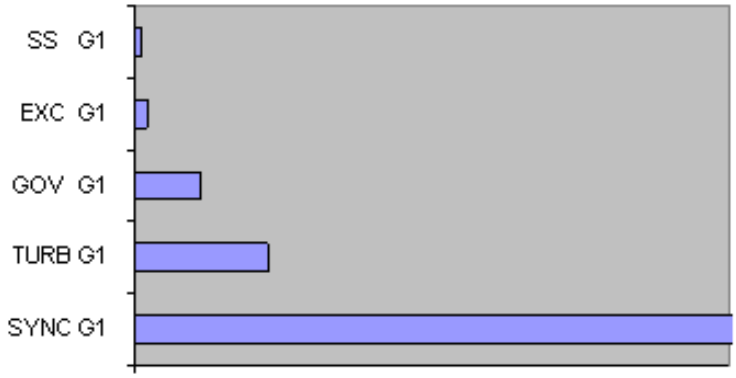

Figure 7.20: Dominant participation factors for inter-area mode

Only the generator and the generator's controllers and turbine will as shown in figure 7.20 be able to influence the inter-area oscillation.

Non-linear time simulations with a three phase fault is not performed since the static load can not supply the system with any reactive power and voltage collapse will therefore occur.

7.3.4 D : DFIG

The same DFIG as used in the simulations in section 7.1 and modelled in section 3.4.1 is placed in Bus 1 and set to produce 100 MW.

Some strange eigenvalues are still occurring and iterative improvement gives roughly the same results as when it was placed in the SMIB network in section 7.1.

D1 : DFIG with VC

As explained in section 3.4.1 and shown in figure 3.11, the AC voltage control block can be used to control the bus voltage by regulating the amount of produced power. This is

possible since the DFIG uses a frequency converter to supply the rotor slip rings of the generator, enabling it to adjust the generators power factor.

Table 7.17: Eigenvalues, D1 : DFIG with VC

Number	Real part [1/s]	Imaginary part [Hz]	Damping ratio [%]
1,2	-28.27	±18.95	23.1
5,6	+3.21	±7.05	-7.22
8,9	-19.50	±1.31	92.11
14,15	-1.13	±0.75	23.28
22,23	-0.04	±0.02	24.17

A total of five pairs with oscillatory eigenvalues where found. Eigenvalue 5,6 have a positive damping but attempts to improve it only works occasionally. Eigenvalues 8,9 represent a local-area eigenvalue and 14,15 is an inter-area eigenvalue.

D2 : DFIG and SVC

The AC voltage control module in the DFIG is disconnected and replaced with an SVC at the same bus.

Table 7.18: Eigenvalues, D2 : DFIG and SVC

Number	Real part [1/s]	Imaginary part [Hz]	Damping ratio [%]
4,5	+3.79	±6.72	-8.95
8,9	-19.37	±1.36	91.54
13,14	-1.32	±0.77	26.33
17,18	-1.40	±0.18	77.96
22,23	-0.001	±0.027	4.53
24,25	-0.09	±0.01	89.67

The same problem as previous section and iterative improvement does not work on most of the eigenvalues.

D3 : DFIG and SCRC

The AC voltage control module is still disconnected and reactive power is produced by a static negative load.

Table 7.19: Eigenvalues, D3 : DFIG and SCRC

Number	Real part [1/s]	Imaginary part [Hz]	Damping ratio [%]
3,4	+3.73	±6.76	-8.75
7,8	-18.22	±1.92	83.37
11,12	-1.32	±0.81	25.05
16,17	-2.56	±0.01	99.96
21,22	-0.051	±0.035	22.61

Eigenvalue analysis shows, as seen in table 7.19, almost the same eigenvalues as with configuration D2. There is still one positive eigenvalue and improvement is not possible to perform.

Summary of D1 ,D2 and D3

Table 7.20: Inter-area and local-area eigenvalues

	Local-area			Inter-area		
Case	1/s	Hz	DR [%]	1/s	Hz	DR [%]
D1	–	–	–	-1.13	± 0.75	23.28
D2	–	–	–	-1.32	± 0.77	26.23
D3	–	–	–	-1.32	± 0.81	25.05

Only one eigenvalue was found to be oscillation against the other area. As seen in table 7.20, this eigenvalue remains almost constant when the voltage control configurations are changed. No clear local-area oscillations where found in the system.

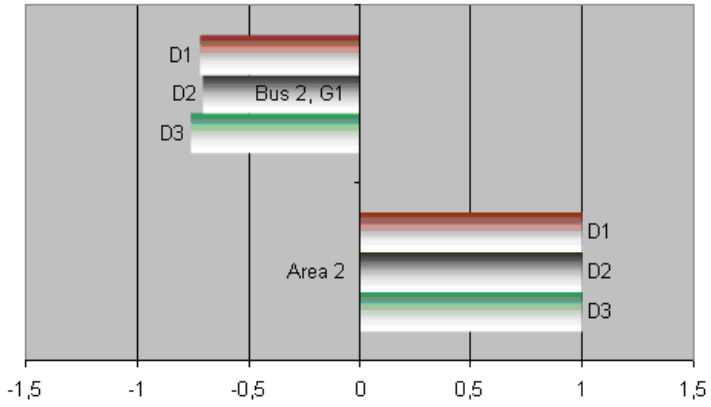

Figure 7.21: Mode shape for inter-area mode

Replacing the voltage controller in the DFIG with other types of voltage control will not give the wind turbine any contribution to the inter-area eigenvalue. The only difference is a slightly increased contribution from G1 when the SCRC is used which might be due to changed load flows.

Calculating the participation matrix did not work and the participation factors are therefore not included for the DFIG.

7.3.5 E : SCIG

A constant wind turbine is simulated using an asynchronous generator connected to a turbine with inertia. The asynchronous generator is modelled as in section 3.3.1. Since there is no voltage regulator included in the model, all reactive power must be produced by an external source.

E2: SCIG and SVC

The SVC produces the reactive power consumed by the SCIG and the power line.

Table 7.21: Eigenvalues, E2: SCIG and SVC

Number	Real part [1/s]	Imaginary part [Hz]	Damping ratio [%]
7,8	-20.00	±1.71	88.06
9,10	-2.01	±3.04	10.46
13,14	-1.57	±0.68	34.27
16,17	-0.70	±0.39	27.09

In addition to the local-area and inter-area eigenvalues that have been observed in all configurations so far, there is also an eigenvalue with higher frequency (3.04 Hz) and quite low damping (10.46 %). This eigenvalue is further analysed in the summary 7.3.5.

E3 : SCIG and SCRC

A SCRC is set to produce the same amount of power as the SVC produced.

Table 7.22: Eigenvalues, E3 : SCIG and SCRC

Number	Real part [1/s]	Imaginary part [Hz]	Damping ratio [%]
6,7	-19.50	±1.87	86.60
8,9	-3.21	±2.91	17.29
11,12	-2.81	±0.99	41.24
14,15	-0.40	±0.54	11.86

One inter-area eigenvalue, one local-area eigenvalue and eigenvalue 8,9 which was also commented in configuration E2, but now with a slightly higher damping.

Summary of E2 and E3

Table 7.23: Inter-area and local-area eigenvalues

	Local-area			Inter-area		
Case	1/s	Hz	DR [%]	1/s	Hz	DR [%]
E2	-1.57	±0.68	34.27	-0.70	± 0.39	27.09
E3	-2.81	± 0.99	41.24	-0.40	± 0.54	16.44

Looking at table 7.23 it can be observed that the damping of the local-area eigenvalue increases when the reactive power production is changed from SVC to SCRC while the inter-area eigenvalue reacts in the opposite way.

The constant speed wind turbine (SCIG) contributes more when used with an SVC compared to when it us used with the SCRC. This explains the weakened inter-area eigenvalue since an asynchronous generator is a more stable construction when it comes to oscillations. The results coincide to a large degree to the results obtained when using only a asynchronous generator.

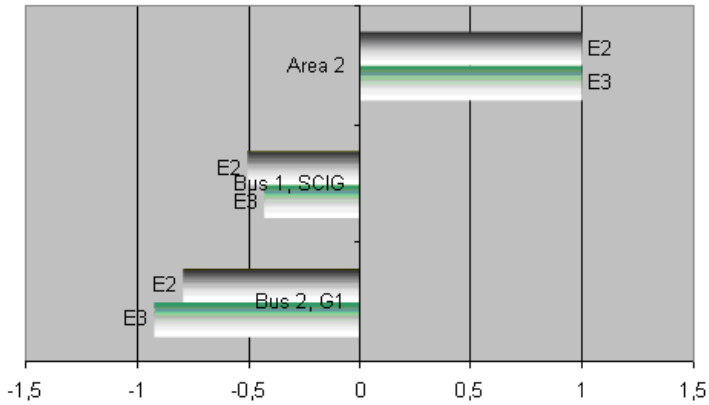

Figure 7.22: Mode shape for inter-area mode

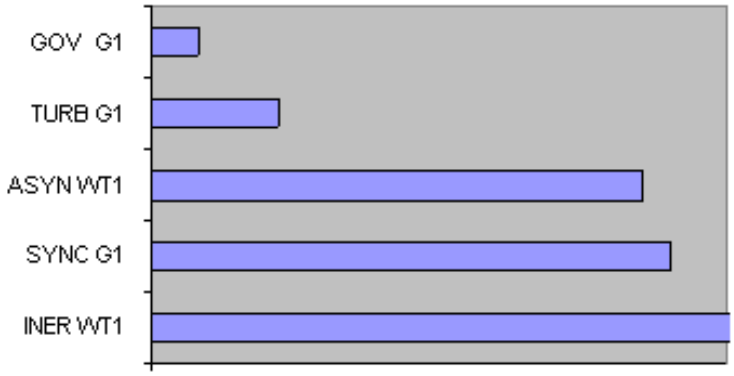

Figure 7.23: Dominant participation factors for inter-area mode

Looking at the participation factors in figure 7.23 it is clear that a two-mass model is required when modelling a constant speed wind turbine. Altering the properties of the inertia group (stiffness of shaft or inertia of the turbine) would the largest change in the inter-area mode.

Table 7.24: Eigenvalue 8,9

	Local-area		
Case	1/s	Hz	DR [%]
E2	-2.01	±3.04	10.46
E3	-3.21	±2.91	17.29

The damping of eigenvalue 8,9 increases when the reactive compensation is changed from SVC to SCRC. As figure 7.22 show the contribution from the SCIG to the inter-area mode is also reduced at the same time so it can be expected that eigenvalue 8,9 can be best controlled by the SCIG.

Eigenvalue 8,9 is as shown in figure 7.24 a local-area oscillation where the SCIG in Bus 1 oscillates against the synchronous generator in Bus 2. Area 2 is only to a very small degree contributing to the oscillations.

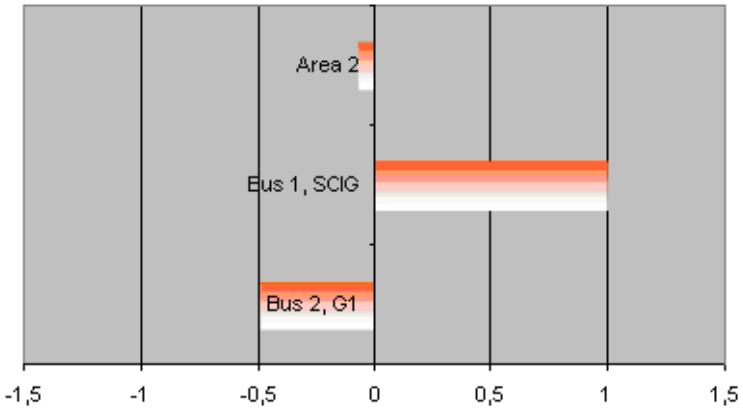

Figure 7.24: Mode shape for local-area mode

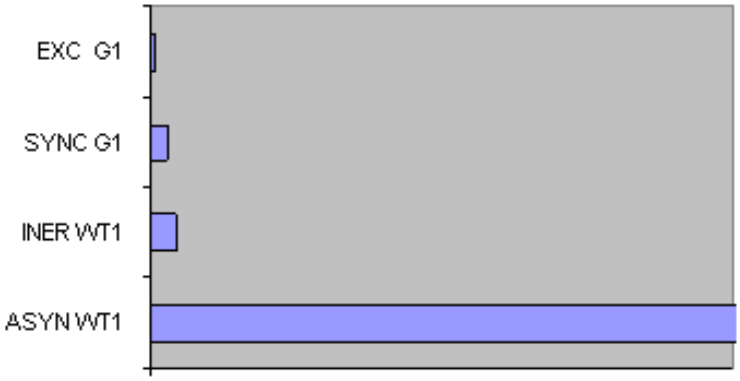

Figure 7.25: Dominant participation factors for inter-area mode 8,9

Altering the local-area eigenvalue 8,9 can best be done at the SCIG but also the inertia block is a good place to investigate in order to improve the damping of this eigenvalue.

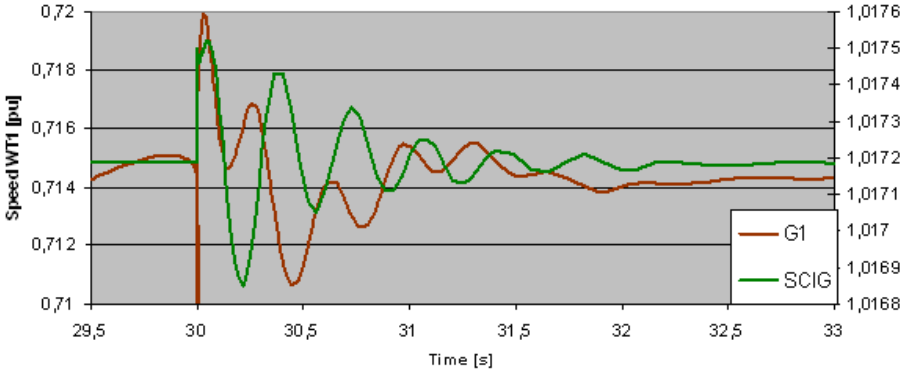

Figure 7.26: Speed response for configuration E2

The synchronous generator's (G1) Y-axis is on the left side and the asynchronous generator is on the right side. Compared to the time simulation on configuration B1 (figure 7.18) the asynchronous generator is now in more anti-phase with the synchronous generator and the oscillations have a higher frequency.

7.3.6 Comparison of Results and Comments

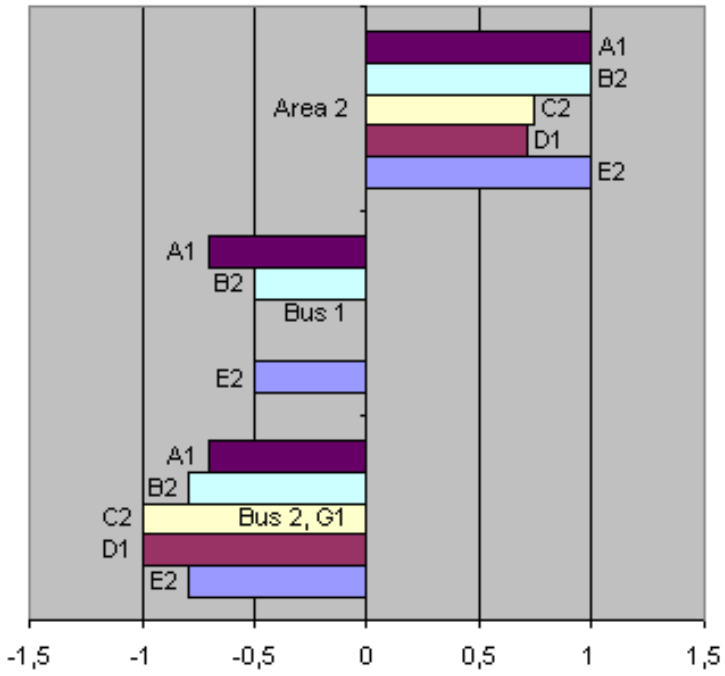

Figure 7.27: Mode shapes inter-area mode, all main configurations

Figure 7.27 shows the mode shapes for the inter-area eigenvalue for configurations A1, B2, C2, D1 and E2. These different configurations are considered to be the most relevant ones since they utilize the production sources' voltage controllers or uses an SVC. The group of bars on the top right side illustrate how observable the oscillations are in area 2. The two groups on the left side show respectively, Bus 1 with the different production sources and Bus 2 with G1.

When using a static production source (C2) or when using the DFIG (D1), the oscillations are as the middle group of bars show, not visible in Bus 1 . For the static production source this is expected since it does not oscillate. The DFIG uses an converter, acting as buffer between the grid and the asynchronous generator, and oscillations are therefore not expected since the converter will decouple the generator from the network.

The two types of asynchronous generators tested, B2 and the SCIG (E2) show the same degree of observability, but as the participation figures 7.17 and 7.23 showed, there is a significant difference in where it is most effective to control the swing mode. For the asynchronous generator without inertia (B) this was most effective at G1, while for the asynchronous generators with inertia, i.e the two mass model, it was most effective to change the inertia.

Figure 7.28 shows how the synchronous generator responds to a three phase fault at Bus 5 that is disconnected after 0.01 seconds. The yellow curve shows the response for configuration A1, when the same generator is used in both buses. The curve named B2 is when an asynchronous generator is used in Bus 1 and the curve E2 is when the SCIG is used in Bus 1. The synchronous generator's oscillations extinguish faster when a asynchronous generator is used in Bus 1. This can also be seen in the eigenvalues

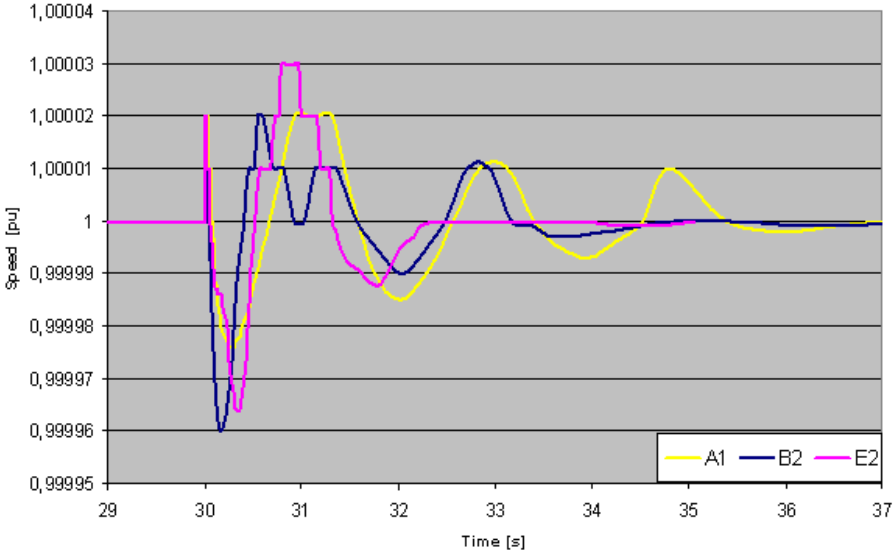

Figure 7.28: G1 Speed response for configuration A1, B2 and E2

analysis where the damping is much lower for configuration A1 compared to B2 and E2.

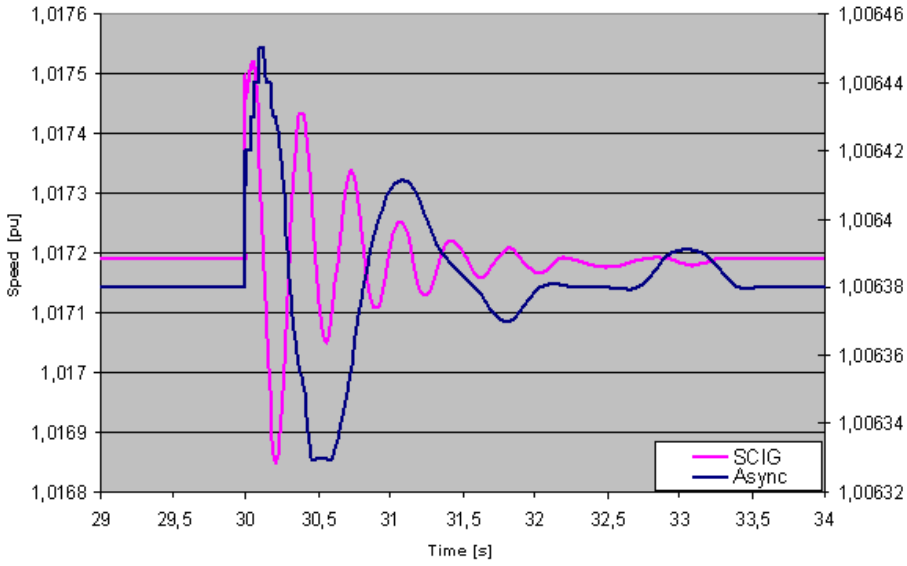

Figure 7.29: Speed response for Synchronous generator and SCIG

Figure 7.29 illustrate the differences in response between the asynchronous generators and the SCIG when the same three phase fault is connected at Bus 5. The right Y-curve is for the asynchronous generator and the left Y-curve is for the SCIG. The SCIG will oscillate at a much higher frequency than the asynchronous generator but the oscillations extinguish at almost the same time. This coincide with the frequency of the eigenvalues presented in table 7.13 for configuration B2 and table 7.23 for configuration E2 where both the local-area and the inter-area eigenvalues for configuration E2 shows a lower frequency than configuration B2.

Chapter 8

Conclusion

The aim of this master thesis has been to utilize the possibilities of modal analysis too see how it can be used as tool to better understand the dynamic behaviour of a power system. A small system with a synchronous generator has been linearized to show how this is done mathematically. Two models, one for variable speed wind turbines, and one for constant speed wind turbines (hereby denoted as DFIG and SCIG) have been tested using both linear analysis and non-linear analysis. The models, and other more simple models, have also been tested in a two-area network in the vicinity of a synchronous generator.

Previous simulations in the specialisation project [17] showed that wind power in general will improve a system's small signal stability due the better damping of the asynchronous generator versus the synchronous generator. The simulations performed in both the wind power models in this thesis also showed that it is for the DFIG immaterial what working point the asynchronous generator is operating at, i.e. how strong the wind speed is. The eigenvalues and thereby the small signal stability will remain the same. This is due to the converter placed between the asynchronous generator and the network, decoupling the asynchronous generator from the network. Some changes in the eigenvalues where found when performing the same analysis on the SCIG, but the damping ratio remained quite unchanged. Since the SCIG is operating at a constant speed this is as expected and the small variations only occur due to the small changes of generator slip.

The eigenvalue analysis performed on the DFIG model, included in SIMPOW, in section 7.1 revealed some problems regarding the iterative improvements. Performing such improvements should normally only lead to minor improvements and, not as experienced with the DFIG, large changes. When testing the DFIG in the two-area network some positive eigenvalues also appeared but none of the simulations revealed that the system was small signal unstable. The same problem also occurred in the specialisation project but due to the non-linear simulations in this thesis and simulations undertaken in other master thesis [18], it can be assumed that the problem is limited to linear analysis. The DFIG model in SIMPOW can therefore be used for system analysis but care must be taken when performing linear analysis.

When testing the SCIG using a two-mass model, the modal analysis revealed that the torsional stiffness of the low speed shaft was the most important contributor to the eigenvalues. Performing a data scanning clearly showed how much the eigenvalues could be improved or aggravated by changing the torsional stiffness of the shaft. Non-linear simulations, with three different torsional stiffness constants, substantiated these measurements.

The comparisons between a normal asynchronous generator and the SCIG showed that

they play an important contribution role to the oscillations in the system, but the participation matrix for the network revealed that the inertia, including the torsional stiffness of the low-speed shaft, had a much more influence of systems small signal stability compared to the normal asynchronous generator. Non-linear analysis also showed that the two different models have a significant different speed response after faults. It can therefore be concluded that it is vital to use a two-mass model when simulating a constant speed wind turbine.

8.1 Further Work

The MATLAB program designed to perform modal analysis of the example network is capable of computing a wide range of parameter but is, as today, limited to only the tested network. A natural extension would be to use a more comprehensive representation of the synchronous generator. The model should also include the regulators normally used on a synchronous generator and take advantage of the possibilities given in MATLAB regarding transfer functions and controller functions.

Simulations verified that the two-mass model is required when modelling a constant speed wind turbine but the model used in this thesis did include an aerodynamic model, representing the blades. A normal extension to this model would therefore be to include an aerodynamic model capable of representing the stall effect of the turbine blades.

Using a larger network would in a more comprehensive way demonstrate the possibilities of modal analysis. The network could be a part of the Norwegian power system or another realistic model. More detailed models of wind turbines could also be used which would, most likely, provide more precise answers.

Bibliography

[1] Paul Gardner, Andrew Garrad, Peter Jamieson, Helen Snodin, and Andrew Tindal. Wind energy, the facts, volume 1. Technical report, Unknown institution, 2006.

[2] Technical University of Denmark (DTU) Wind Energy Department, Risø National Laboratory. Wind atlas, europe. web, 1989. `http://www.windatlas.dk`.

[3] European Wind Energy Association. Powering change, ewea annual report 2007. Technical report, European Wind Energy Association (EWEA), January 2008.

[4] P.E Sørensen, A.D.Hansen, P.Christensen, M. Mieritz, J. Bech, B. Bak-Jensen, and H. Nielsen. Simulations and verification of transient events in large wind power installations. Technical report, Risø publication 1331, oct 2003.

[5] Johannes Gerlof Slootweg. *Wind Power, modelling and impact on power system dynamics*. PhD thesis, Technische Universiteit Delft, 2003.

[6] AncaD. Hansen, P.E Sørensen, Lorand Janosi, and J. Bech. Wind farm modelling for power quality. Technical report, IEEE, 2001.

[7] Simpow. Simpow manual. Technical report, STRI AB, 2006.

[8] Asbjørn Benjamin Hovd and Frode Karstein Novik. Electric power system stability. Technical report, NTNU, 2007.

[9] Jonas Persson. Using linear analysis to find eigenvalues and eigenvectors in power system. Technical report, ABB Utilities, Jun 2002.

[10] unknown author. The wikibook of: Control systems and control engineering. web, 11.11.07. `http://en.wikibooks.org/wiki/Control_Systems`.

[11] Jonas Persson. *Bandwidth-reduced Linear Models of Non-continuous Power System Components*. PhD thesis, Royal Institute of Technology (KHT), 2006.

[12] Jan Machowski, Janusz W. Bialek, and James R. Bumby. *Power system dynamics and stability*. JOHN WILEY and SONS, LTD, 1997.

[13] Angelo Mendonca and J.A. Pecas Lopes. Impact of large scale wind power integration on small signal stability. Technical report, IEEE, 2005.

[14] unknown author. History of wind power. web, 26.10.07. `http://en.wikipedia.org/wiki/History_of_wind_power`.

[15] J.F Manwell, J.G McGowan, and A.L Rogers. *Wind Energy Explained*. JOHN WILEY and SONS, LTD, 2006.

[16] Norges Vassdrags og energidirektorat (NVE). Vindkraft. Web, 25.10.07. http://webb2.nve.no/modules/module_109/publisher_view_product.asp?iEntityId=10101.

[17] Asbjørn Benjamin Hovd. Large scale wind power integration - impact on small signal stability. Technical report, NTNU, 2007.

[18] Tarjei Benum Solvang. Large-scale wind power integration in nordland. Technical report, NTNU, June 2007.

[19] 38.01.07 Cigre task force. Analysis and control of power system oscillations (111). Technical report, International Council on Large Electric Systems (CIGRE), 1996.

[20] IEEE Power System Engineering Committee. Proposed terms and definitions for power system stability. Technical report, IEEE Trans, July 1982.

[21] K R Padiyar. *Power system dynamics, Stability and control.* JOHN WILEY and SONS, LTD, 1995.

[22] A. Ishchenko, J.M.A. Myrzik, and W.L. Kling. Linearization of dynamic model of squirrel cage generator wind turbine. Technical report, IEEE, 2007.

[23] J. Persson, J.G. Slootweg, L. Rouco, L. Sôder, and W.L King. A comparison of eigenvalues obtained with two dynamic simulation software packages. Technical report, IEEE, 2003.

[24] Prabha Kundur. *Power system stability and control.* TATA McGRAW-HILL, 1994.

[25] Tet 4180, electromechanical dynamics- small disturbances. Assignment 4, 2007.

[26] Eric W Weisstein. "'eigenvectors"' from mathworld. a wolfram web resource. web, 14.11.07. http://mathworld.wolfram.com/Eigenvector.html.

[27] J.l. Sancha and I.J. Pérez-Arriaga. Selective modal analysis of power system oscillatory instability. Technical report, IEEE, 1998.

[28] Hadi Saadat. *Power System Analysis.* Mc Graw Hill, 2004.

Index

Appendices

Appendix A

Practical use of Linear Analysis

A.1 Linearization Of a Synchronous Generator

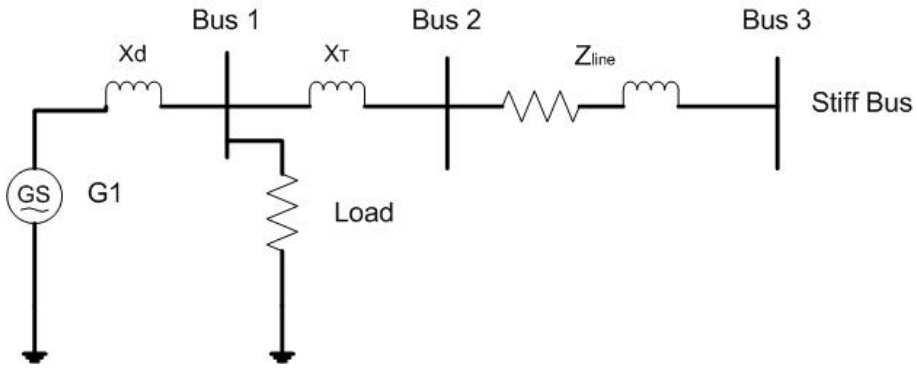

Figure A.1: Three bus example

Parameters for the Synchronous generator used in the example:

Table A.1: Parameters for Synchronous Generator

Synchronous Generator			
Symbol	Simpow	Value	Unit
S_n	SN	100	MVA
V_n	UN	0.69	kV
H	H	6.5	MWs/MVA
X_d	XD	1.8	pu
$X_d^{'}$	XDP	0.3	pu
$X_d^{''}$	XDB	0.25	pu
X_q	XQ	1.7	pu
$X_q^{'}$	XQP	0.55	pu
$X_q^{''}$	XQB	0.25	pu
$T_{d0}^{'}$	TD0P	8.0	pu
$T_{d0}^{''}$	TD0B	0.03	pu
$T_{q0}^{'}$	TQ0P	0.4	pu
$T_{q0}^{''}$	TQ0B	0.05	pu
K_d	D	0	torque/pu

The generator data is taken from Kundur's two are system [24]. The Damping, D, is

modelled in Kundur as $D = 0$ but is calculated to the real value in the linearization example.

Values in Bold are known predefined values, the other values are calculated:

Table A.2: Predefined and calculated values

Power Flow							
BUS	Type	V [Pu]	Angle [δ]	P_{prod} [Pu]	Q_{prod} [Pu]	P_{load} [Pu]	Q_{load} [Pu]
1	PQ	1.068	8.46	**1.0**	**0.1**	**0.5**	**0**
2	–			**0**	**0**	**0**	**0**
3	Swing	**1.0**	**0**	**0**			

Table A.3: Line data

From Bus	To Bus	Resistance [Pu]	Reactance [Pu]
G1	1	0	0.3
1	2	0	0.15
2	3	0.02	0.2

A.2 MATLAB Program

All the formulas have entered into a MATLAB program for verification but also since this a good way to perform more in-depth analysis of the network. The MATLAB program in capable of calculating the change in, eigenvalues, eigenvectors and participation matrix, when changing several of the network's parameters.

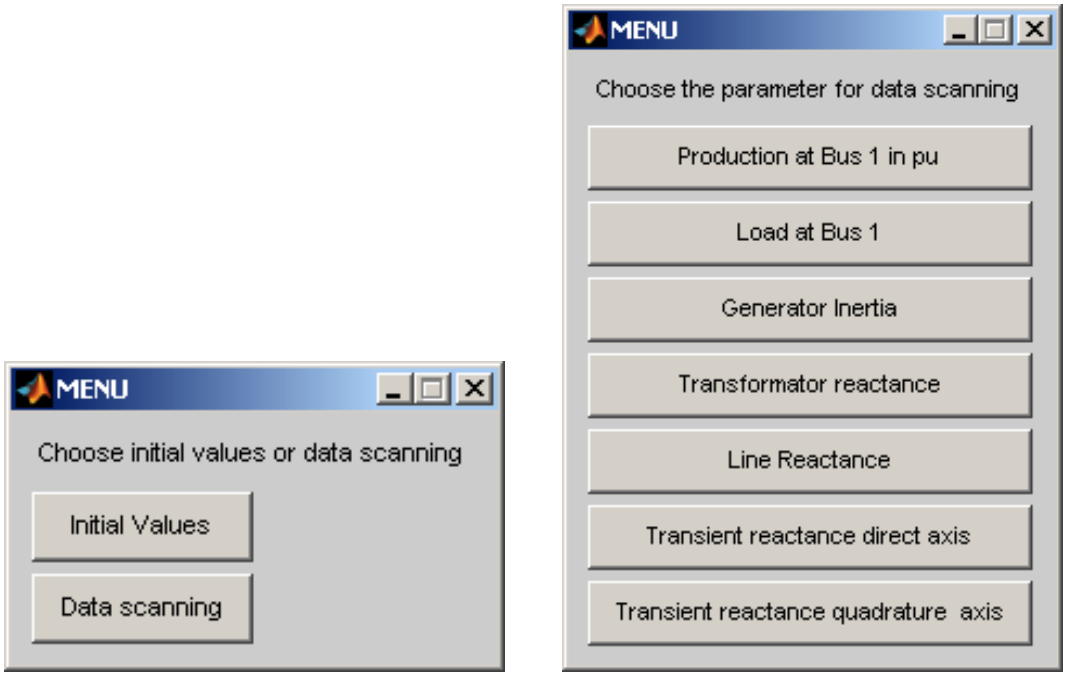

(a) Window 1 **(b)** Window 2

Figure A.2: The MATLAB program

When started the program prompts the user to choose between "Initial values" and "Data scanning". "Initial values" will calculate all the values found in section 6.2 and display them. "Data Scanning" will open a window which allow the user to perform a data scan of a wide variety of parameters. The program will then display the results in a graph as shown in figure 6.6.

```
  clear all

K = menu('Choose initial values or data scanning ','Initial Values',...
         'Data scanning');   %


%%%%%%%%%%%%%%%%%%Network parameters%%%%%%%%%%%%%%%%%
P1=1.0;  P1_load=0.5; Q1=0.1i;
U3=1.0+0i; %U3_angle=0;
f=50;
W0=2 *pi* f;

%%%%%%%%%%%%%%%Generator initial Parameters%%%%%%%%
Xt=0.15;
Xd=1.8; Xdp=0.3; Xdb=0.25;
Xqp=0.55; Xqb=0.25;
Xl=0.2; Rl=0.02;   %
```

```
  TD0B=0.03; TQ0B=0.05;
  H=6.5; f=50;               %Values from Kundur, frequency changed to 50Hz

  %%%%%%%%%%%%%%Data scanning%%%%%%%%%%%%%%%%5
  P1_2=(P1*ones(10,1)); P1_load_2=(P1_load*ones(10,1)); Q1_2=0.1i;
  U3_2=1.0+0i;

  Xt_2=(Xt*ones(10,1)); Xl_2=(Xl*ones(10,1));
  Xdp_2=(Xdp*ones(10,1)); Xqp_2=(Xqp*ones(10,1));
  Xdb_2=0.25; Xqb_2=0.25;
  H_2=(H*ones(10,1));               %Change of inertia


  if K==2

  X = menu('Choose the parameter for data scanning ','Production at Bus 1 in pu',...
            'Load at Bus 1','Generator Inertia','Transformator reactance',...
               'Line Reactance','Transient reactance direct axis',...
                'Transient reactance quadrature  axis');

  M = input('Input Start value [Default=1]: ');  % Start value for data scanning
if isempty(M)
    M = [1];;
   end
   P = input('Input Stop value [Default=1]: ');  % End value for data scanning
if isempty(P)
    P = [1];;

end

step=(P-M)/9;
S=   [M;M+step;M+2*step;M+3*step;M+4*step;M+5*step;M+6*step;M+7*step;M+8*step;M+9*step];;
            %Makes 10 values from start value to end value

  if X==1
      P1_2=S;
  end
  if X==2
      P1_load_2=S;
  end
  if X==3
      H_2=S;
  end
   if X==4
      Xt_2=S;
   end
   if X==5
      Xl_2=S;
   end
   if X==6
      Xdp_2=S;
   end
   if X==7
      Xqp_2=S;
   end


  end
  %%%%%%%%%%%%%%%%Calculactions %%%%%%%%%%%%%%%%%%%%%%
  for a=1:10
```

```
P1_line_2(a,1)=P1_2(a)-P1_load_2(a);   %Power from Bus1 and through the line

Xtot_2(a,1)=Xt_2(a)+Xl_2(a);
xd_2(a,1)=Xdp_2(a)+Xtot_2(a);           %Total reactance direct axis
xq_2(a,1)=Xqp_2(a)+Xtot_2(a);           %Total reactance q axis

U1_mat_2(:,:,a)=[1 -U3_2 (-conj(P1_line_2(a,1)+Q1_2)*Xtot_2(a,1)*i)];
U1_2(:,:,a) = roots(U1_mat_2(:,:,a));

I_line_2(a,1)=conj(P1_line_2(a,1)+Q1_2)/U1_2(1,1,a);
                                        %calculates the current through the line
Itot_2(a,1)=I_line_2(a,1) + (P1_load_2(a)/abs(U1_2(1,1,a))); %total current

Eg_2(a,1)=U1_2(1,1,a)+Xdp_2(a)*i*Itot_2(a,1);
                        %Calulates transient voltage behind generator reactance

Eg_angle_deg_2(a,1)=((angle(Eg_2(a,1)))*360)/(2*pi); %from radians to degrees

Eg_abs_2(a,1)=abs(Eg_2(a,1));                          %E in absolute value

Eg_angle_rad_2(a,1)=((Eg_angle_deg_2(a,1))/360)*2*pi; % Angle in rad

Ks_2(a,1)=((Eg_abs_2(a,1)*abs(U3_2))/xd_2(a,1))*cos (Eg_angle_rad_2(a,1));
                             % Synchronizing torque coefficient

Ks2_2(a,1)=(((Eg_abs_2(a,1)*abs(U3_2))/xd_2(a,1))*cos (Eg_angle_rad_2(a,1)))+...
              ((abs(U3_2))^2*((xd_2(a,1)-xq_2(a,1))/(xd_2(a,1)*xq_2(a,1)))...
               *cos(2*Eg_angle_rad_2(a,1)));
                            %Synchronoizing torque coefficient, salient pole

Kd_2(a,1)=(U3_2*(((Xdp_2(a)-Xdb_2)/(xd_2(a,1))^2)*TD0B*...
          (sin(Eg_angle_rad_2(a,1)))^2+((Xqp_2(a)-Xqb_2)/(xq_2(a)^2)...
           *TQ0B*(cos(Eg_angle_rad_2(a,1)))^2)))*W0;
                                        %calculates the damping coefficient

A_2(:,:,a)=[(-(Kd_2(a,1)/(2*H_2(a)))) (-(Ks2_2(a,1)/(2*H_2(a))));W0 0];
                                        %constructs ten different A matrixes

[V_2(:,:,a),D_2(:,:,a)] = eig(A_2(:,:,a));  % D=Eigenvalues V=Right Eigenvectors

U_2(:,:,a)=V_2(:,:,a)^-1;                              % U= Left eigenvectors

P_cart_2(:,:,a)=[(V_2(1,1,a)*U_2(1,1,a)) (V_2(1,2,a)*U_2(2,1,a));
(V_2(2,1,a)*U_2(1,2,a)) (V_2(2,2,a)*U_2(2,2,a))];
                                        %Constructs the Participation matrix

D_real_2(a,1)=real(D_2(1,1,a));         %1X10 matrix with real eigenvalues
D_imag_2(a,1)=imag(D_2(1,1,a));         %1X10 matrix with imag eigenvalues in rad
D_hz_2(a,1)=(D_imag_2(a,1))/(2* pi);    %1X10 matrix with imag eigenvalues in Hz
DR_2(a,1)=(-D_real_2(a,1))/(sqrt((-D_real_2(a,1))^2+(D_imag_2(a,1))^2))*100;



end

if K==1

disp('----------Calculated Values----------')
disp('----Synchronizing torque efficient and Damping power----------')
```

```
   Ks2_2(1,1)
   Kd_2(1,1)

   disp('----Eigenvalue and Damping ratio----------')

   D_2(:,:,1)
   DR_2(1,1)

   disp('----Left and Right Eigenvectors----------')
   U_2(:,:,1)
   V_2(:,:,1)

    disp('----Participation matrix----------')
   P_cart_2(:,:,1)




   end



   if K==2

    figure(1), subplot(2,1,1), plot(D_real_2, D_hz_2, '--rs','LineWidth',2,...
               'MarkerEdgeColor','k',...
               'MarkerFaceColor','g',...
               'MarkerSize',8)      , grid    %plot the eigenvalues

 xlabel('real \sigma, 1/s '), ylabel('Imag, Hz')
    %subplot(2,1,2), plot(t,f), grid
    %xlabel('t, sec'), ylabel('f, Hz')
figure(1), subplot(2,1,2), plot(S, DR_2, '--rs','LineWidth',2,...
               'MarkerEdgeColor','k',...
               'MarkerFaceColor','g',...
               'MarkerSize',8)      , grid      %plot the damping ratio

 xlabel('Inertia, H '), ylabel('Damping ratio (%)')

 end
```

A.3 SIMPOW

The example is tested in SIMPOW to verify that the calculated values are correct, the system in SIMPOW is modelled as close to the example as possible:

The eigenvalues found by SIMPOW is identical to the values found by the MATLAB program. Figure A.4 shows the change in eigenvalues when performing a data scan of the generator inertia from $H = 1$ to $H = 10$

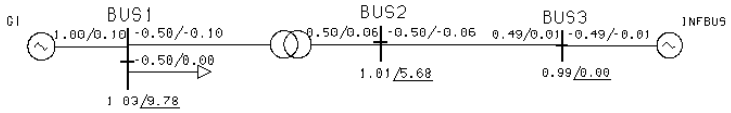

Figure A.3: Load flow from SIMPOW

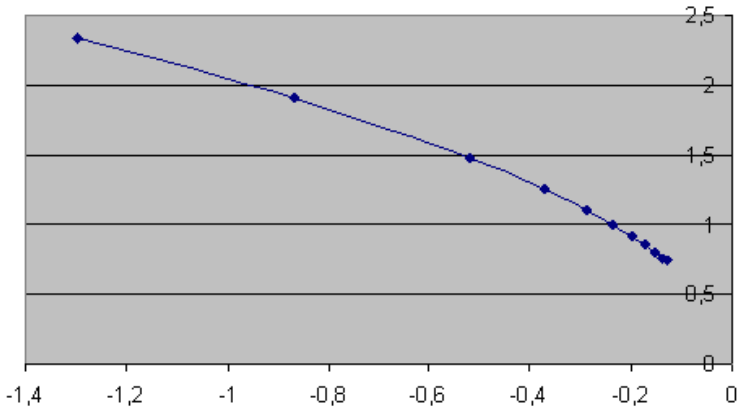

Figure A.4: Eigenvalues in SIMPOW when changing inertia from 1 to 10

A.3.1 SIMPOW OPTPOW file

```
Example in OPTPOW
**

GENERAL
 SN=100
 LBASE=100
END



NODES
 BUS1   UB=0.69 AREA=1
 BUS2   UB=20.2 AREA=1
 BUS3   UB=20.2 AREA=1
 END


LINES
 BUS2  BUS3   TYPE=11  R=0.001    X=0.01  L=20 !L=20
 !BUS3  BUS4   TYPE=11  R=0.001    X=0.01  L=50
END


TRANSFORMERS
 BUS1 BUS2  SN=100  UN1=0.69  UN2=20  ER12=0  EX12=0.15
 END


LOADS
```

```
 BUS1  P=50   Q=0  MP=0  MQ=0
END


POWER CONTROL
 BUS1   TYPE=NODE  RTYP=PQ  Q=10  P=100    NAME=G1
 BUS3   TYPE=NODE  RTYP=SW  U=20.0  FI=0     NAME=INFBUS
END

END
```

A.3.2 SIMPOW DYNPOW file

```
Example in DYNPOW
**



CONTROL DATA
 TEND=10
END


GENERAL
 FN=50
END

NODES
   BUS3 TYPE=1
END

SYNCHRONOUS MACHINE


G1  BUS1  TYPE=4  UN=0.69 SN=100 XD=1.8 XQ=1.7 XDP=0.3
          H=1.3861  D=5.1933



END


END
```

Appendix B

Models

All models used in the simulations are modeled in SIMPOW. The aggregations, calculations and SIMPOW files can be found in this chapter.

B.1 DFIG Model

B.1.1 DFIG Aggregation

The aggregation of the DFIG wind turbine ensures that the ratio between nominal power, blade length and turbines speed remains the same. The theory for the aggregation is from [18].

Equation 2.1 in section 2.2 describing the power produced from the wind is here repeated for convenience:

$$P_{wind} = \frac{1}{2} C_p \rho_{air} A_{rotor} v_{wind}^3 \tag{B.1}$$

This can be written as:

$$P_{wind} = \frac{1}{2} C_p(\Lambda, \beta) \rho_{air} \pi R_{blade}^2 v_{wind}^3 \tag{B.2}$$

Where the power coefficient C_p is a function of the tip speed ratio ,λ, and the blade angle, β. The air density and the wind speed can be assumed to be the same for the aggregated wind turbine.

The value of the tip speed ratio must remain constant in order to get the right power coefficient. The value of the tip speed ratio is given by:

$$\Lambda = \frac{\Omega * R_{blade}}{v_{wind}} \tag{B.3}$$

This yields the following formula for blade length:

$$\begin{aligned} \frac{P_{agg}}{P_{std}} &= \frac{0.5 C_p(\Lambda, \beta) \rho_{air} \pi R_{agg}^2 v_{wind}^3}{0.5 C_p(\Lambda, \beta) \rho_{air} \pi R_{org}^2 v_{wind}^3} \\ R_{agg} &= \sqrt{R_{org}^2 \frac{P_{agg}}{P_{std}}} \end{aligned} \tag{B.4}$$

And for Rotational speed:

$$\Lambda = \frac{\Omega_{std} * R_{std}}{v} = \frac{\Omega_{agg} * R_{agg}}{v}$$
$$\Omega_{agg} = \frac{\Omega_{std} R_{std}}{R_{agg}} \tag{B.5}$$

The aggregated values for the DFIG wind turbine can now be calculated:

Table B.1: Original -and aggregated values for DFIG

Symbol	Standard	Aggregated	Units
S_N	2.05	140	MVA
Ω	18.0	2.18	rpm
R	36.0	297.5	m

B.1.2 Calculation of w_{ref}

The speed measured by the speed control is changed into an optimal rotational speed and compared with the actual rotational speed. This is done by using the C_p/Λ to obtain the coefficients used in the calculation.

If the default C_p/Λ-curve and the aggregated values for the wind turbine is used while assuming air density to be $1.2kg/m^3$ the coefficients can be found by assuming the pitch angle to be $\beta = 0$:

$$\omega_{opt} = \frac{60 * \Lambda_{opt}}{2pi * R * \Omega_{nom}} v_w* = K_1 * v_w$$
$$P_{eg,opt} = \frac{0.5 C_{p_{opt}} \rho_{air} \pi R^2}{S_n} v_w^3 = K_2 * V_w^3 = K_2 * \frac{w_{opt}^3}{K_1^3} \tag{B.6}$$

The default C_p/Λ-curve in [7] is used , this gives $C_{p_{opt}} = 0.504$ at $\Lambda_{opt} = 7.5$. K_1 and K_2 can now be calculated:

$$\Omega_{opt} = \frac{60 * 7.5}{2pi * 2.2 * 297.5} v_w* = 0.1094 * v_w \Rightarrow K_1 = 0.1094$$
$$P_{eg,opt} = \frac{0.5 * 0.504 * 1.2 * \pi * 297.5^2}{140 * 10^6} v_w^3 = 6.01 * 10^{-4} * V_w^3 = K_2 * \frac{w_{opt}^3}{K_1^3} \Rightarrow K_2 = 6.01 * 10^{-4} \tag{B.7}$$

By assuming three different wind speeds the following matrix system can be set up to derive the three coefficients:

$$K_1 * \begin{pmatrix} v_{w,1} \\ v_{w,2} \\ v_{w,3} \end{pmatrix} = \begin{pmatrix} K_2^2 * v_{m,1}^6 & K_2 * v_{m,1}^3 & 1 \\ K_2^2 * v_{m,2}^6 & K_2 * v_{m,2}^3 & 1 \\ K_2^2 * v_{m,3}^6 & K_2 * v_{m,2}^3 & 1 \end{pmatrix} * \begin{pmatrix} A_2 \\ A_1 \\ A_0 \end{pmatrix} \tag{B.8}$$

$$\begin{pmatrix} A_2 \\ A_1 \\ A_0 \end{pmatrix} = \begin{pmatrix} K_1 * v_{w,1} \\ K_1 * v_{w,2} \\ K_1 * v_{w,3} \end{pmatrix} * \begin{pmatrix} K_2^2 * v_{m,1}^6 & K_2 * v_{m,1}^3 & 1 \\ K_2^2 * v_{m,2}^6 & K_2 * v_{m,2}^3 & 1 \\ K_2^2 * v_{m,3}^6 & K_2 * v_{m,2}^3 & 1 \end{pmatrix}^{-1} \tag{B.9}$$

And using wind speeds of 7, 9 and 11 m/s the coefficients are:

$$\begin{aligned} \begin{pmatrix} A_2 \\ A_1 \\ A_0 \end{pmatrix} &= \begin{pmatrix} 0.1094 * 7 \\ 0.1094 * 9 \\ 0.1094 * 11 \end{pmatrix} * \begin{pmatrix} (6.01 * 10^{-4})^2 * 7^6 & 6.01 * 10^{-4} * 7^3 & 1 \\ (6.01 * 10^{-4})^2 * 9^6 & 6.01 * 10^{-4} * 9^3 & 1 \\ (6.01 * 10^{-4})^2 * 11^6 & 6.01 * 10^{-4} * 11^3 & 1 \end{pmatrix}^{-1} = \\ &= \begin{pmatrix} 0.7658 \\ 0.9846 \\ 1.2034 \end{pmatrix} * \begin{pmatrix} (0.0425 & 0.206 & 1 \\ (0.192 & 0.438 & 1 \\ (0.640 & 0.800 & 1 \end{pmatrix}^{-1} = \\ &= \begin{pmatrix} 0.7658 \\ 0.9846 \\ 1.2034 \end{pmatrix} * \begin{pmatrix} 7.27 & -11.92 & 4.66 \\ -9.00 & 12.00 & -3.00 \\ 2.54 & -1.96 & 0.42 \end{pmatrix} = \begin{pmatrix} -0.571 \\ 1.311 \\ 0.520 \end{pmatrix} \end{aligned} \tag{B.10}$$

The speed calculation in the speed control block will then be:

$$W_{ref} = -0.571 P_{eg}^2 + 1.311 P_{eg} + 0.520 \tag{B.11}$$

B.1.3 OPTPOW File

```
ASYNCHRONOUS
  WT1 BUS1 TYPE=DSLS/MACHOPT/  SN=140 UN=0.69 H=4.5
      RS=0.00619 RR=0.02 XS=0.135952 XR=0.112143
      XM=3.904762 PG=100 A2=-0.571 A1=1.311 A0=0.520
END
```

B.1.4 DYNPOW File

```
GLOBALS
   MA1_PORD TYPE=REAL
   MA1_QORD TYPE=REAL
   MA1_DW TYPE=REAL
   MA1_RCBIN TYPE=REAL
END

ASYNCHRONOUS MACHINES
  WT1 TYPE=DSLS/MACHDYN/ H=4.0 TURB=5
R2=0.03  X2=0.25 MODE=1
    PORD=MA1_PORD  RCBIN=MA1_RCBIN  QORD=MA1_QORD
END
```

```
TURBINES
  5  TYPE=DSLS/WINDTURB/ NOM_POWER=200  AIRDENS=1.22
     NOM_TURBSPEED=2.18
     BLADELENGTH=297.5 GOV=2 !WINDCURVE=22

  2   TYPE=DSLS/PICON/ KPP=150 KPC=3 KIP=25
      KIC=30 TP=0.3 BMAX=27 BMIN=0 DBTMAX=10 DBTMIN=-10
      BLOCK=0  DW=MA1_DW  PORD=MA1_PORD
END

MISCELLANEOUS
 SPC1 TYPE=DSLS/SPCON/ KS=0.6 TPC=0.05 KP=3.0
     PMIN=0.1 PMAX=1.0 DPMIN=-0.45 DPMAX=0.45
     WMAX=1.50 WMIN=0.70 A2=-0.571 A1=1.311 A0=0.520
     DW=MA1_DW   PORD=MA1_PORD ASYN=WT1

 CRC1 BUS1 TYPE=DSLS/CRCON/ N=1 UMIN=0.9
      UMAX=1.05 INDELAY=0.0 BLOCK=0
      RCBIN=MA1_RCBIN ASYN=WT1
 VCC1 BUS1 TYPE=DSLS/VCCON/ N=1 KA=4 TA=0.02
      KP=10 QMAX=0.3 QMIN=-0.3 BLOCK=1
      QORD=MA1_QORD ASYN=WT1
END
```

B.2 SCIG

B.2.1 Parameters

Table B.2: Parameters for SCIG from [4] and [7]

Given parameters			SIMPOW parameters		
Symbol	Value	Unit	Group	Value	Unit
Wind turbine generator					
S_n	2.3	MVA	SN		MVA
V_n	0.96	kV	UN	0.96	kV
N_o	1500	rpm			
R_s	0.004	Ω	R1	0.01	PU
X_s	0.05	Ω	X1S	0.125	PU
X_m	1.6	Ω	XM	4.0	PU
$R_r^{'}$	0.004	Ω	–	–	–
$X_r^{'}$	0.05	Ω	X2S	0.125	PU
I_{gen}	93.22	kgm^2	H	0.5	MWs/MVA
Mechanical System					
I_{wtr}	4.18E+06	kgm^2	H	3.5	MWs/MVA
k_{ms}	8.95E+07	Nm/rad	K	0.477	pu/rad
f	80	ratio	–	–	–

Values for the asynchronous machine are in SIMPOW given in local PU. Values are therefore changed to PU values using the PU formulas:

$$Z_{ref,gen} = \frac{U_{n,gen}^2}{S_{n,gen}} \tag{B.12}$$

$$Z_{pu,local} = \frac{Z}{Z_{ref,gen}} \tag{B.13}$$

The inertia constant in H is as given by [12]:

$$H = \frac{0.5 * J\omega_{sm}^2}{S_n} \tag{B.14}$$

With a rotational speed of 1500 rpm and a 1/80 ratio between the low speed shaft and the high speed shaft we get:

$$\begin{aligned} H_{gen} &= \frac{0.5 * 93.22kgm^2(2 * \Pi\frac{1500}{60})^2 * 10^{-6}}{2.3MVA} = 0.5\frac{MWs}{MVA} \\ H_{wtr} &= \frac{0.5 * 4.176 * 10^6 kgm^2(2 * \Pi\frac{1500}{60*80})^2 * 10^{-6}}{2.3MVA} = 3.5\frac{MWs}{MVA} \end{aligned} \tag{B.15}$$

The torsional spring constant in pu will be:

$$K_{ms_{pu}} = \frac{k_{ms}}{S_n * f} = \frac{8.95 * 10^6 Nm/rad}{2.3MVA * 80} = 0.477Pu/rad \tag{B.16}$$

Since the model used in the simulations have a rating of $S = 140MVA$ all the above values have been changed in order to fit the aggregated model:

B.2.2 OPTPOW File

```
ASYNCHRONOUS
  WT1 BUS1 TYPE=1A SN=140 UN=0.960  H=0.5
                   R1=0.01 X1S=0.125 X2S=0.125
                   XM=4.00 RTAB=7  NCON= 0
END

TABLES
 7    TYPE=2  F=-1 0.01
                1 0.01
END
```

B.2.3 DYNPOW File

```
ASYNCHRONOUS MACHINES
  WT1  TURB=3
END

TURBINES
 3  TYPE=22  TAB=15  INER=11
```

```
END

TABLES

 15  TYPE=0  F   0.0  1
                 0.10 1
                 5.0  1
                 5.0  1
                 10.0 1
                 15.0 1
                 20.0 1
                 100  1
 END

INERTIA
 11  TYPE=0  INER=0 RATIO=1 H=3.500 K=0.477 DM=0.000 D=0.000
END
```

B.3 Synchronous Generator

The Simpow modeling of the synchronous generator is shown in appendix C.3.2 and C.3.3

B.4 Asynchronous Generator

Identical to the SCIG but without the Inertia.

B.5 SVC

B.5.1 OPTPOW File

```
POWER CONTROL
 BUS1  TYPE=NODE  RTYP=UP    U=0.69    P=0.0   CNODE=BUS1   QMIN=-80  QMAX=80  NAME=SVC1
END
```

B.5.2 DYNPOW File

```
SVC
 SVC1 BUS1 SN=100 REG=5 CNODE=BUS1 !SHUNT=BUS1
END

REGULATORS
 5    TYPE=SVS BMAX=0.8 BMIN=-0.8 !QMAX=80 QMIN=-80
      RTYP=3 KP=100 KA=15.0 TF=0.01 VPMIN=-1.2 VPMAX=1.2 T1=1.0 T2=10.0
END
```

Appendix C

Simulations

C.1 Variable Speed Wind Turbine

C.1.1 DFIG at Constant Power

```
List of Eigenvalues
*******************

    1 -1026.569580 1/s, +0.000000 Hz
    2 -0.334904 1/s, +7.590780 Hz
    3 -0.334904 1/s, -7.590780 Hz
    4 -30.009499 1/s, +3.063104 Hz
    5 -30.009499 1/s, -3.063104 Hz
    6 -17.856327 1/s, +0.000000 Hz
    7 -1.188428 1/s, +0.000000 Hz
    8 -0.559672 1/s, +0.000000 Hz
    9 -0.127117 1/s, +0.000000 Hz
   10 -10.333776 1/s, +0.000000 Hz
   11 -10.000000 1/s, +0.000000 Hz
   12 -166.666672 1/s, +0.000000 Hz
   13 -999.999939 1/s, +0.000000 Hz
   14 -10000.000000 1/s, +0.000000 Hz
   15 -100.000000 1/s, +0.000000 Hz
```

(a) No improvement

```
List of Eigenvalues
*******************

    1 -1026.569580 1/s, +0.000000 Hz
    2 -9.978876 1/s, +0.000000 Hz
    3 -0.334904 1/s, -7.590780 Hz
    4 -30.009499 1/s, +3.063104 Hz
    5 -30.009499 1/s, -3.063104 Hz
    6 -17.856300 1/s, +0.000000 Hz
    7 -1.188428 1/s, +0.000000 Hz
    8 -0.559672 1/s, +0.000000 Hz
    9 -0.127117 1/s, +0.000000 Hz
   10 -10.333800 1/s, +0.000000 Hz
   11 -10.000000 1/s, +0.000000 Hz
   12 -166.666672 1/s, +0.000000 Hz
   13 -999.999939 1/s, +0.000000 Hz
   14 -10000.000000 1/s, +0.000000 Hz
   15 -100.000000 1/s, +0.000000 Hz
```

(b) Improved

Figure C.1: All eigenvalues before and after improvement

Eigenvalues after changing the gain settings in the voltage controller:

```
List of Eigenvalues
*******************

    1 -1037.156372 1/s, +0.000000 Hz
    2 -9.978897 1/s, +0.000000 Hz
    3 -0.332923 1/s, -7.594117 Hz
    4 -44.424500 1/s, +0.000000 Hz
    5 -15.589605 1/s, +0.000000 Hz
    6 -15.571761 1/s, +0.000000 Hz
    7 -1.188854 1/s, +0.000000 Hz
    8 -0.558801 1/s, +0.000000 Hz
    9 -0.127052 1/s, +0.000000 Hz
   10 -10.331264 1/s, +0.000000 Hz
   11 -9.999995 1/s, +0.000000 Hz
   12 -166.666672 1/s, +0.000000 Hz
   13 -999.999939 1/s, +0.000000 Hz
   14 -10000.000000 1/s, +0.000000 Hz
   15 -100.000000 1/s, +0.000000 Hz
```

Figure C.2: Eigenvalues with changed KP and KS

C.1.2 DFIG at Different Wind Speeds

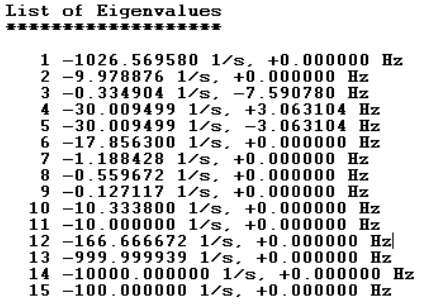

(a) 28 m/s

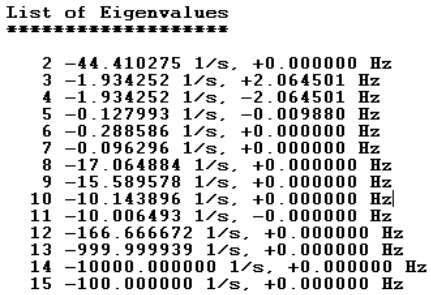

(b) 10 m/s

Figure C.3: Eigenvalues at different wind speeds.

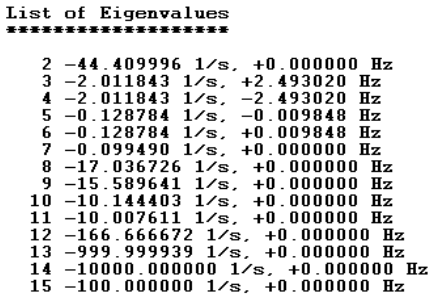

(c) 8 m/s

Figure C.3: Eigenvalues at different wind speeds.

C.2 Constant Speed Wind Turbine

C.2.1 SCIG at Constant Power

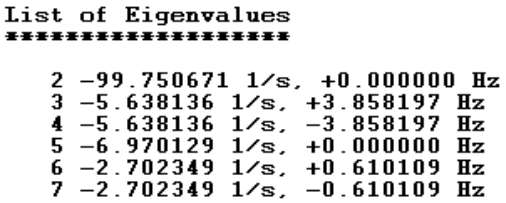

Figure C.4: Eigenvalues, constant power

C.2.2 SCIG at Variable Power

```
List of Eigenvalues
*******************

   2 -99.714531 1/s, +0.000000 Hz
   3 -3.600276 1/s, +4.647572 Hz
   4 -3.600276 1/s, -4.647572 Hz
   5 -2.344797 1/s, +0.780746 Hz
   6 -2.344797 1/s, -0.780746 Hz
   7 -11.782408 1/s, +0.000000 Hz
```

(a) 0.2

```
List of Eigenvalues
*******************

   2 -99.727318 1/s, +0.000000 Hz
   3 -3.700323 1/s, +4.606624 Hz
   4 -3.700323 1/s, -4.606624 Hz
   5 -11.140387 1/s, +0.000000 Hz
   6 -2.561035 1/s, +0.769264 Hz
   7 -2.561035 1/s, -0.769264 Hz
```

(b) 0.5

Figure C.5: Eigenvalues with different torque

```
List of Eigenvalues
*******************

   2 -99.740517 1/s, +0.000000 Hz
   3 -3.924355 1/s, +4.505193 Hz
   4 -3.924355 1/s, -4.505193 Hz
   5 -9.229947 1/s, +0.000000 Hz
   6 -3.288052 1/s, +0.739043 Hz
   7 -3.288052 1/s, -0.739043 Hz
```

(c) 0.8

```
List of Eigenvalues
*******************

   2 -99.754799 1/s, +0.000000 Hz
   3 -4.447855 1/s, +4.293509 Hz
   4 -4.447855 1/s, -4.293509 Hz
   5 -5.859522 1/s, +0.997406 Hz
   6 -5.859522 1/s, -0.997406 Hz
   7 -3.037029 1/s, +0.000000 Hz
```

(d) 1.1

Figure C.5: Eigenvalues with different torque

C.3 Two Area Network

C.3.1 Network Data

Table C.1: Bus data

Power Flow						
BUS	Type	V [Kv]	P_{prod} [MW]	Q_{prod} [Mvar]	P_{load} [MW]	Q_{load} [Mvar]
1	Synch	0.69	100	0	50	0
2	Synch	0.69	100	0	50	0
3	-	20	0	0	0	0
4	-	20	0	0	0	0
5	-	20	0	0	0	0
6	STIFF	20	-	-	-	-

Table C.2: Line data

From Bus	To Bus	Resistance	Reactance	Charging	Tap ratio
1	3	0	0	0	0
2	4	0	0	0	0
3	5	0.02	0.2	0	0
4	5	0.02	0.2	0	0
5	6	0.05	0.5	0	0

Table C.3: Transformer data

From Bus	To Bus	Sn	V_{N1}	V_{N2}	E_{R12}	E_{X12}
1	3	200	0.69	20	0	0.15
2	4	200	0.69	20	0	0.15

C.3.2 Optpow File

```
Network 1, Six-bus network to test small-signal stability.
**  network1.optpow  **

GENERAL
 SN=100
END

NODES
 BUS1 UB=0.69  AREA=1
 BUS2 UB=0.69  AREA=1
 BUS3 UB=20    AREA=1
 BUS4 UB=20    AREA=1
 BUS5 UB=20    AREA=1
 BUS6 UB=20    AREA=2
END
```

```
TRANSFORMERS
 BUS1 BUS3  SN=200  UN1=0.69  UN2=20  ER12=0  EX12=0.15
 BUS2  BUS4  SN=200  UN1=0.69  UN2=20  ER12=0  EX12=0.15
END

LINES
 BUS3  BUS5   TYPE=11  R=0.001    X=0.01  L=20
 BUS4  BUS5   TYPE=11  R=0.001    X=0.01  L=20
 BUS5  BUS6   TYPE=11  R=0.001    X=0.01  L=50
END

LOADS
 BUS1  P=50   Q=0  MP=0  MQ=0
 BUS2  P=50   Q=0  MP=0  MQ=0
END


POWER CONTROL
 BUS1   TYPE=NODE  RTYP=UP  U=0.69  P=100    NAME=G2
 BUS2   TYPE=NODE  RTYP=UP  U=0.69  P=100    NAME=G1
 BUS6   TYPE=NODE  RTYP=SW  U=20.0  FI=0     NAME=INFBUS

END

END
```

C.3.3 Dynpow File

```
**

CONTROL DATA
 TEND=50
END

GENERAL DATA
 FN=50
END

NODES
 BUS6 TYPE=1 NAME=INFBUS
END

SYNCHRONOUS MACHINE

 G1  BUS2  TYPE=1  XD=1.8    XQ=1.7    XA=0.2    XDP=0.3    XQP=0.55
                     XDB=0.25  XQB=0.25  RA=0.0025 TD0P=8.0   TQ0P=0.4
                     TD0B=0.03 TQ0B=0.05 TAB=1     TURB=7
                     H=6.5     SN=200    UN=0.69     D=0        VREG=2

 G2  BUS1  TYPE=1  XD=1.8    XQ=1.7    XA=0.2    XDP=0.3    XQP=0.55
                       XDB=0.25  XQB=0.25  RA=0.0025 TD0P=8.0   TQ0P=0.4
                       TD0B=0.03 TQ0B=0.05 TAB=1     TURB=7
                       H=6.5     SN=200    UN=0.69     D=0        VREG=2
END

REGULATORS
!!!! Regulators constructed with the DSL Code Generator:
```

```
 2    TYPE=DSL/EXC_HTG/    KA=200    TR=0.01 SWS=4
 4    TYPE=DSL/STABILISER/ KSTAB=20  TW=10   T1=0.05 T2=0.02 T3=3  T4=5.4
END

DSL-TYPE
 STABILISER(W,T4,T3,T2,T1,TW,KSTAB,VS,VS0)
 EXC_HTG(VC,TR,KA,VS/0/,UF,UF0)
END

TURBINES
 10 TYPE = SGC YMAX=1 YMIN = -1 K = 20 T1 = 0.1
 7  TYPE = ST1 GOV=10 TC = 0.3 KH = 0.6 TR   7
END

LOADS
 BUS1 MP=0 MQ=0
 BUS2 MP=0 MQ=0
END

TABLES
 1 TYPE=1 F 0.000 0.00 0.700 0.70
            0.800 0.80 0.830 0.83
            0.860 0.86 0.962 0.94
            0.974 0.95 1.039 1.00
            1.113 1.05 1.202 1.10
            1.315 1.15 1.467 1.20
            1.682 1.25 1.998 1.30
            2.478 1.35
END

END
```

C.3.4 A : Synchronous Generator

```
List of Eigenvalues
*******************

   1 -96.932800 1/s, +0.000000 Hz
   2 -95.678154 1/s, +0.000000 Hz
   3 -50.406578 1/s, +0.000000 Hz
   4 -50.150848 1/s, +0.000000 Hz
   5 -40.708668 1/s, +0.000000 Hz
   6 -37.690395 1/s, +0.000000 Hz
   7 -19.606709 1/s, +2.388914 Hz
   8 -19.606709 1/s, -2.388914 Hz
   9 -19.496094 1/s, +0.771047 Hz
  10 -19.496094 1/s, -0.771047 Hz
  11 -2.152705 1/s, +1.000469 Hz
  12 -2.152705 1/s, -1.000469 Hz
  13 -10.388031 1/s, +0.000000 Hz
  14 -10.175660 1/s, +0.000000 Hz
  15 -0.489530 1/s, +0.570185 Hz
  16 -0.489530 1/s, -0.570185 Hz
  17 -5.745210 1/s, +0.000000 Hz
  18 -5.266892 1/s, +0.000000 Hz
  19 -2.570154 1/s, +0.000000 Hz
  20 -2.614272 1/s, +0.000000 Hz
  21 -0.181310 1/s, +0.000000 Hz
  22 -0.178090 1/s, +0.000000 Hz
  23 -0.134358 1/s, +0.000000 Hz
  24 -0.142073 1/s, +0.000000 Hz
  25 -0.101779 1/s, +0.000000 Hz
  26 -0.103450 1/s, +0.000000 Hz
  27 -0.060620 1/s, +0.000000 Hz
```

(a) A1

```
List of Eigenvalues
*******************

   1 -2115.407715 1/s, +0.000000 Hz
   2 -96.400864 1/s, +0.000000 Hz
   3 -50.290585 1/s, +0.000000 Hz
   4 -46.212967 1/s, +0.000000 Hz
   5 -39.493732 1/s, +0.000000 Hz
   6 -36.021713 1/s, +0.000000 Hz
   7 -19.638775 1/s, +1.653531 Hz
   8 -19.638775 1/s, -1.653531 Hz
   9 -1.190434 1/s, +0.923349 Hz
  10 -1.190434 1/s, -0.923349 Hz
  11 -10.389594 1/s, +0.054687 Hz
  12 -10.389594 1/s, -0.054687 Hz
  13 -10.375851 1/s, +0.000000 Hz
  14 -5.529146 1/s, +0.000000 Hz
  15 -0.323663 1/s, +0.564972 Hz
  16 -0.323663 1/s, -0.564972 Hz
  17 -2.863234 1/s, +0.000000 Hz
  18 -2.581543 1/s, +0.000000 Hz
  19 -0.973382 1/s, +0.000000 Hz
  20 -0.206008 1/s, +0.000000 Hz
  21 -0.179807 1/s, +0.000000 Hz
  22 -0.060391 1/s, +0.000000 Hz
  23 -0.133353 1/s, +0.000000 Hz
  24 -0.141214 1/s, +0.000000 Hz
  25 -0.102864 1/s, +0.000000 Hz
  26 -0.100003 1/s, +0.000000 Hz
```

(b) A2

Figure C.6: Eigenvalues A : Synchronous generator.

```
List of Eigenvalues
*******************

   1 -96.274902 1/s, +0.000000 Hz
   2 -50.271278 1/s, +0.000000 Hz
   3 -19.381851 1/s, +1.813304 Hz
   4 -19.381851 1/s, -1.813304 Hz
   5 -40.713978 1/s, +0.000000 Hz
   6 -37.882744 1/s, +0.000000 Hz
   7 -35.819660 1/s, +0.000000 Hz
   8 -1.108712 1/s, +0.912122 Hz
   9 -1.108712 1/s, -0.912122 Hz
  10 -10.386034 1/s, +0.000000 Hz
  11 -10.246272 1/s, +0.000000 Hz
  12 -7.509776 1/s, +0.000000 Hz
  13 -0.309700 1/s, +0.558180 Hz
  14 -0.309700 1/s, -0.558180 Hz
  15 -5.379985 1/s, +0.000000 Hz
  16 -2.889988 1/s, +0.000000 Hz
  17 -2.614113 1/s, +0.000000 Hz
  18 -0.179615 1/s, +0.000000 Hz
  19 -0.136047 1/s, +0.000000 Hz
  20 -0.144267 1/s, +0.000000 Hz
  21 -0.103965 1/s, +0.000000 Hz
  22 -0.059987 1/s, +0.000000 Hz
  23 -0.083467 1/s, +0.000000 Hz
```

(c) A3

Figure C.6: Eigenvalues A : Synchronous generator.

Example on how to calculate damping and frequency of an oscillation:

Values are taken from figure 7.15

$$T_{peak-peak} = 32.870571 - 32.870571 = 1.762588S \tag{C.1}$$

$$F = 1/1.762588 = 0.57Hz \tag{C.2}$$

Table C.4: Peak to Peak values

Amplitude		
Peak Nr	Time [s]	Speed [pu]
1	31.107983	1.0004
2	32.870571	1.00017

Determining when the oscillations stops is always a bit difficult so the number given here are just an estimate:

Table C.5: Damping

Start [s]	End [s]
30.02	45

$$1\tau = (45 - 30.02 = 14.98)/5 = 2.996 \tag{C.3}$$

$$Damping = 1/2.996 = 0.33 \tag{C.4}$$

And the properties of the oscillation written as an eigenvalue will be:

$$\lambda = -0.33 \ \pm J0.57 \ hz \tag{C.5}$$

C.3.5 B : Asynchronous Generator

```
List of Eigenvalues
*******************

   1 -9814.333984 1/s, +0.000000 Hz
   2 -2273.759521 1/s, +0.000000 Hz
   3 -96.401062 1/s, +0.000000 Hz
   4 -100.157394 1/s, +0.000000 Hz
   5 -50.270008 1/s, +0.000000 Hz
   6 -39.202644 1/s, +0.000000 Hz
   7 -19.593906 1/s, +1.642247 Hz
   8 -19.593906 1/s, -1.642247 Hz
   9 -2.186934 1/s, +1.059607 Hz
  10 -2.186934 1/s, -1.059607 Hz
  11 -10.325260 1/s, +0.000000 Hz
  12 -9.579246 1/s, +0.000000 Hz
  13 -5.566081 1/s, +0.000000 Hz
  14 -0.575761 1/s, +0.605016 Hz
  15 -0.575761 1/s, -0.605016 Hz
  16 -2.620765 1/s, +0.000000 Hz
  17 -0.997675 1/s, +0.000000 Hz
  18 -0.179815 1/s, +0.000000 Hz
  19 -0.138216 1/s, +0.000000 Hz
  20 -0.054788 1/s, +0.000000 Hz
  21 -0.102777 1/s, +0.000000 Hz
  22 -0.100002 1/s, +0.000000 Hz
  23 +0.001764 1/s, +0.000000 Hz
```

(a) B1

```
List of Eigenvalues
*******************

   1 -9843.854492 1/s, +0.000000 Hz
   2 -100.203072 1/s, +0.000000 Hz
   3 -96.843651 1/s, +0.000000 Hz
   4 -50.260719 1/s, +0.000000 Hz
   5 -39.125065 1/s, +0.000000 Hz
   6 -19.456306 1/s, +1.767564 Hz
   7 -19.456306 1/s, -1.767564 Hz
   8 -10.321856 1/s, +0.000000 Hz
   9 -2.709077 1/s, +1.031356 Hz
  10 -2.709077 1/s, -1.031356 Hz
  11 -5.180639 1/s, +0.000000 Hz
  12 -0.627665 1/s, +0.599214 Hz
  13 -0.627665 1/s, -0.599214 Hz
  14 -2.666158 1/s, +0.060850 Hz
  15 -2.666158 1/s, -0.060850 Hz
  16 -0.180818 1/s, +0.000000 Hz
  17 -0.138566 1/s, +0.000000 Hz
  18 -0.101753 1/s, +0.000000 Hz
  19 -0.054888 1/s, +0.000000 Hz
```

(b) B3

Figure C.7: Eigenvalues, B : Asynchronous generator.

C.3.6 C : Static Production

```
List of Eigenvalues
*******************

    1 -8949.471680 1/s, +0.000000 Hz
    2 -96.360573 1/s, +0.000000 Hz
    3 -50.193726 1/s, +0.000000 Hz
    4 -38.487808 1/s, +0.000000 Hz
    5 -20.138439 1/s, +1.678937 Hz
    6 -20.138439 1/s, -1.678937 Hz
    7 -10.360929 1/s, +0.000000 Hz
    8 -0.803249 1/s, +0.694898 Hz
    9 -0.803249 1/s, -0.694898 Hz
   10 -5.202071 1/s, +0.000000 Hz
   11 -2.611723 1/s, +0.000000 Hz
   12 -0.988598 1/s, +0.000000 Hz
   13 -0.179790 1/s, +0.000000 Hz
   14 -0.138208 1/s, +0.000000 Hz
   15 -0.055008 1/s, +0.000000 Hz
   16 -0.102807 1/s, +0.000000 Hz
   17 -0.100000 1/s, +0.000000 Hz
```

(a) C2

```
List of Eigenvalues
*******************

    1 -96.044662 1/s, +0.000000 Hz
    2 -50.217072 1/s, +0.000000 Hz
    3 -37.951893 1/s, +0.000000 Hz
    4 -19.673561 1/s, +2.033593 Hz
    5 -19.673561 1/s, -2.033593 Hz
    6 -10.369279 1/s, +0.000000 Hz
    7 -0.649230 1/s, +0.686836 Hz
    8 -0.649230 1/s, -0.686836 Hz
    9 -5.342459 1/s, +0.000000 Hz
   10 -2.702171 1/s, +0.000000 Hz
   11 -0.180844 1/s, +0.000000 Hz
   12 -0.138551 1/s, +0.000000 Hz
   13 -0.101714 1/s, +0.000000 Hz
   14 -0.055250 1/s, +0.000000 Hz
```

(b) C3

Figure C.8: Eigenvalues C : Static production.

C.3.7 D : DFIG

```
List of Eigenvalues
*******************

   1 -28.272511 1/s, +18.954269 Hz
   2 -28.272511 1/s, -18.954269 Hz
   3 -96.501297 1/s, +0.000000 Hz
   4 -50.328705 1/s, +0.000000 Hz
   5 +3.206786 1/s, +7.051509 Hz
   6 +3.206786 1/s, -7.051509 Hz
   7 -39.620731 1/s, +0.000000 Hz
   8 -19.502300 1/s, +1.311584 Hz
   9 -19.502300 1/s, -1.311584 Hz
  10 -18.453978 1/s, +0.000000 Hz
  11 +4.879964 1/s, +0.000000 Hz
  12 -10.197964 1/s, +0.000000 Hz
  13 -7.015681 1/s, +0.000000 Hz
  14 -1.131107 1/s, +0.752055 Hz
  15 -1.131107 1/s, -0.752055 Hz
  16 -9.999993 1/s, +0.000000 Hz
  17 -2.735205 1/s, +0.000000 Hz
  18 -1.542365 1/s, +0.121364 Hz
  19 -1.542365 1/s, -0.121364 Hz
  20 -1.053261 1/s, +0.000000 Hz
  21 +0.157733 1/s, +0.000000 Hz
  22 -0.038352 1/s, +0.024502 Hz
  23 -0.038352 1/s, -0.024502 Hz
  24 -0.179917 1/s, +0.000000 Hz
  25 -0.102515 1/s, +0.000000 Hz
  26 -0.133916 1/s, +0.000000 Hz
  27 -0.142101 1/s, +0.000000 Hz
  28 -166.666672 1/s, +0.000000 Hz
  29 -999.999939 1/s, +0.000000 Hz
  30 -10000.000000 1/s, +0.000000 Hz
  31 -100.000000 1/s, +0.000000 Hz
```

(a) D1

```
List of Eigenvalues
*******************

   1 -10.000000 1/s, +0.000000 Hz
   2 -8560.508789 1/s, +0.000000 Hz
   3 -96.615395 1/s, +0.000000 Hz
   4 +3.794516 1/s, +6.724682 Hz
   5 +3.794516 1/s, -6.724682 Hz
   6 -50.327099 1/s, +0.000000 Hz
   7 -39.596542 1/s, +0.000000 Hz
   8 -19.372658 1/s, +1.356143 Hz
   9 -19.372658 1/s, -1.356143 Hz
  10 -17.844873 1/s, +0.000000 Hz
  11 -10.150915 1/s, +0.000000 Hz
  12 -7.239502 1/s, +0.000000 Hz
  13 -1.325925 1/s, +0.773043 Hz
  14 -1.325925 1/s, -0.773043 Hz
  15 +3.640623 1/s, +0.000000 Hz
  16 -10.000009 1/s, +0.000000 Hz
  17 -1.400395 1/s, +0.179051 Hz
  18 -1.400395 1/s, -0.179051 Hz
  19 -2.713590 1/s, +0.000000 Hz
  20 -1.076824 1/s, +0.000000 Hz
  21 -0.925251 1/s, +0.000000 Hz
  22 -0.007484 1/s, +0.026229 Hz
  23 -0.007484 1/s, -0.026229 Hz
  24 -0.094475 1/s, +0.007423 Hz
  25 -0.094475 1/s, -0.007423 Hz
  26 -0.100756 1/s, +0.000000 Hz
  27 -0.179945 1/s, +0.000000 Hz
  28 -0.142200 1/s, +0.000000 Hz
  29 -0.100000 1/s, +0.000000 Hz
  30 -166.666672 1/s, +0.000000 Hz
  31 -999.999939 1/s, +0.000000 Hz
  33 -100.000000 1/s, +0.000000 Hz
```

(b) D2

Figure C.9: Eigenvalues D : DFIG.

```
List of Eigenvalues
*******************

   1 -10.000000 1/s, +0.000000 Hz
   2 -96.197113 1/s, +0.000000 Hz
   3 +3.733888 1/s, +6.762556 Hz
   4 +3.733888 1/s, -6.762556 Hz
   5 -50.383400 1/s, +0.000000 Hz
   6 -39.311939 1/s, +0.000000 Hz
   7 -18.216156 1/s, +1.920070 Hz
   8 -18.216156 1/s, -1.920070 Hz
   9 -17.999586 1/s, +0.000000 Hz
  10 +4.641632 1/s, +0.000000 Hz
  11 -1.315224 1/s, +0.808907 Hz
  12 -1.315224 1/s, -0.808907 Hz
  13 -8.105865 1/s, +0.000000 Hz
  14 -10.129807 1/s, +0.000000 Hz
  15 -9.999992 1/s, +0.000000 Hz
  16 -2.561651 1/s, +0.012019 Hz
  17 -2.561651 1/s, -0.012019 Hz
  18 -1.151075 1/s, +0.060408 Hz
  19 -1.151075 1/s, -0.060408 Hz
  20 +0.090090 1/s, +0.000000 Hz
  21 -0.050721 1/s, +0.034786 Hz
  22 -0.050721 1/s, -0.034786 Hz
  23 -0.102068 1/s, +0.000000 Hz
  24 -0.181466 1/s, +0.000000 Hz
  25 -0.137039 1/s, +0.000000 Hz
  26 -0.144004 1/s, +0.000000 Hz
  27 -166.666672 1/s, +0.000000 Hz
  28 -999.999939 1/s, +0.000000 Hz
  29 -10000.000000 1/s, +0.000000 Hz
  30 -100.000000 1/s, +0.000000 Hz
```

(c) D3

Figure C.9: Eigenvalues D : DFIG.

C.3.8 E : SCIG

List of Eigenvalues
****

```
 1 -9578.259766 1/s, +0.000000 Hz
 2 -4120.912598 1/s, +0.000000 Hz
 3 -96.333733 1/s, +0.000000 Hz
 4 -101.643326 1/s, +0.000000 Hz
 5 -50.217838 1/s, +0.000000 Hz
 6 -38.590725 1/s, +0.000000 Hz
 7 -20.001719 1/s, +1.712989 Hz
 8 -20.001719 1/s, -1.712989 Hz
 9 -2.011993 1/s, +3.045180 Hz
10 -2.011993 1/s, -3.045180 Hz
11 -10.394231 1/s, +0.000000 Hz
12 -9.103911 1/s, +0.000000 Hz
13 -1.565154 1/s, +0.682928 Hz
14 -1.565154 1/s, -0.682928 Hz
15 -5.220181 1/s, +0.000000 Hz
16 -0.690968 1/s, +0.390831 Hz
17 -0.690968 1/s, -0.390831 Hz
18 -2.593623 1/s, +0.000000 Hz
19 -1.013753 1/s, +0.000000 Hz
20 -0.179337 1/s, +0.000000 Hz
21 -0.137300 1/s, +0.000000 Hz
22 -0.055288 1/s, +0.000000 Hz
23 -0.102950 1/s, +0.000000 Hz
24 -0.100000 1/s, +0.000000 Hz
```

(a) E2

List of Eigenvalues
****

```
 1 -9727.297852 1/s, +0.000000 Hz
 2 -102.022606 1/s, +0.000000 Hz
 3 -96.864136 1/s, +0.000000 Hz
 4 -50.207485 1/s, +0.000000 Hz
 5 -38.429623 1/s, +0.000000 Hz
 6 -19.504894 1/s, +1.874839 Hz
 7 -19.504894 1/s, -1.874839 Hz
 8 -3.210676 1/s, +2.910499 Hz
 9 -3.210676 1/s, -2.910499 Hz
10 -10.369321 1/s, +0.000000 Hz
11 -2.818912 1/s, +0.991126 Hz
12 -2.818912 1/s, -0.991126 Hz
13 -4.425564 1/s, +0.000000 Hz
14 -0.402171 1/s, +0.535717 Hz
15 -0.402171 1/s, -0.535717 Hz
16 -2.600408 1/s, +0.000000 Hz
17 -0.169021 1/s, +0.000000 Hz
18 -0.149742 1/s, +0.002022 Hz
19 -0.149742 1/s, -0.002022 Hz
20 -0.069900 1/s, +0.000000 Hz
21 -0.064819 1/s, +0.000000 Hz
```

(b) e3

Figure C.10: Eigenvalues E : SCIG.